Exoplanetary atmospheres: Observations and modelling

Benjamin Charnay

ARIEL-School, *Biarritz, 2019*

Introduction

A diversity of exoplanets

I) Observational techniques

- Transit
- Direct imaging
- Medium/high spectral resolution
- Lessons from observations of exoplanets

II) Modelling exoplanetary atmospheres

- Radiative transfer
- Thermal structure
- Clouds & aerosols

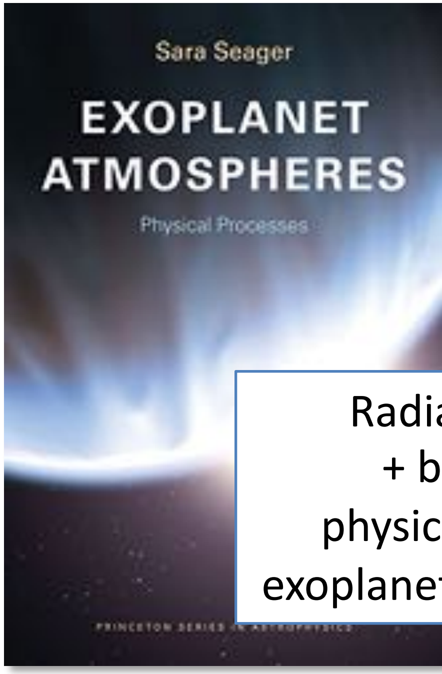

Radiative transfer
+ basics about
physics/chemistry of
exoplanetary atmospheres

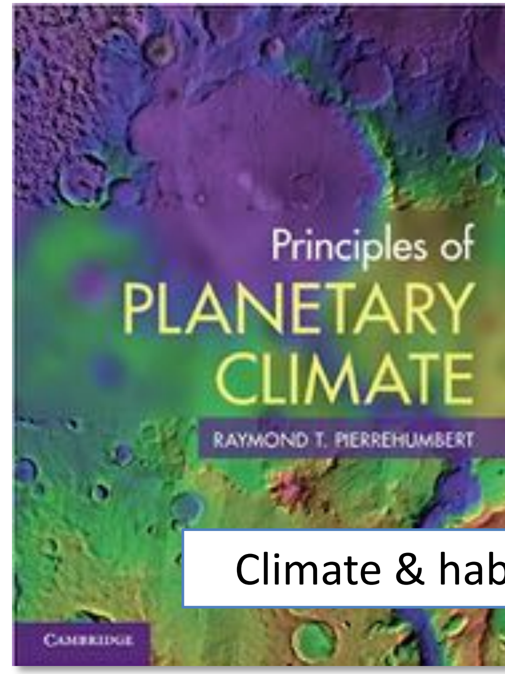

Climate & habitability

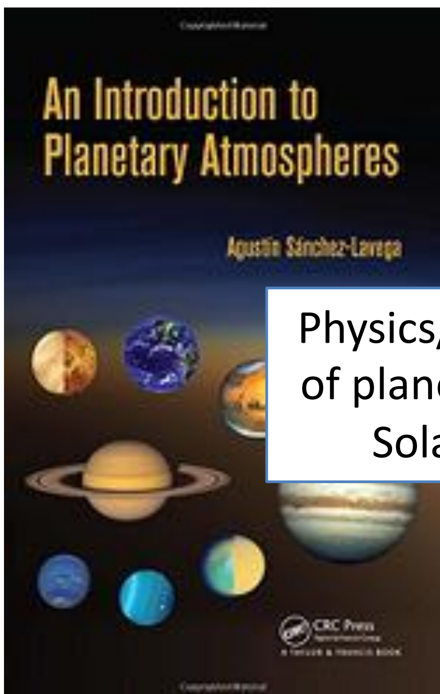

Physics/chemistry/dynamics
of planetary atmospheres &
Solar System planets

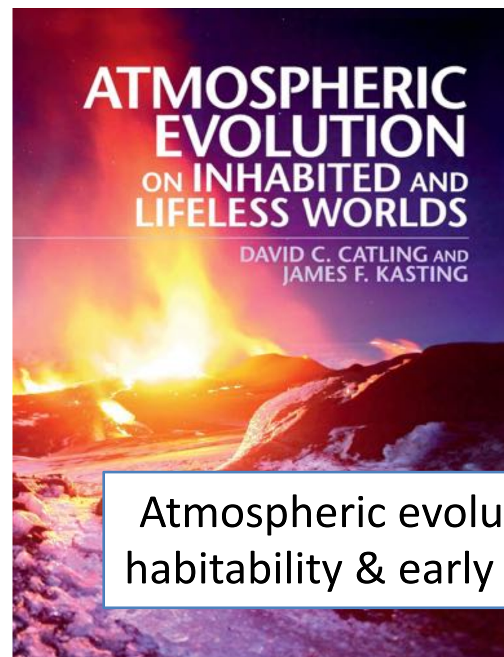

Atmospheric evolution,
habitability & early Earth

Not really a statistically significant sample

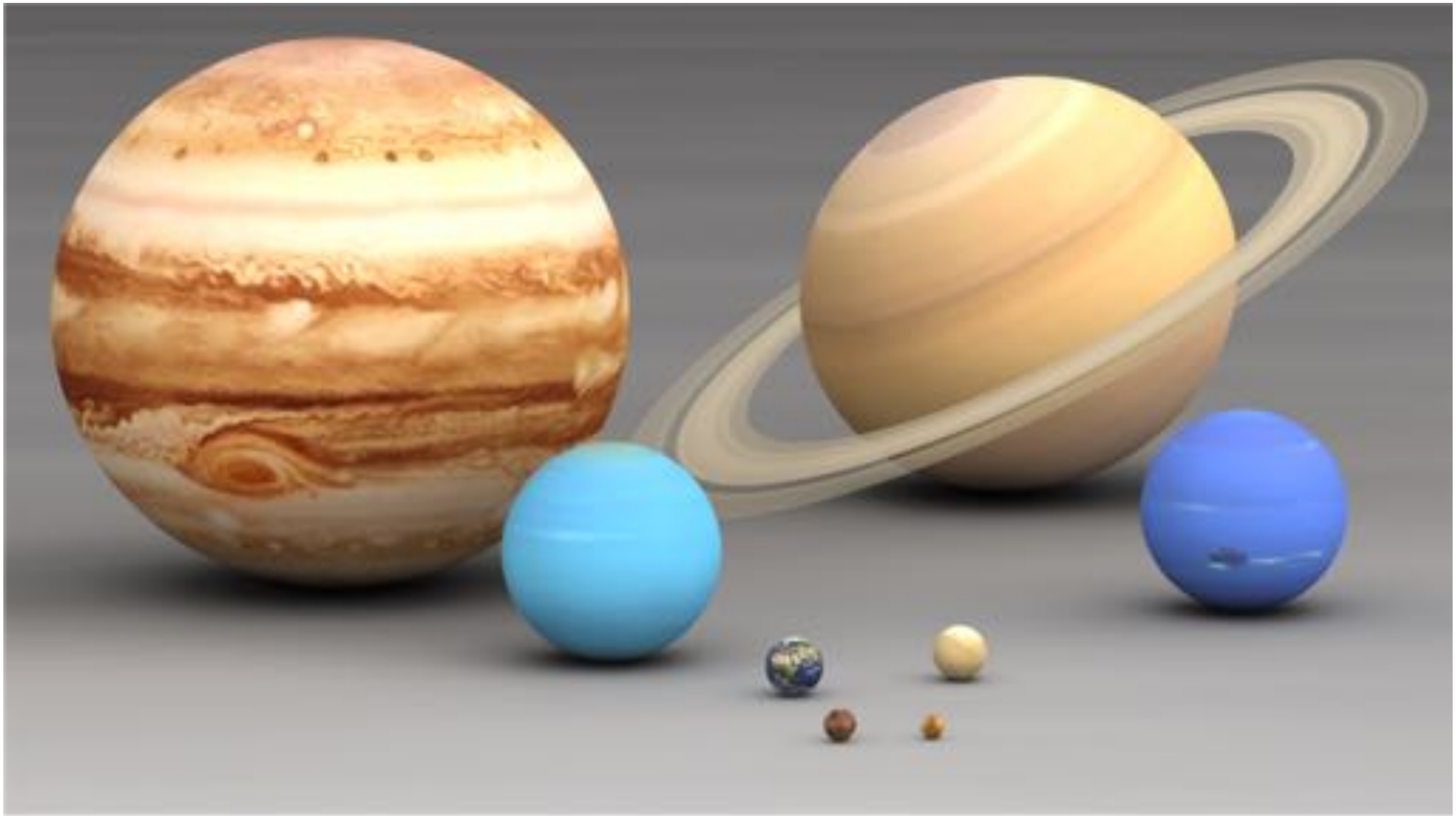

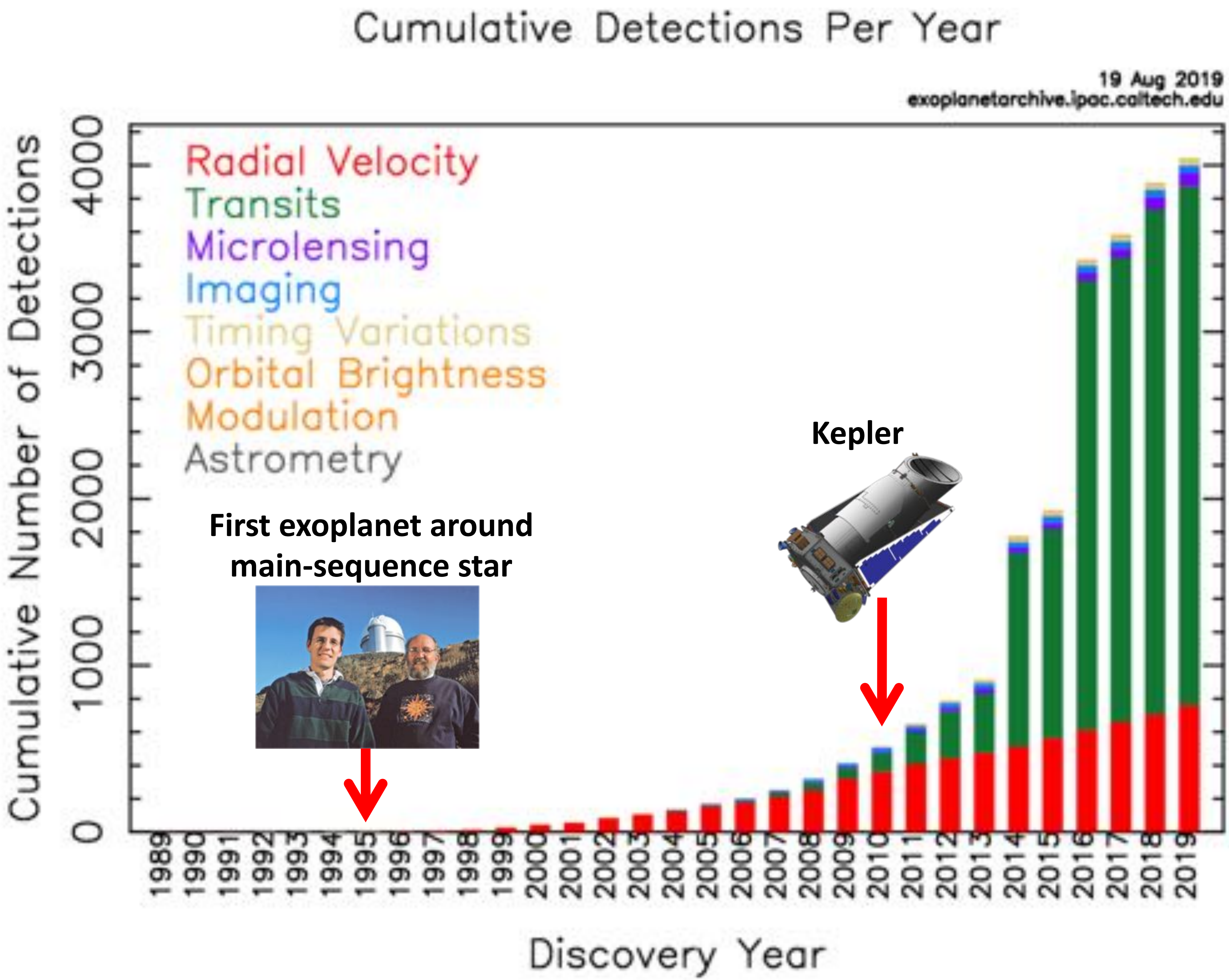

Cumulative Detections Per Year
19 Aug 2019
exoplanetarchive.ipac.caltech.edu
Radial Velocity
Transits
Microlensing
Imaging
Timing Variations
Orbital Brightness
Modulation
Astrometry
Cumulative Number of Detections
0
1000
2000
3000
4000
First exoplanet around
main-sequence star
Kepler
1989
1990
1991
1992
1993
1994
1995
1996
1997
1998
1999
2000
2001
2002
2003
2004
2005
2006
2007
2008
2009
2010
2011
2012
2013
2014
2015
2016
2017
2018
2019
Discovery Year

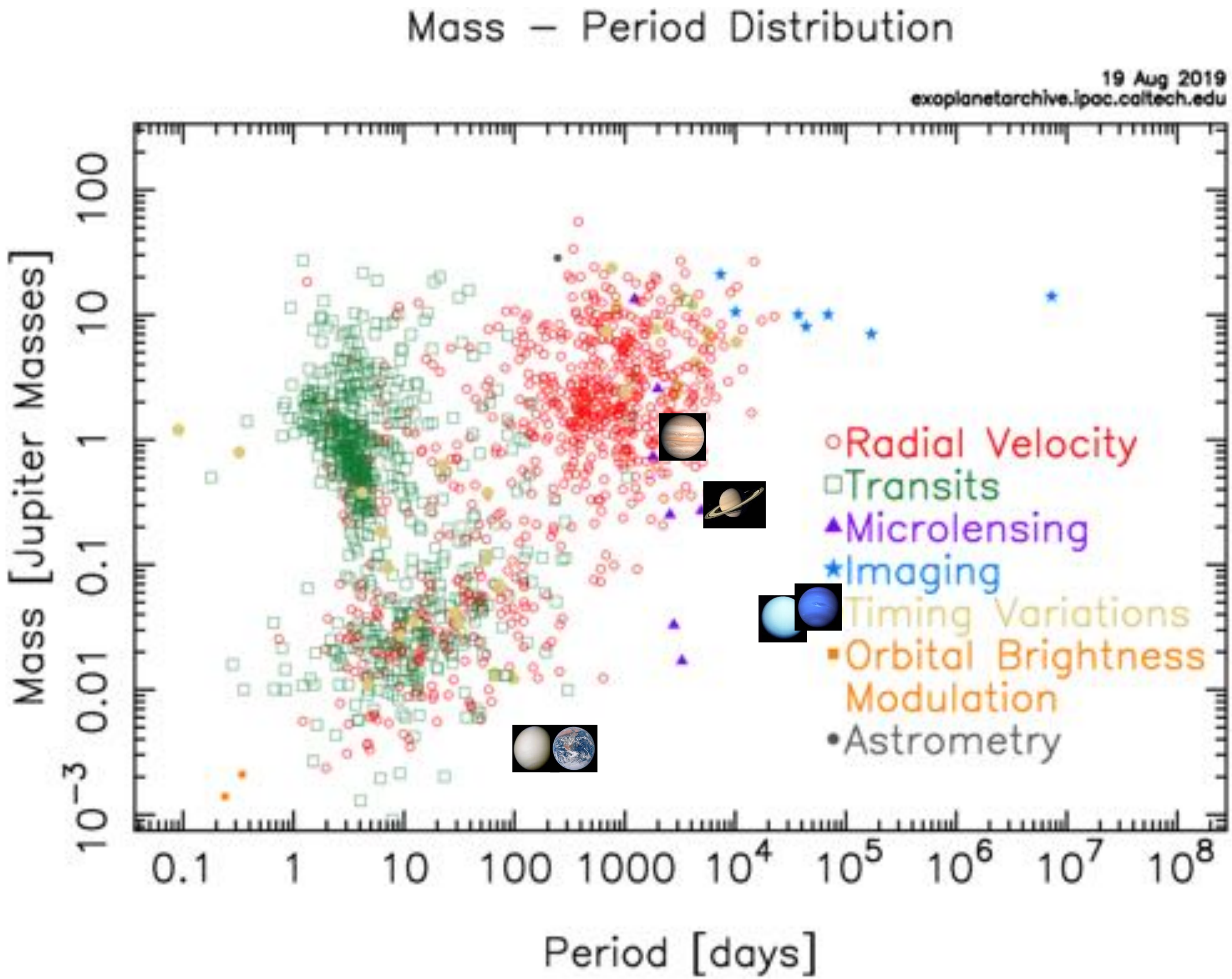

Mass – Period Distribution
19 Aug 2019
exoplanetarchive.ipac.caltech.edu
Mass [Jupiter Masses]
Period [days]
100
10
1
0.1
0.01
10^{-3}
0.1
1
10
100
1000
10^4
10^5
10^6
10^7
10^8
Radial Velocity
Transits
Microlensing
Imaging
Timing Variations
Orbital Brightness Modulation
Astrometry

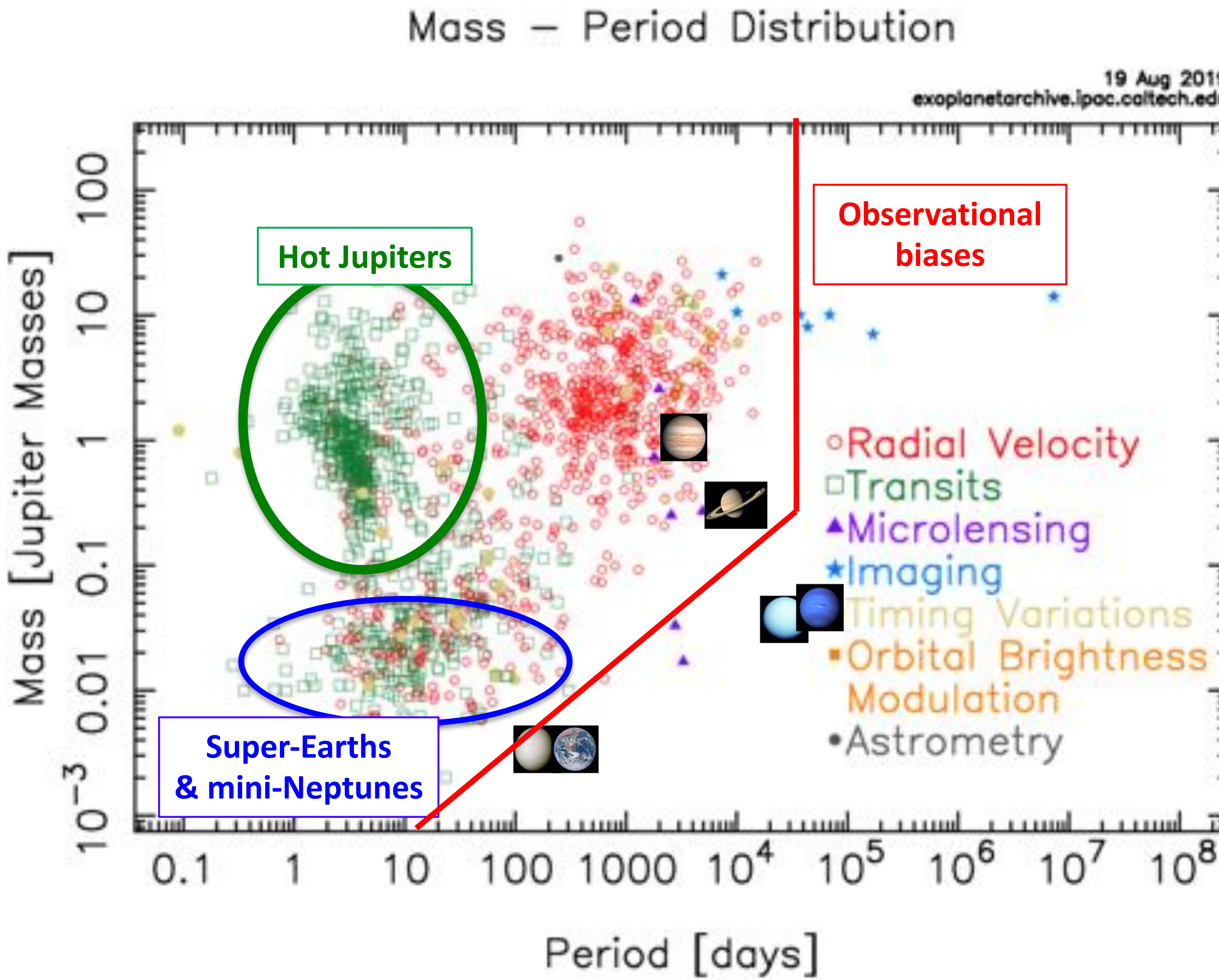

Mass – Period Distribution
19 Aug 2019
exoplanetarchive.ipac.caltech.edu
Hot Jupiters
Observational biases
Super-Earths & mini-Neptunes
Radial Velocity
Transits
Microlensing
Imaging
Timing Variations
Orbital Brightness Modulation
Astrometry
Mass [Jupiter Masses]
100
10
1
0.1
0.01
10^{-3}
0.1
1
10
100
1000
10^4
10^5
10^6
10^7
10^8
Period [days]

Occurrence rate of planets

$$\text{Occ. Rate} = \frac{\text{Num. of (real) Planet}}{\text{Completeness}}$$

(Number of stars for which a planet would be detected if it's there)

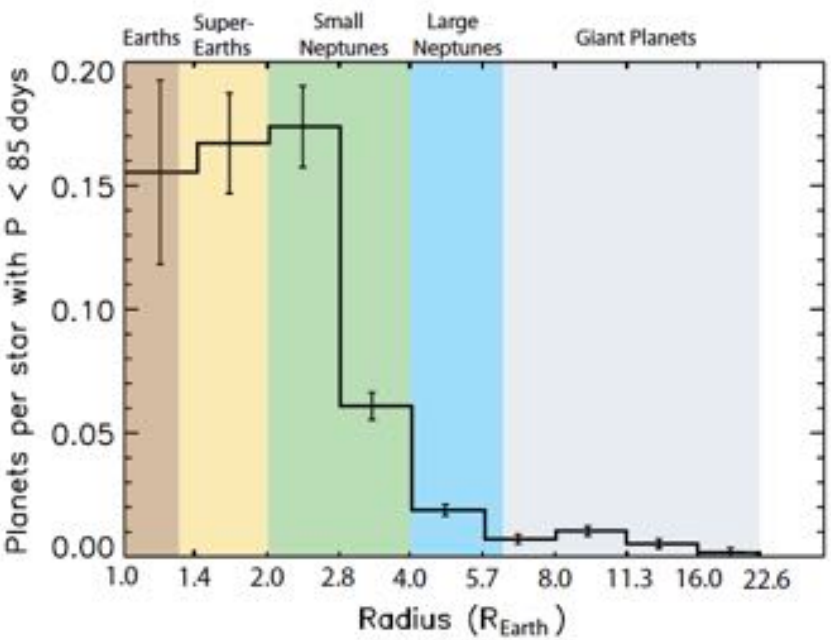

Fressin et al. (2013)

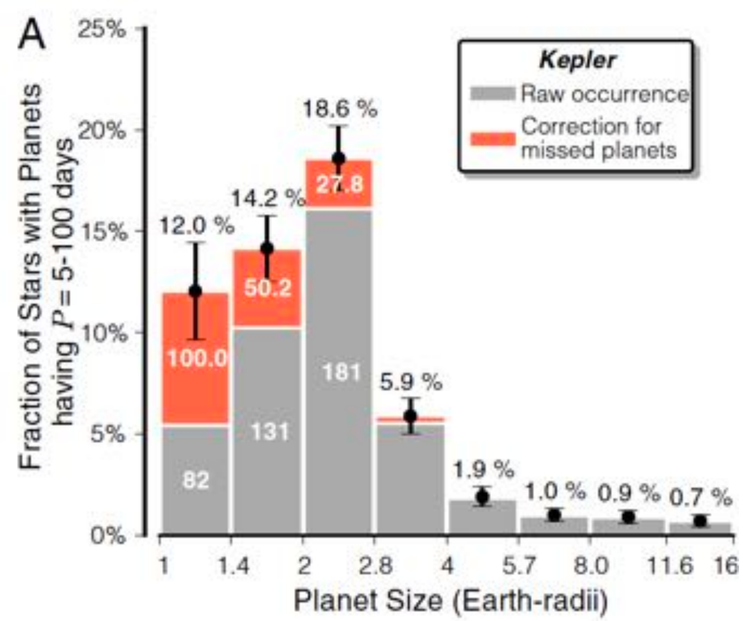

Petigura et al. (2013)

Planets around Sun-like stars are very common
High fraction of super-Earths and mini-Neptunes

Planet formation: core accretion model

$T_{\rm disk} < 10^7 {\rm yr}$

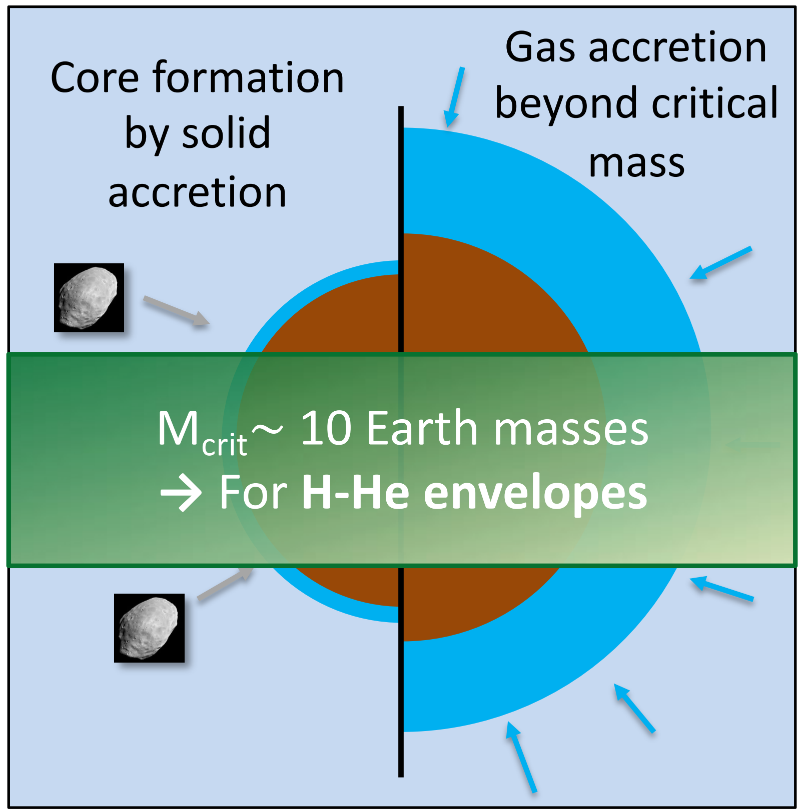

(Perri & Cameron 1974, Mizuno 1978, Bondeheimer & Pollack 1986, Pollack et al. 1996)

Planet formation: core accretion model

$T_{\mathrm{disk}} < 10^7 \mathrm{yr}$

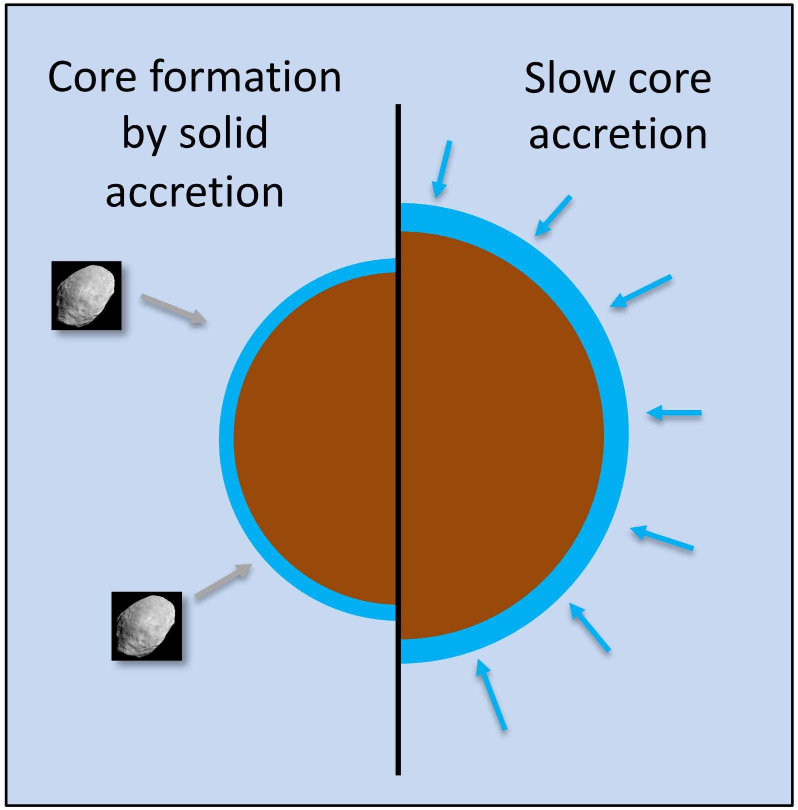

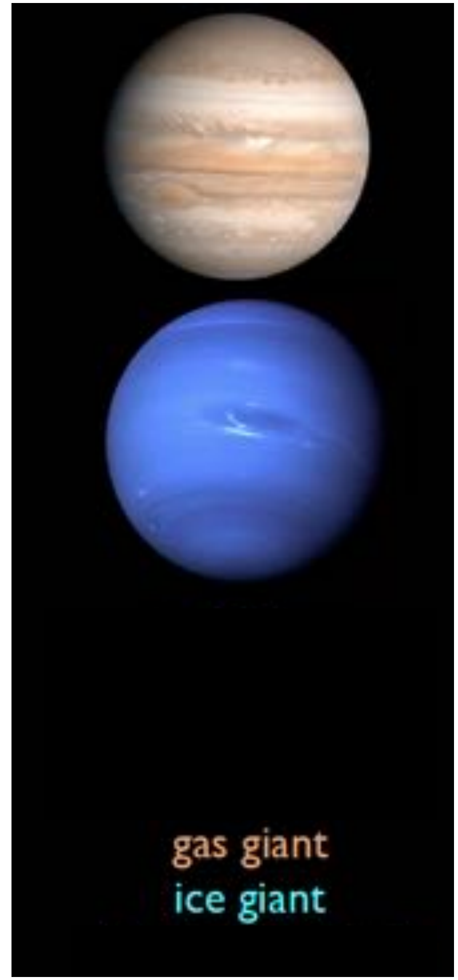

Planet formation: core accretion model

$T_{\text{disk}} < 10^7\text{yr}$

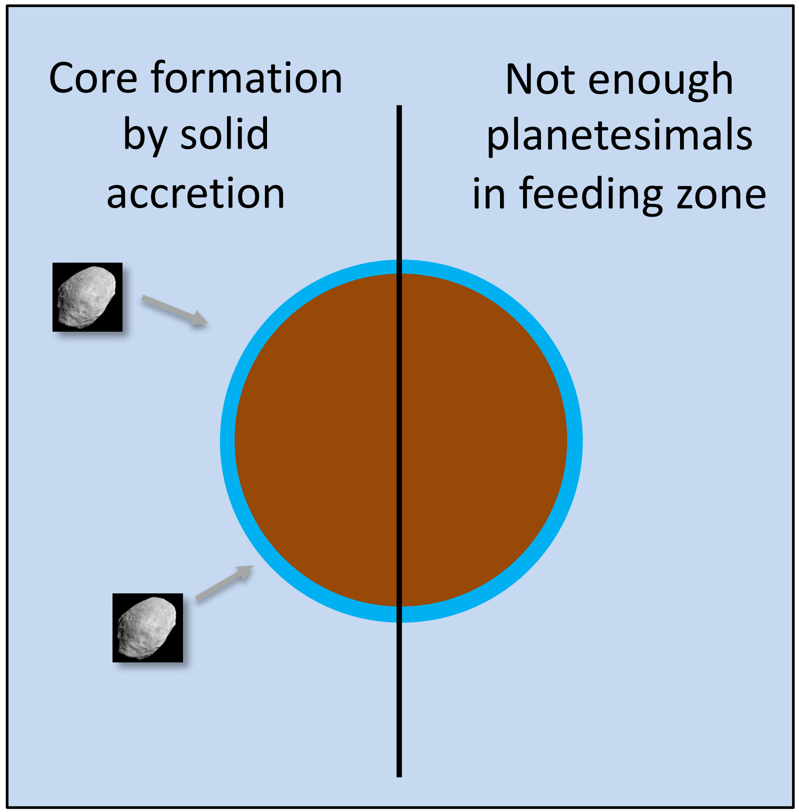

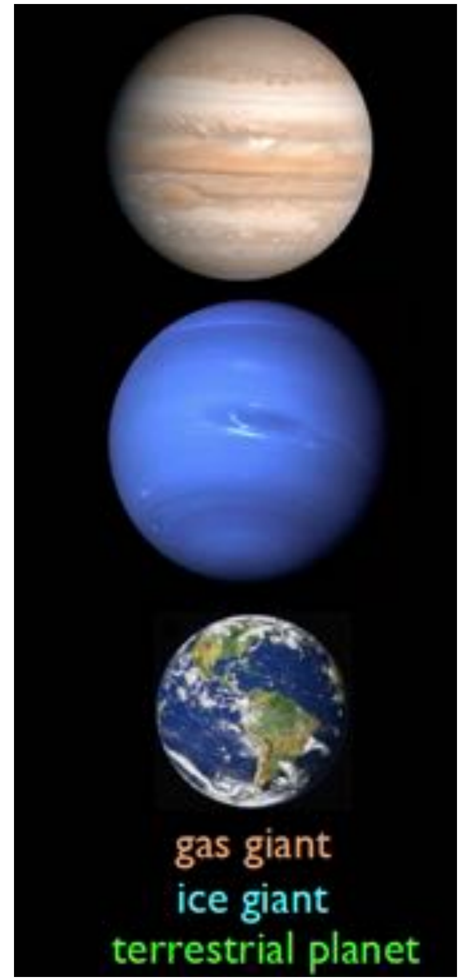

Atmospheres as a probe of planetary interior and formation

Metallicity = fraction of heavy elements (heavier than H and He)
For Solar System atmospheres, metallicity ≈ $[C]/[C]_{solar}$
For exoplanetary atmospheres, metallicity ≈ $[O]/[O]_{solar}$

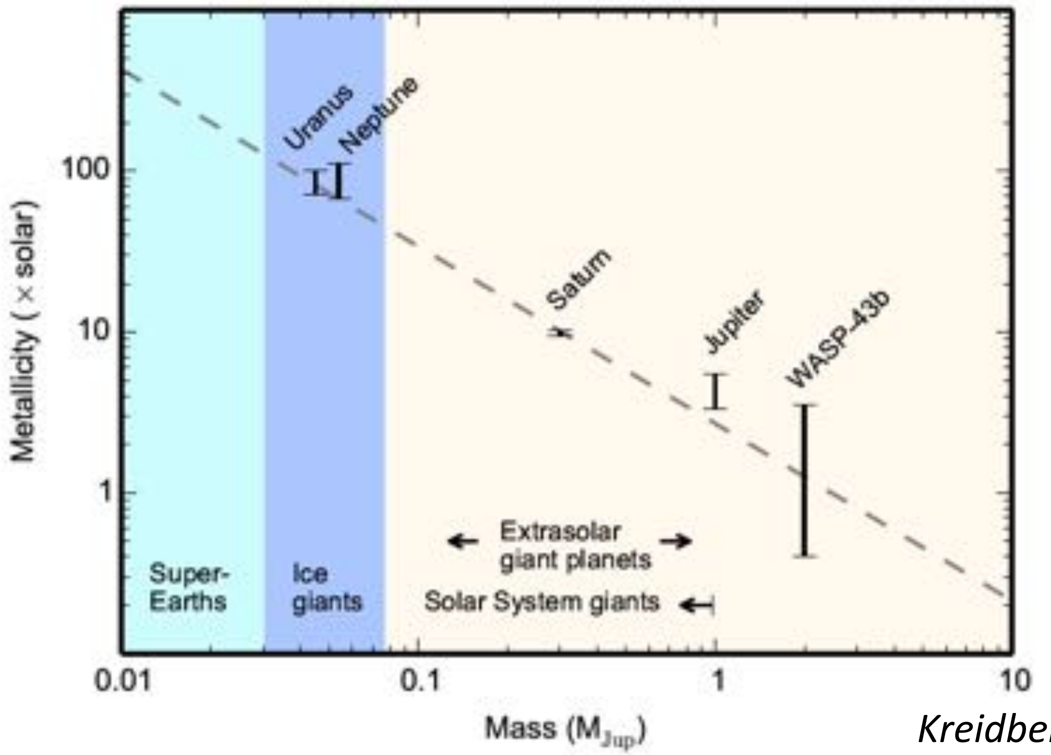

Kreidberg et al. (2015)

- Metallicity decreases with planetary mass in the Solar System
- Sub-Neptunes/Neptunes planets formed in-situ should have a relatively low metallicity

→ Measuring the metallicity allows to test formation and migration mechanisms

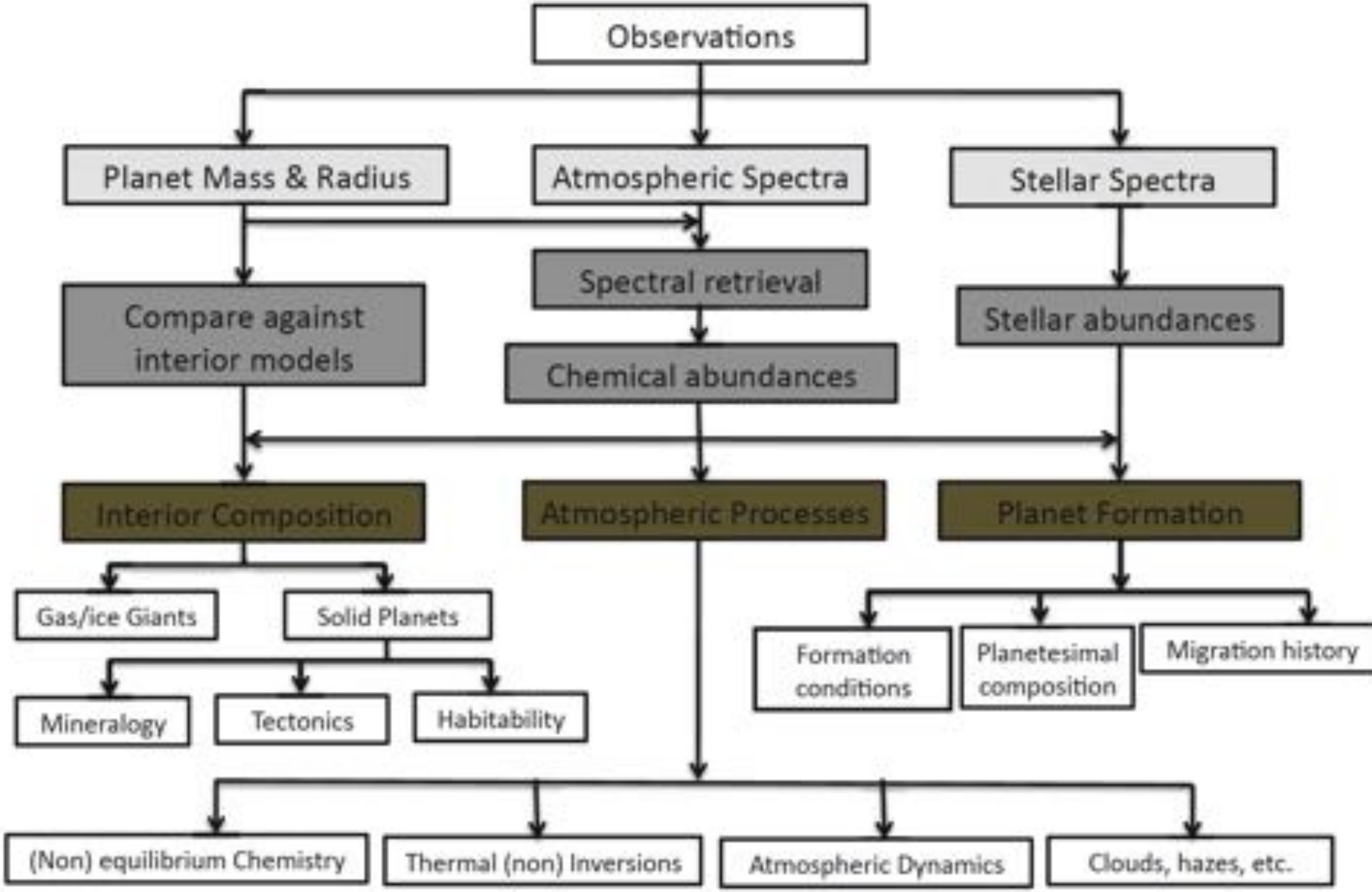

Madhusudhan et al. (2014)

Introduction

A diversity of exoplanets

I) Observational techniques

- Transit
- Direct imaging
- Medium/high spectral resolution
- Lessons from observations of exoplanets

II) Modelling exoplanetary atmospheres

- Radiative transfer
- Thermal structure
- Clouds & aerosols

I) Transit

Probability of transit

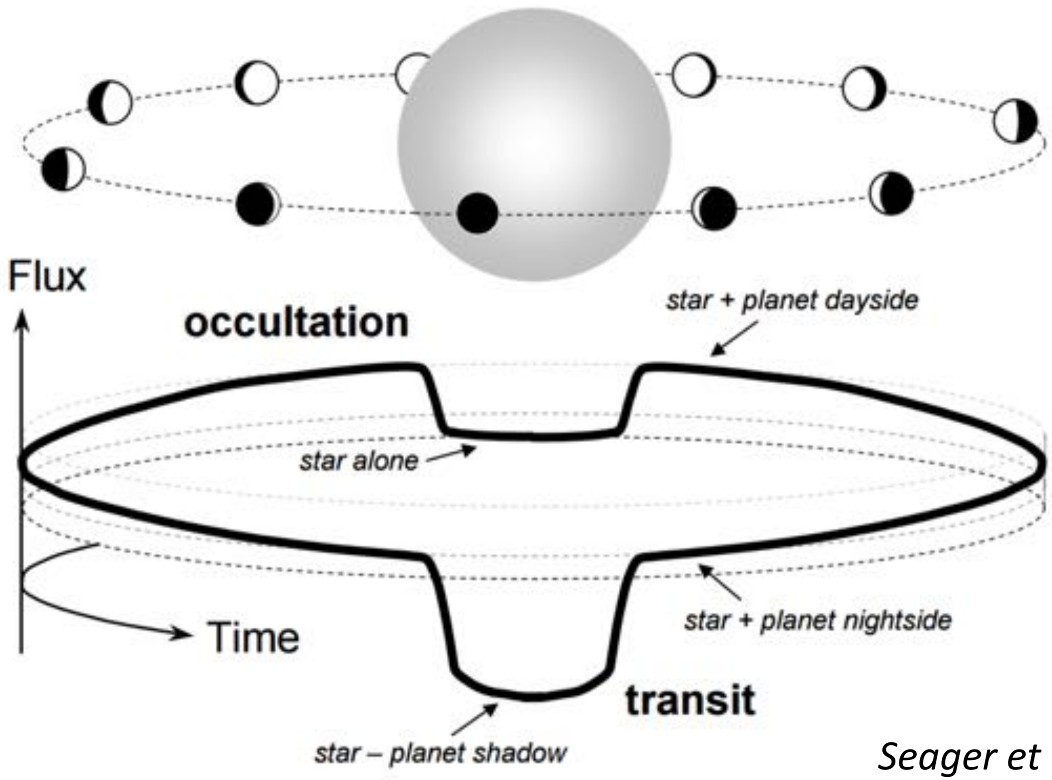

Seager et al. (2010)

Prob. of full transit: $p_{tra} = \left(\frac{R_\star - R_p}{a}\right)\left(\frac{1+e\sin\omega}{1-e^2}\right)$

Prob. of full occultation: $p_{occ} = \left(\frac{R_\star - R_p}{a}\right)\left(\frac{1-e\sin\omega}{1-e^2}\right)$

If $R_\star \gg R_p$ and $e \sim 0$: $p_{tra} = p_{occ} \approx 0.005\left(\frac{R_\star}{R_\odot}\right)\left(\frac{a}{1\ AU}\right)^{-1}$

I) Transit

Probability of transit

Interest of ultra-cool stars

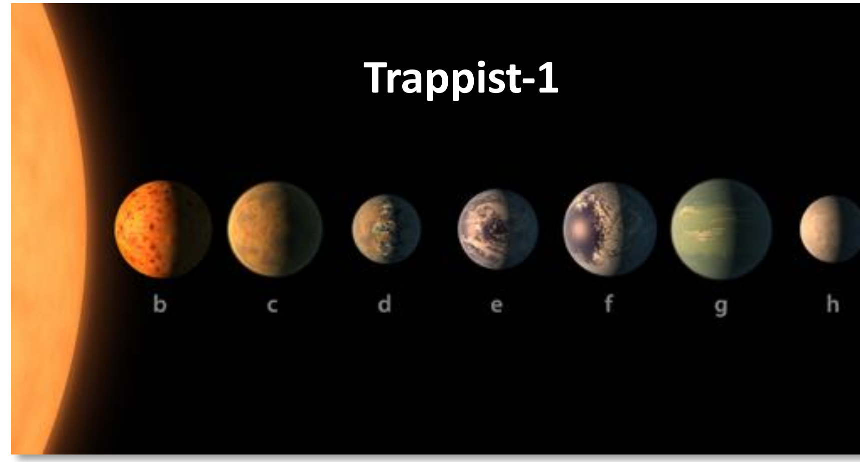

Probability of transit of an Earth-size planet at Teff=255K

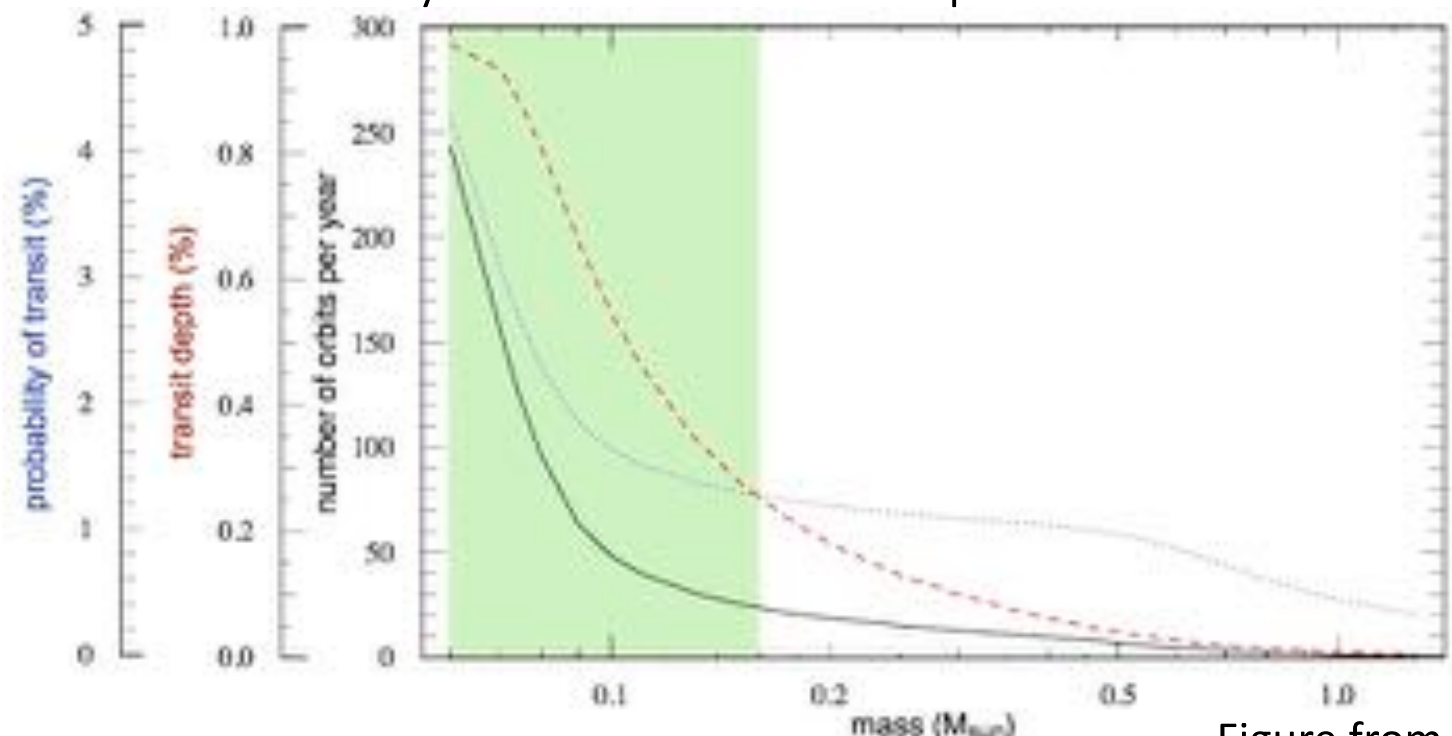

Figure from A. Triaud

I) Transit

Photometry

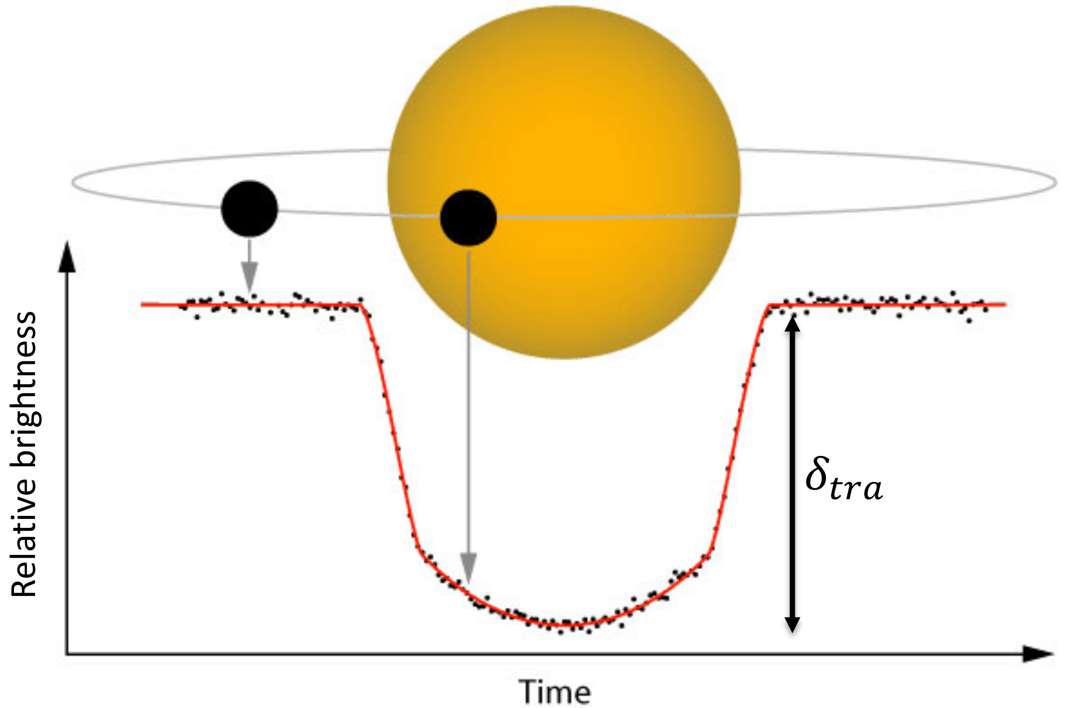

<u>Transit depth:</u>

$$\delta_{tra} = \left(\frac{R_p}{R_\star}\right)^2$$

<u>Occultation depth:</u>

$$\delta_{occ} = \frac{I_p}{I_\star}\left(\frac{R_p}{R_\star}\right)^2$$

I) Transit

Effect of limb darkening

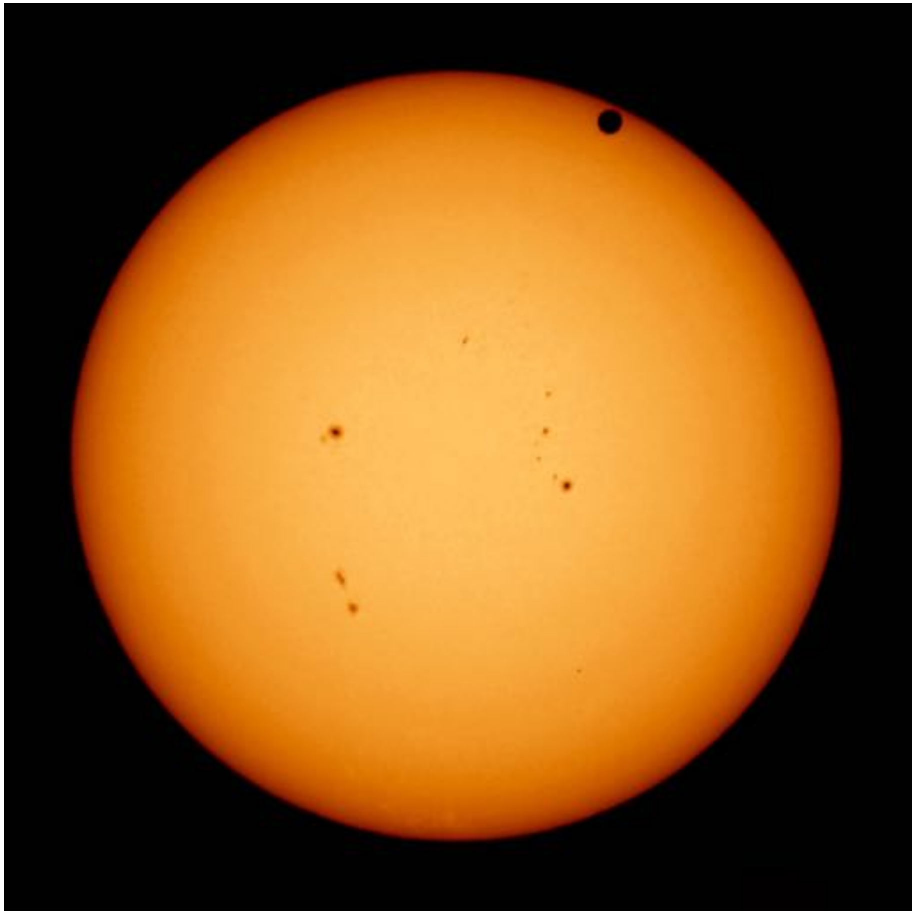

Transit of Venus

I) Transit

Effect of limb darkening

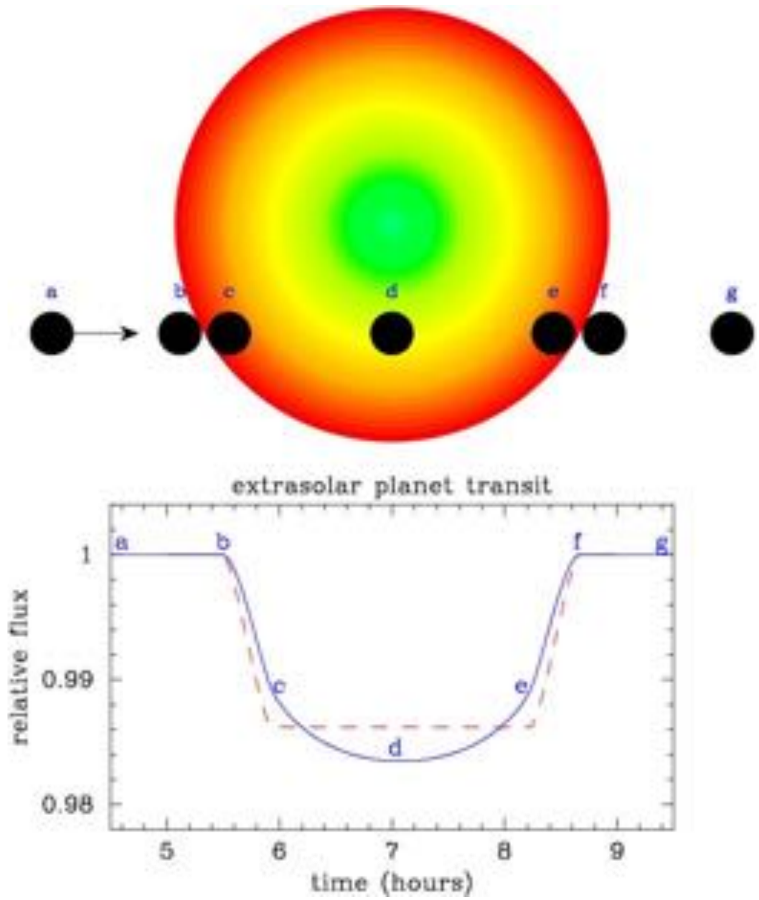

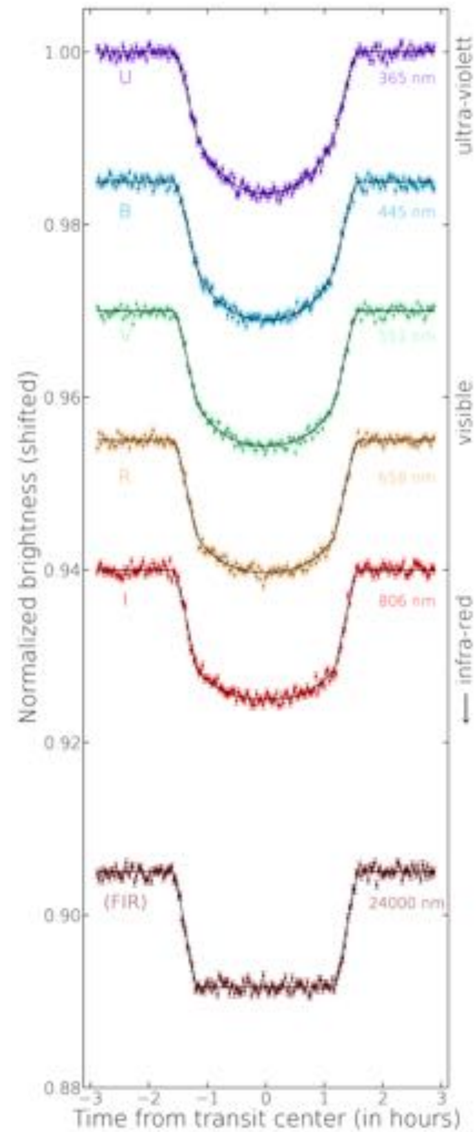

I) Transit

Atmospheric characterization with photometric transit lightcurves

- **Measure of radius and density**

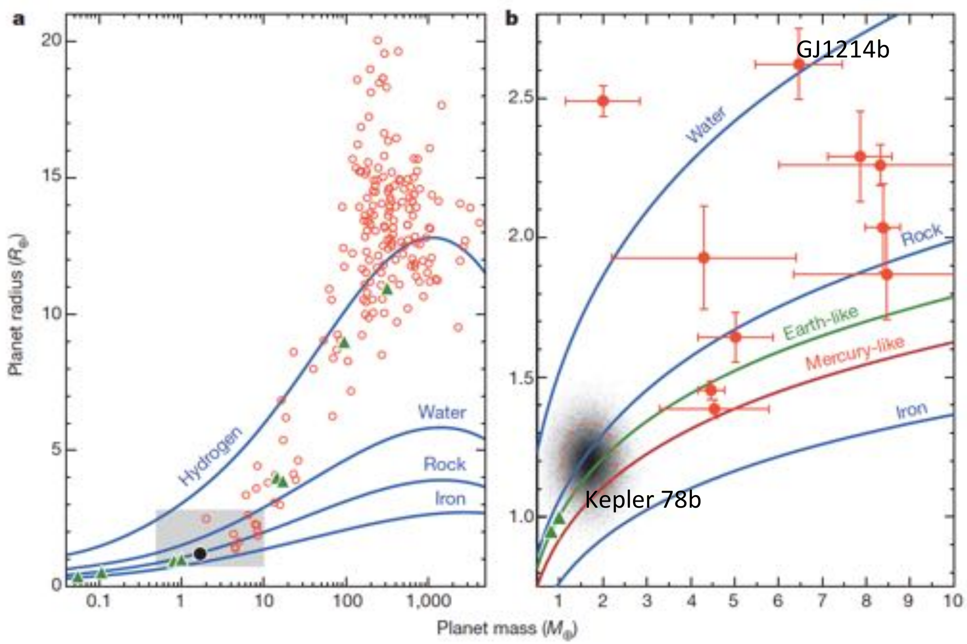

Howard et al. (2013)

- **Measure of thermal emission and reflected light during occultations**

→ effective temperature and geometric albedo

I) Transit

Spectroscopy

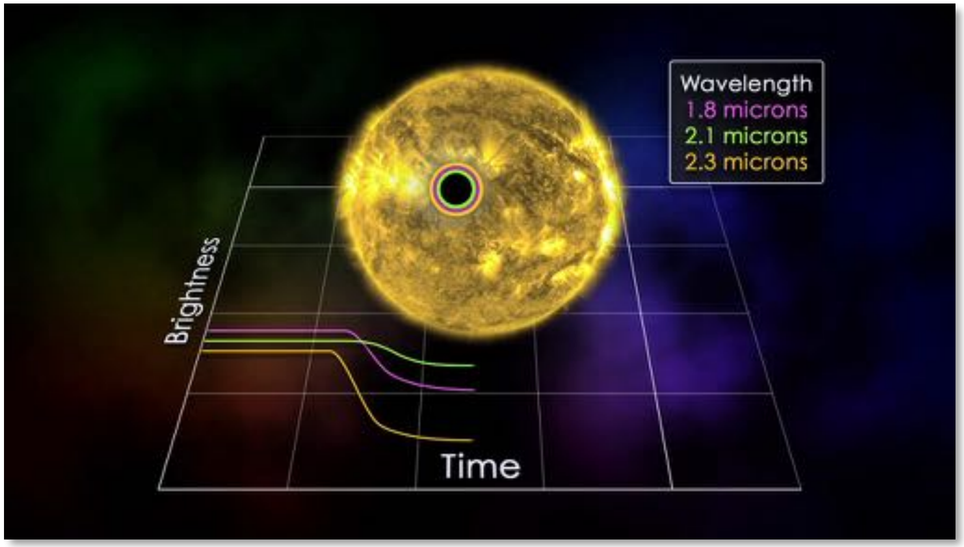

Effect of mean molecular weight

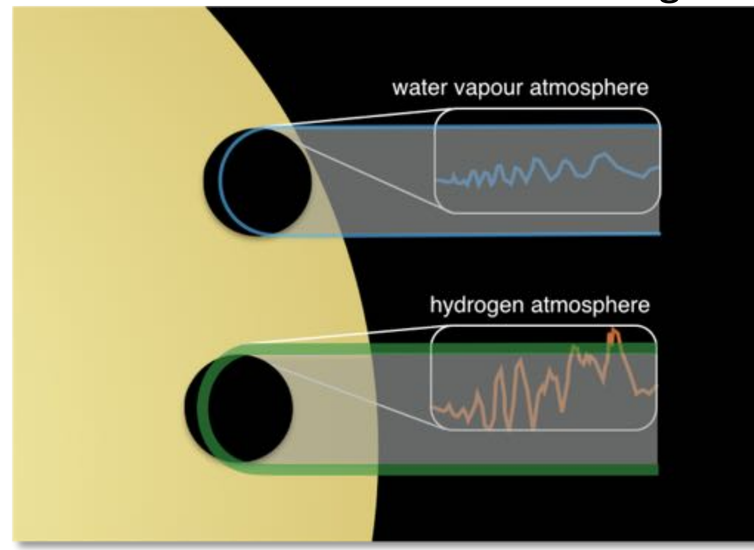

Variation of transit depth:

$$\Delta\delta_{tra} = \frac{\pi(R_p + N_H H)^2}{\pi R_\star^2} - \frac{\pi R_p^2}{\pi R_\star^2} \approx 2N_H \delta_{tra}\left(\frac{H}{R_p}\right)$$

Scale height: $H = \frac{RT}{Mg}$; Number of scale heights: $N_H \approx 7$ (for low resolution)

→ Transit spectroscopy easier for high scale height (e.g. hot giant planets)

I) Transit

Spectroscopy

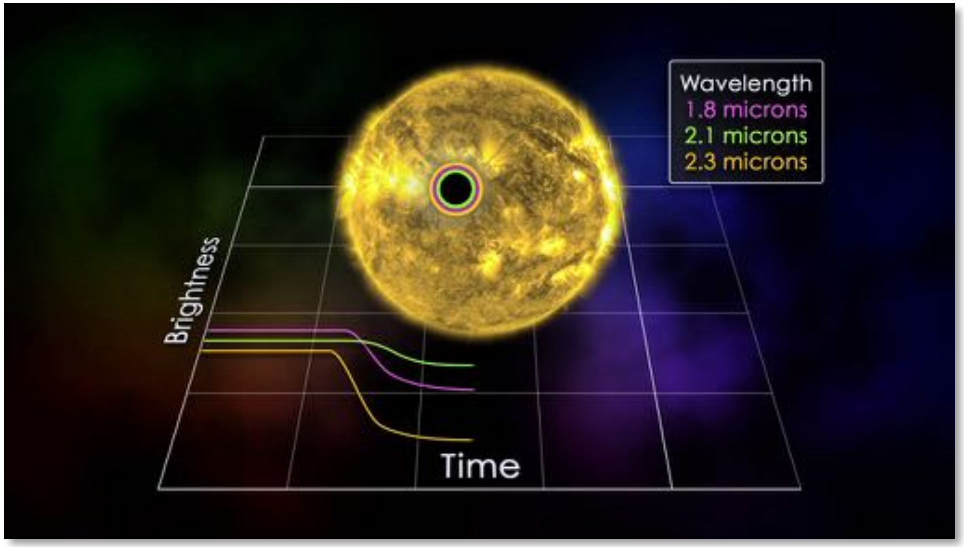

Effect of mean molecular weight

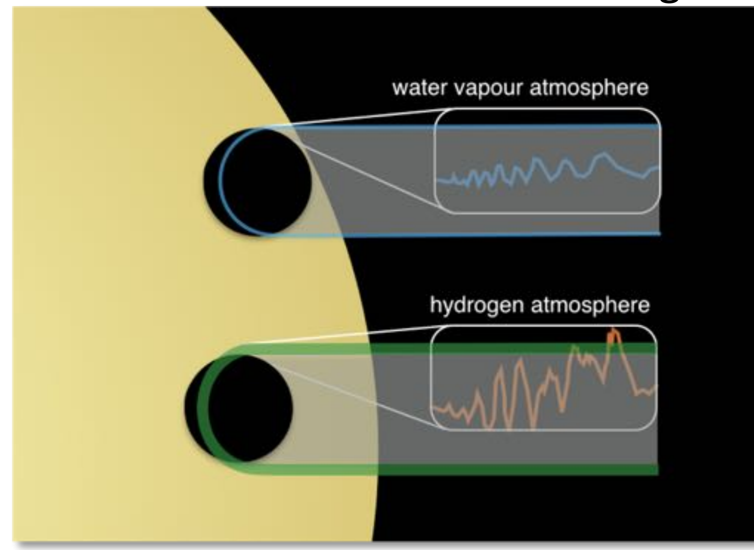

Variation of transit depth:

$$\Delta\boldsymbol{\delta}_{tra} = \frac{\pi(R_p + N_H H)^2}{\pi R_\star{}^2} - \frac{\pi R_p{}^2}{\pi R_\star{}^2} \approx 2N_H\delta_{tra}\left(\frac{H}{R_p}\right)$$

Scale height: $H = \frac{RT}{Mg}$; Number of scale heights: $N_H \approx 7$ (for low resolution)

For an Sun-like star:

- Hot Jupiter (T=1300 K, g=25 m s^{-2}, M=2.3 g/mol): $\delta_{tra} \approx 0.01$, $\Delta\delta_{tra} \approx 4.10^{-4}$
- Earth-like planet (T=280 K, g=10 m s^{-2}, M=28g/mol): $\delta_{tra} \approx 10^{-4}$, $\Delta\delta_{tra} \approx 2.10^{-6}$

I) Transit

Spectroscopy

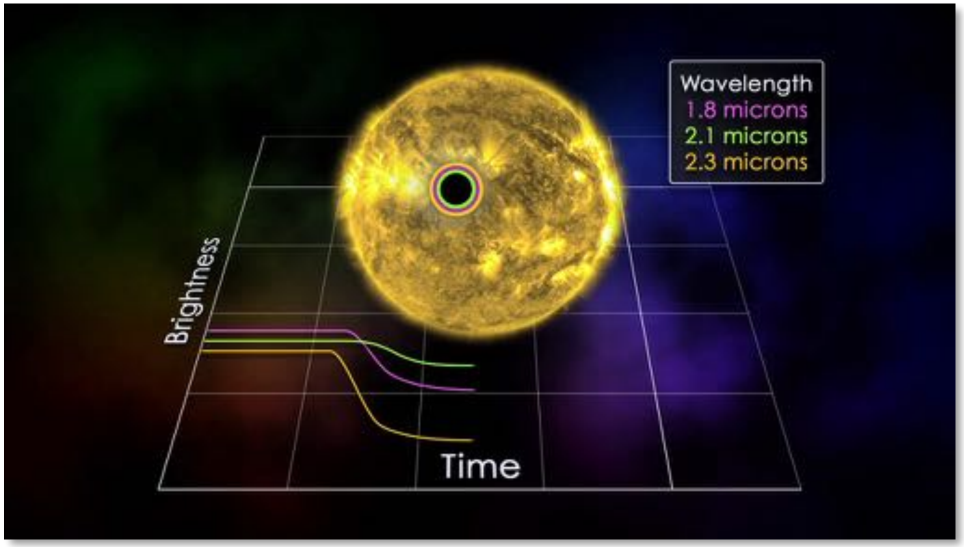

Effect of mean molecular weight

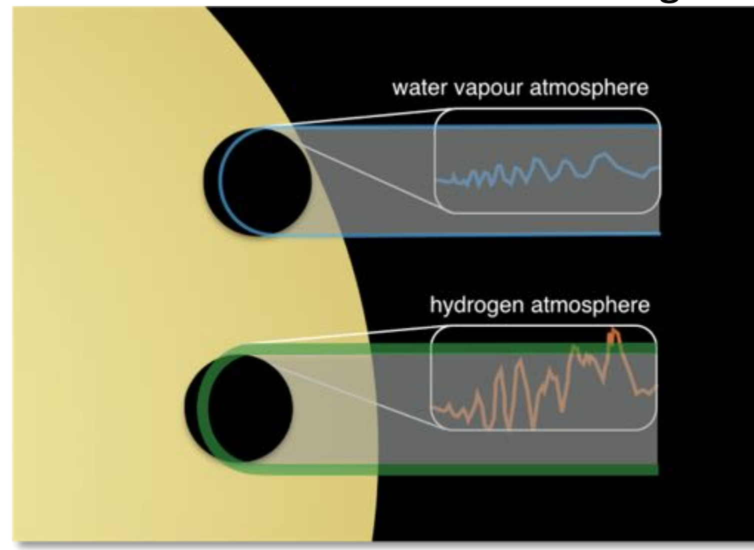

<u>Variation of transit depth:</u>

$$\Delta\boldsymbol{\delta_{tra}} = \frac{\pi(R_p+N_H H)^2}{\pi {R_\star}^2} - \frac{\pi {R_p}^2}{\pi {R_\star}^2} \approx 2N_H\delta_{tra}\left(\frac{H}{R_p}\right)$$

Scale height: $\boldsymbol{H} = \frac{RT}{Mg}$; Number of scale heights: $\boldsymbol{N_H \approx 7}$ (for low resolution)

<u>For Trappist-1 (0.015 R_S):</u>

- Hot Jupiter (T=1300 K, g=25 m s^{-2}, M=2.3 g/mol): $\delta_{tra} \approx 0.7$, $\Delta\delta_{tra} \approx 2.10^{-2}$
- Earth-like planet (T=280 K, g=10 m s^{-2}, M=28g/mol): $\delta_{tra} \approx 6.10^{-3}$, $\Delta\delta_{tra} \approx 10^{-4}$

I) Transit

Spectroscopy

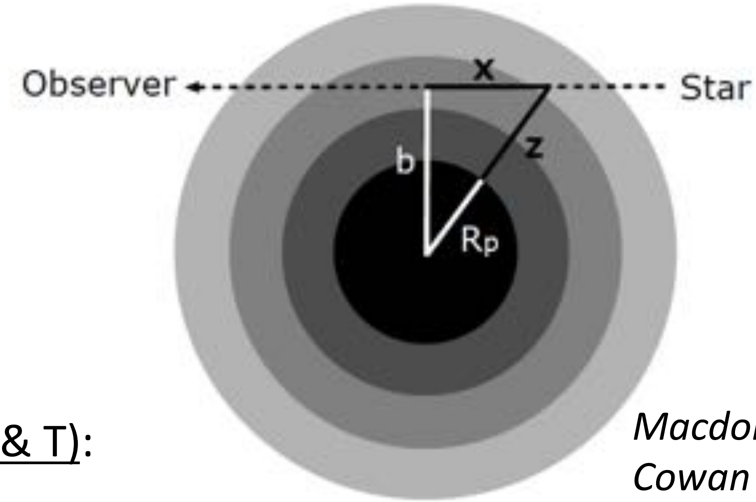

Macdonald & Cowan (2019)

<u>Assumptions: hydrostatic+isothermal</u>

$$p(z) = p(z_0)\exp\left(-\frac{z-z_0}{H}\right) \text{ with } H = \frac{RT}{Mg}$$

<u>Optical depth (cross-section independent of P & T)</u>:

$$\tau(b,\lambda) = \sum_i \int_{-\infty}^{+\infty} \sigma_i(\lambda) n_i(x) dx$$

$$n_i(x) = n_{i0} e^{-z/H} \; with \; z = \sqrt{b^2 + x^2} - R_p \approx b - Rp + \frac{x^2}{2b}$$

$$\tau(b,\lambda) \approx \sum_i \sigma_i(\lambda) n_{i0} e^{-(b-Rp)/H} \int_{-\infty}^{+\infty} e^{-x^2/2RpH} dx = \sum_i \sigma_i(\lambda) n_{i0} e^{-(b-Rp)/H} \sqrt{2\pi b H}$$

<u>Comparison with vertical optical depth:</u>

$$\eta = \frac{\tau_H}{\tau_V} = \sqrt{\frac{2\pi Rp}{H}}$$

Earth: $\eta \sim 75$
Jupiter: $\eta \sim 128$
HD209458b: $\eta \sim 38$

I) Transit

Spectroscopy

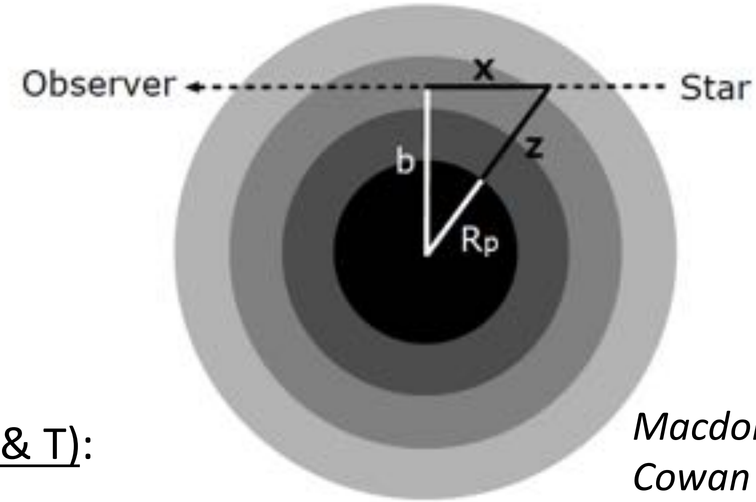

Macdonald & Cowan (2019)

Assumptions: hydrostatic+isothermal

$$p(z) = p(z_0)\exp\left(-\frac{z-z_0}{H}\right) \text{ with } H = \frac{RT}{Mg}$$

Optical depth (cross-section independent of P & T):

$$\tau(b,\lambda) = \sum_i \sigma_i(\lambda) n_{i0} e^{-(b-Rp)/H}\sqrt{2\pi b H}$$

Transit depth:

$$D(\lambda) = \left(\frac{R_p}{R_\star}\right)^2 + \frac{2}{{R_\star}^2}\int_{R_p}^{R_\star} b\left(1-e^{-\tau(b,\lambda)}\right)db = \left(\frac{R_p+h_\lambda}{R_\star}\right)^2$$

Equivalent altitude:

$$h_\lambda = -Rp + \sqrt{{R_p}^2 + 2\int_{R_p}^{R_\star} b(1-e^{-\tau(b,\lambda)})db} \approx 0.577H + H ln\left(\sqrt{2\pi H Rp}\sum_i \sigma_i(\lambda) n_{i0}\right)$$

$$\boldsymbol{h_\lambda \approx b(\tau = 0.56) - Rp}$$

see *De Wit & Seager* (2013) and *Macdonald & Cowan* (2019)

I) Transit

Spectroscopy

Synthetic Earth's transit spectrum

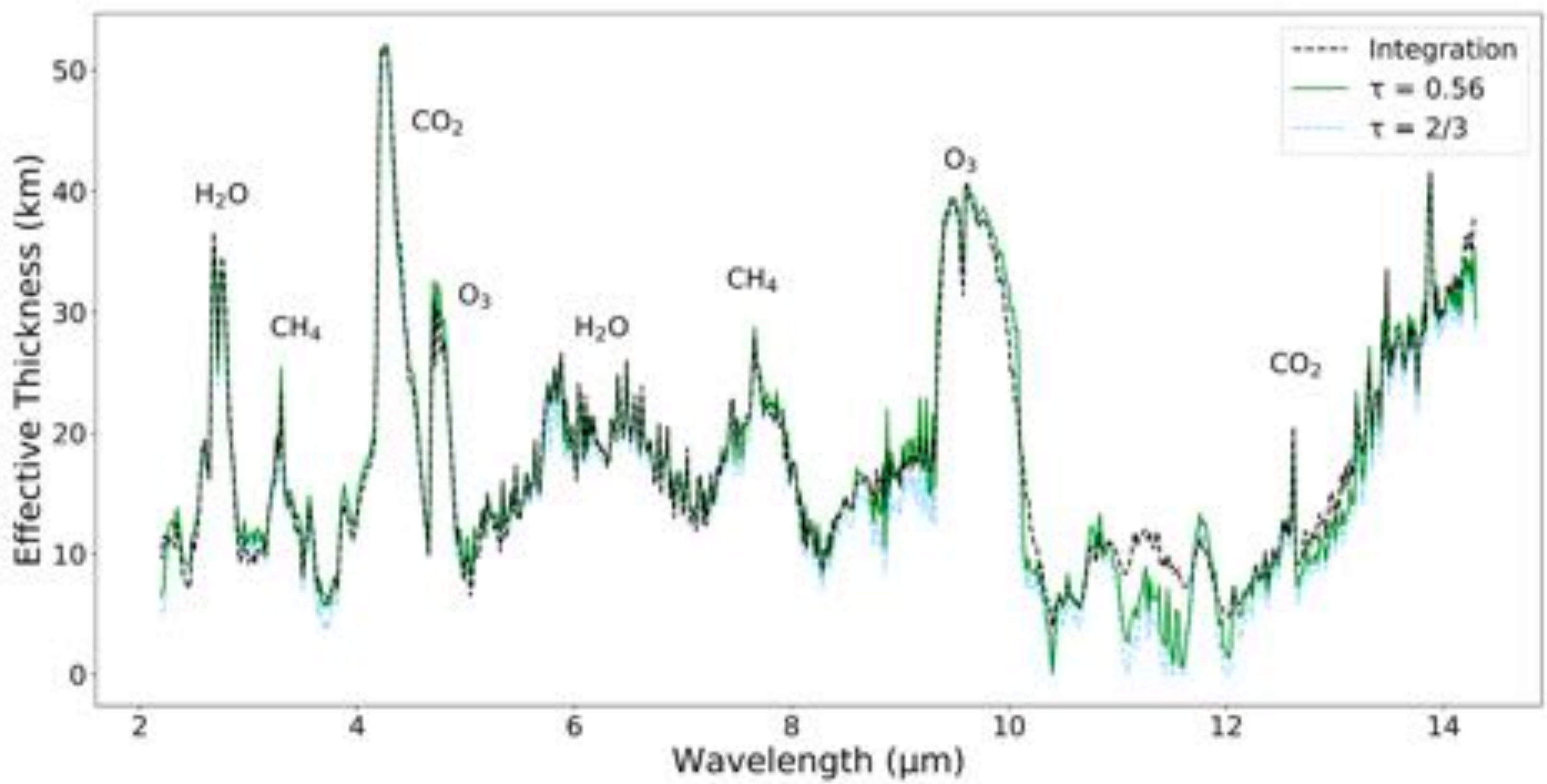

Macdonald & Cowan (2019)

I) Transit

Phase curves

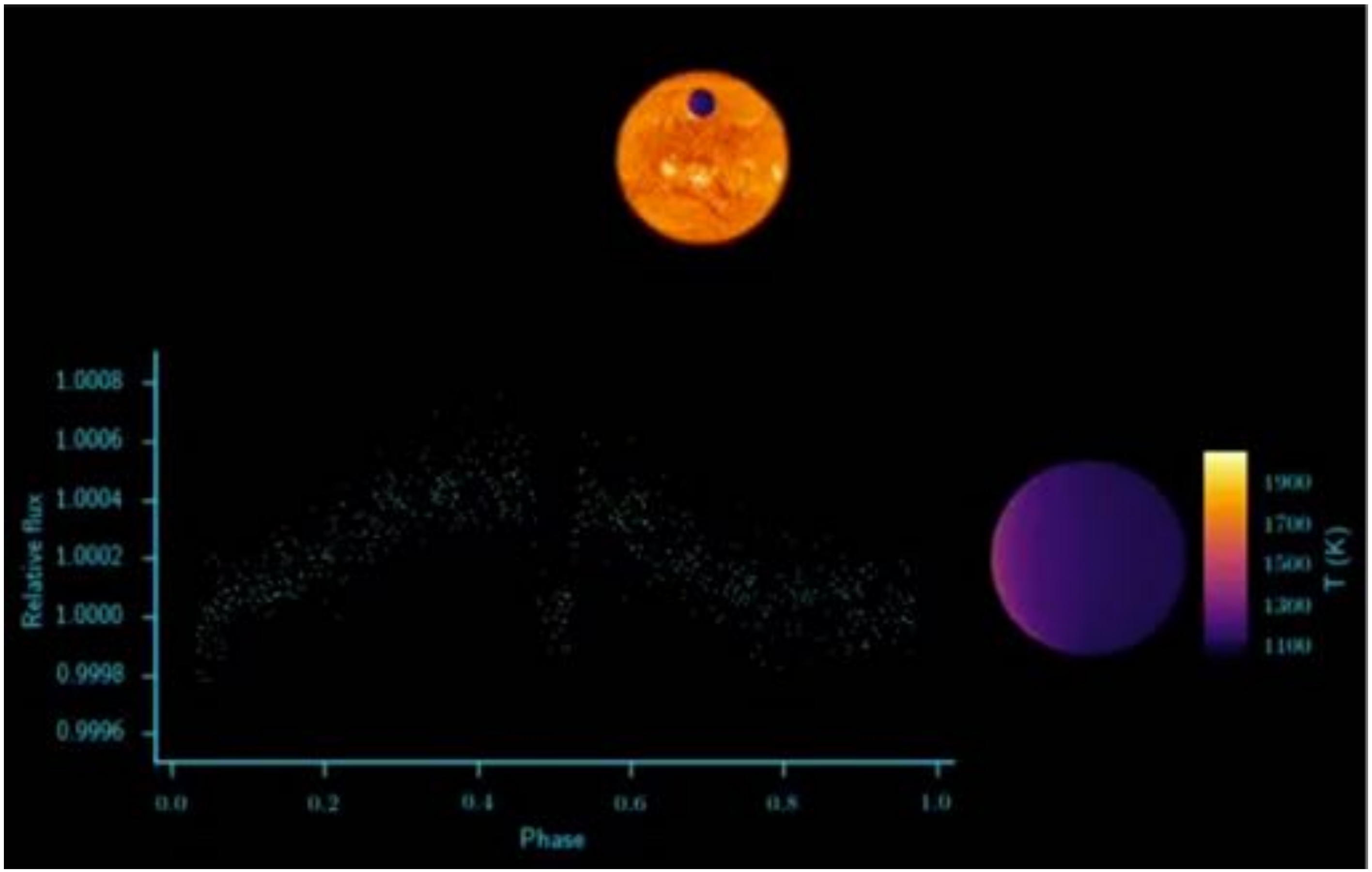

Courtesy Tom Louden

I) Transit

Phase curves

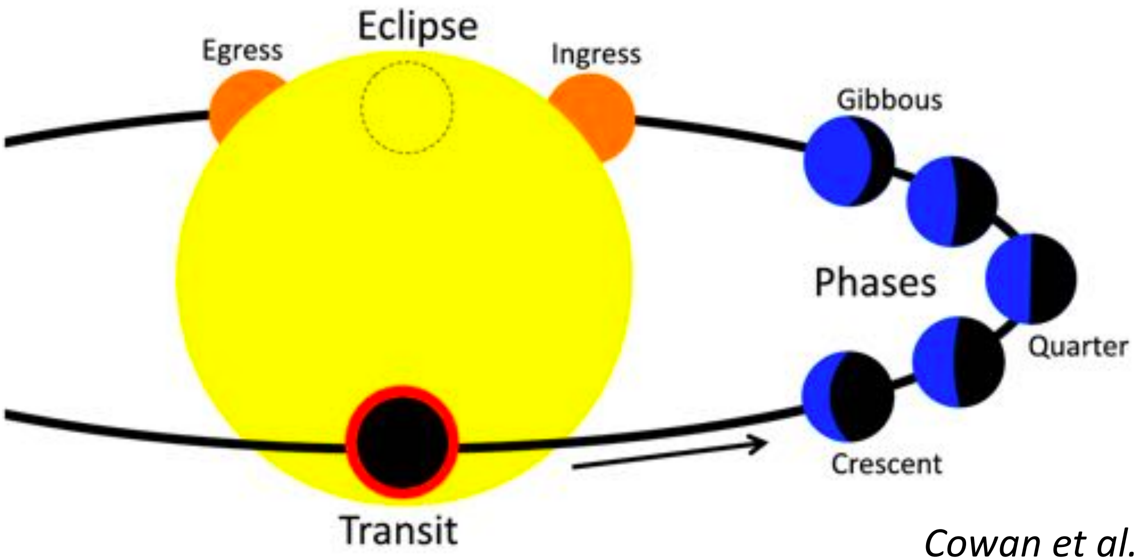

Cowan et al. (2014)

Photometric phase curve (ex: Spitzer)

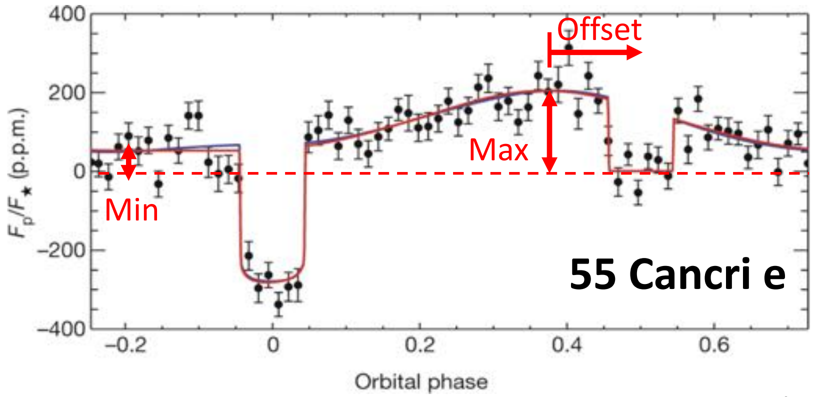

Demory et al. (2016)

Spectrally resolved phase curve (ex: HST)

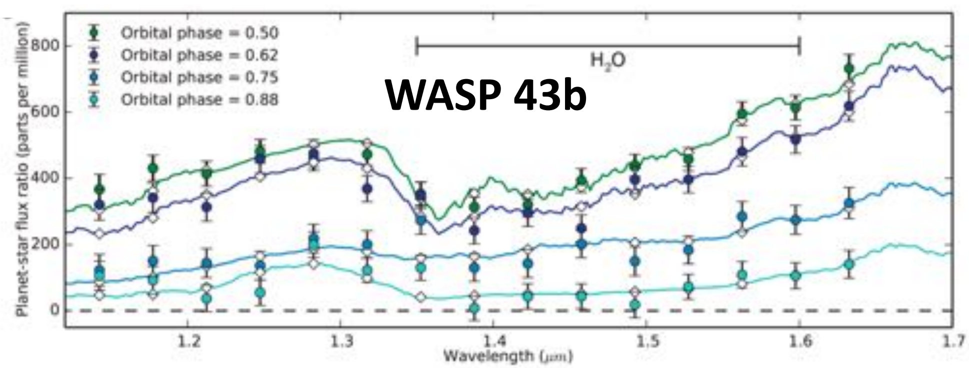

Stevenson et al. (2014)

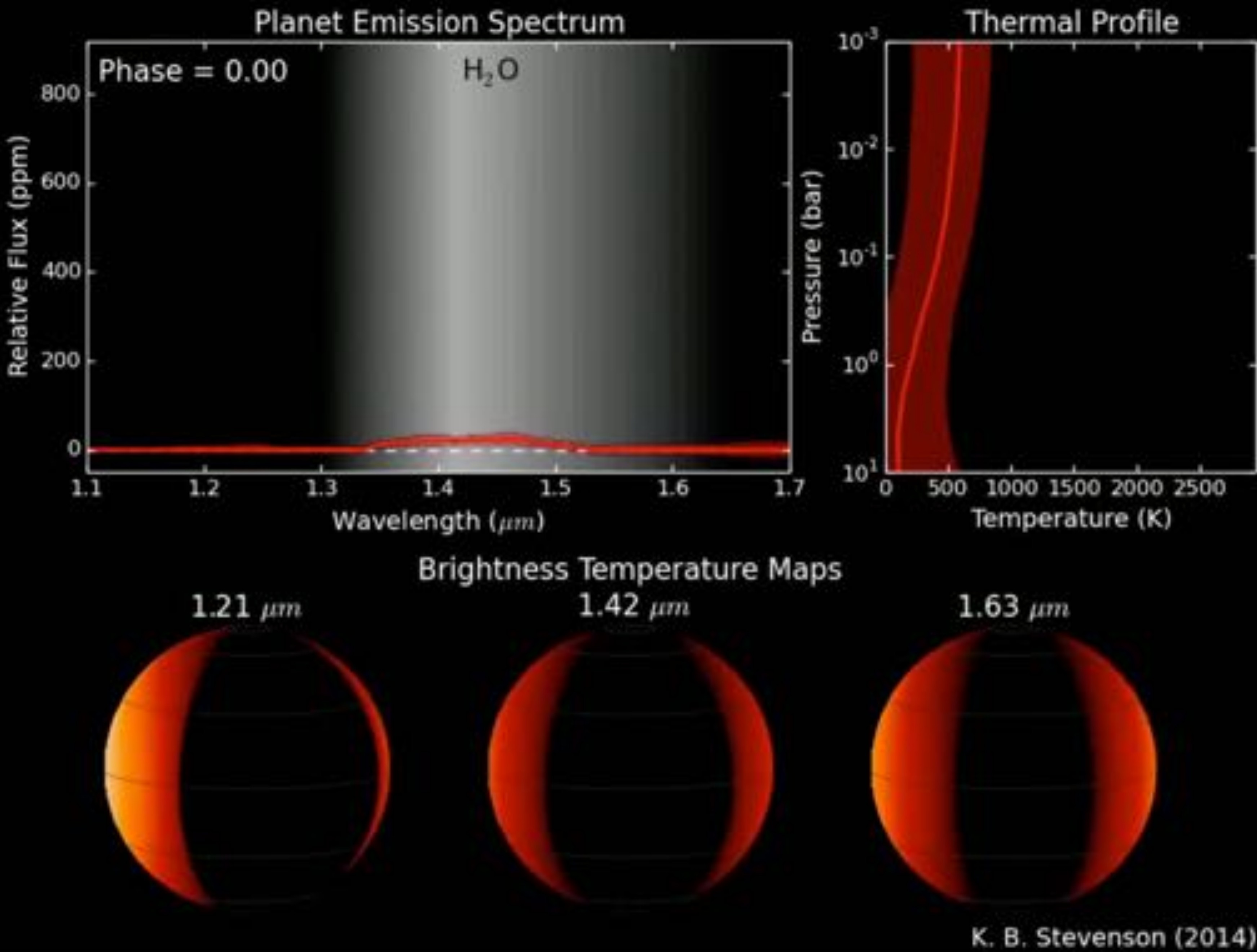
Planet Emission Spectrum
Phase = 0.00
H_2O
Relative Flux (ppm)
800
600
400
200
0
1.1
1.2
1.3
1.4
1.5
1.6
1.7
Wavelength (μm)
Thermal Profile
Pressure (bar)
10^{-3}
10^{-2}
10^{-1}
10^{0}
10^{1}
0
500
1000
1500
2000
2500
Temperature (K)
Brightness Temperature Maps
1.21 μm
1.42 μm
1.63 μm
K. B. Stevenson (2014)

I) Transit

Open-access codes for lightcurve fitting

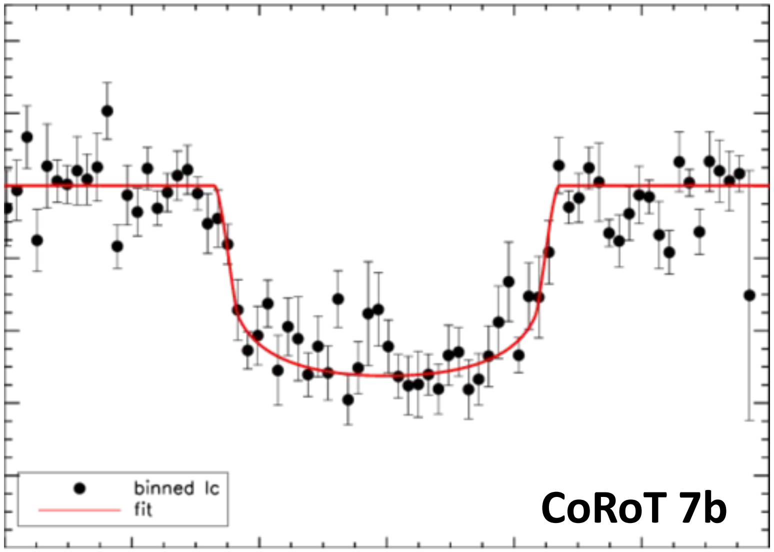

For transits:
Transit routines (IDL, FORTRAN): https://faculty.washington.edu/agol/transit.html
batman (Python): https://www.cfa.harvard.edu/~lkreidberg/code.html
STARRY (Python): https://github.com/rodluger/starry
ExoCTK (Python): https://exoctk.stsci.edu/lightcurve_fitting

For secondary eclipses & phase curves:
STARRY (Python): https://github.com/rodluger/starry
spiderman (Python): https://www.cfa.harvard.edu/~lkreidberg/code.html#spiderman

II) Direct imaging

Limitations

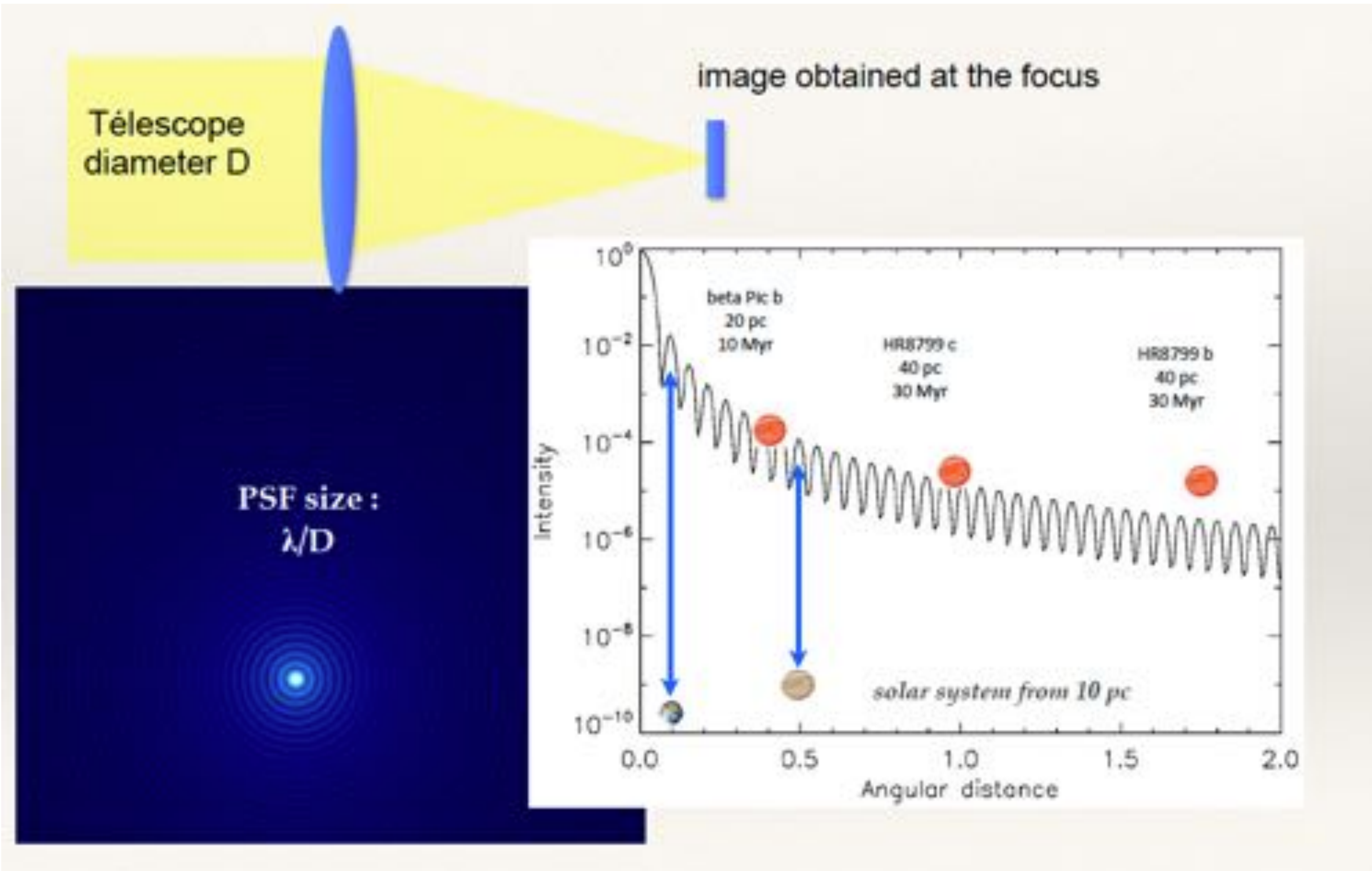

II) Direct imaging

Ingredients to overcome limitations

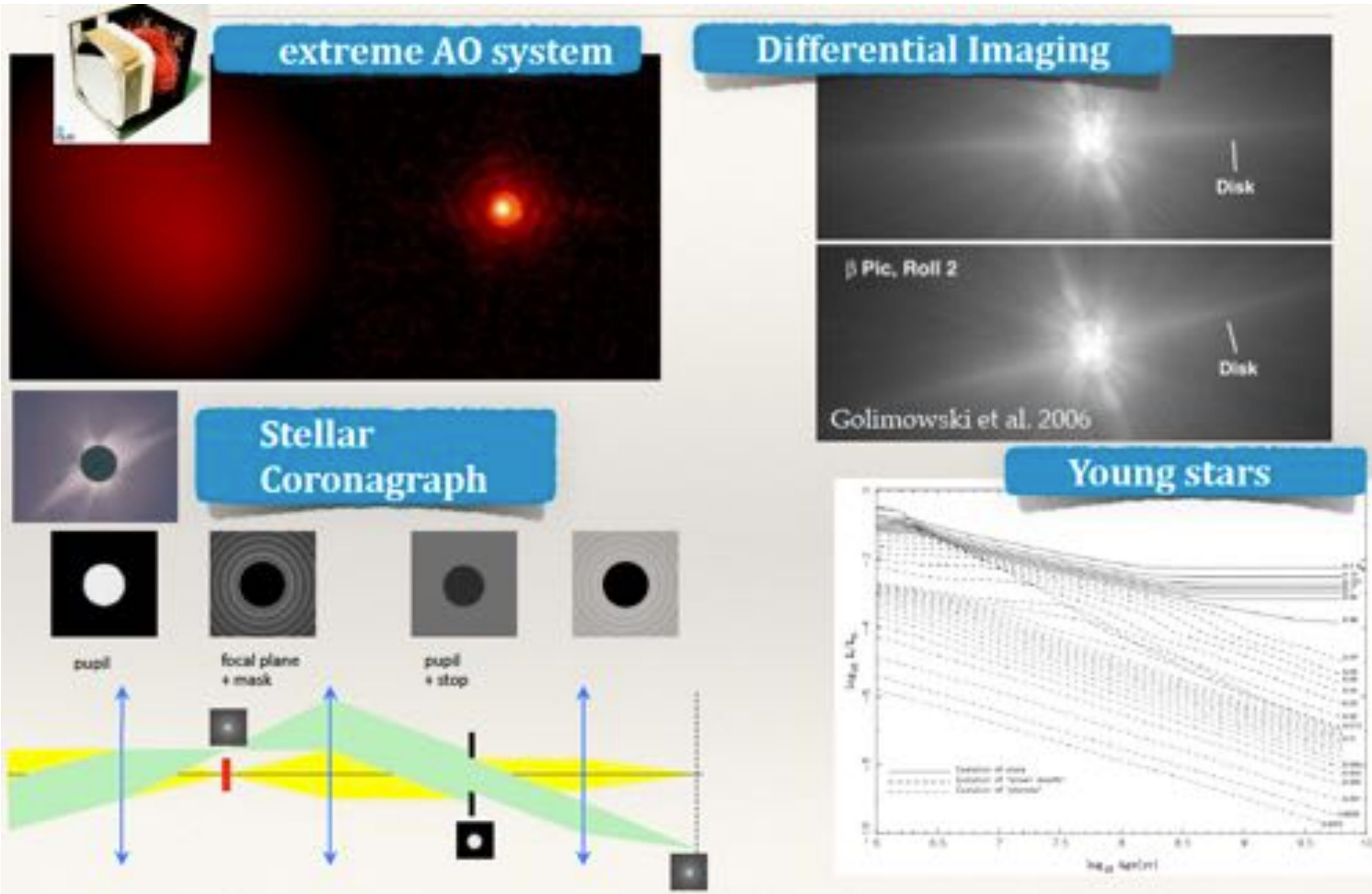

III) Medium/high spectral resolution

- **Low resolution:** $R = \frac{\lambda}{\Delta\lambda} < 1000$ (e.g. HST, ARIEL)

→ absorption bands

- **Medium resolution:** $R = \frac{\lambda}{\Delta\lambda} \sim 1000 - 10000$ (e.g. JWST, VLT/SINFONI)

→ strong molecular lines

- **High resolution:** $R = \frac{\lambda}{\Delta\lambda} > 10000$ (e.g. VLT/CRIRES, VLT/ESPRESSO)

→ resolve line shape and doppler shift

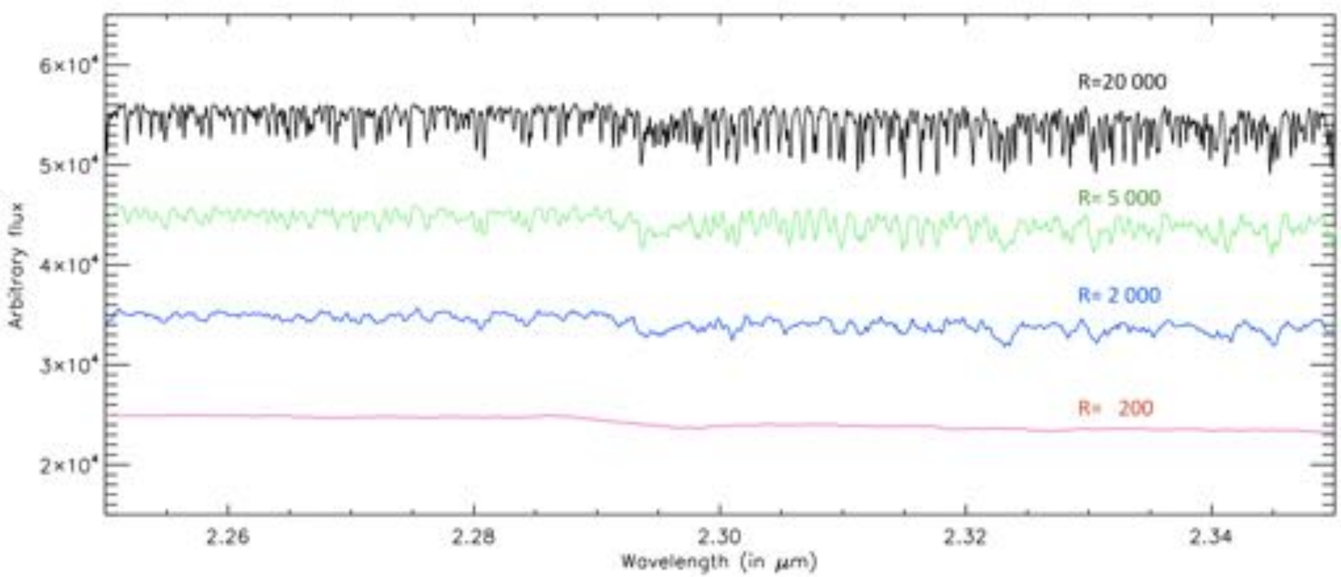

III) Medium/high spectral resolution

Medium resolution for direct imaging

- Distinguish planetary signal from stellar noise (speckles) thanks to intrinsic molecular lines
- Cross-correlation between the high-passing observed spectrum S_{obs} and a model spectrum S_{th}

$$CCF(V_0) = \int S_{obs}(\nu)\times Sth(\nu + \nu\times V_0/c)d\nu$$

with normalization: $\int S^2(\nu)d\nu = 1$

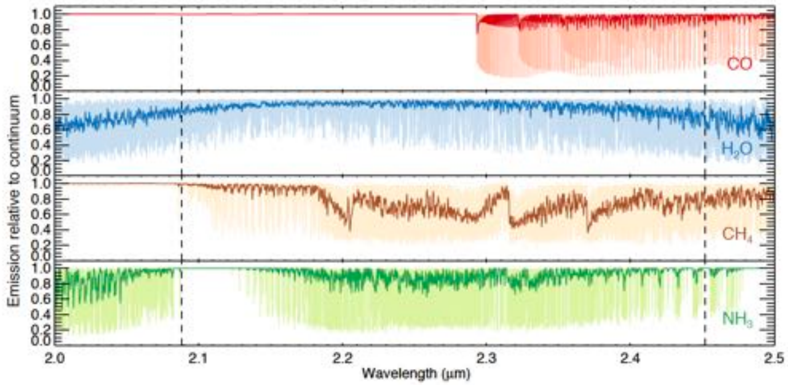

Wavelength-averaged image of beta Pic b with VLT-SINFONI

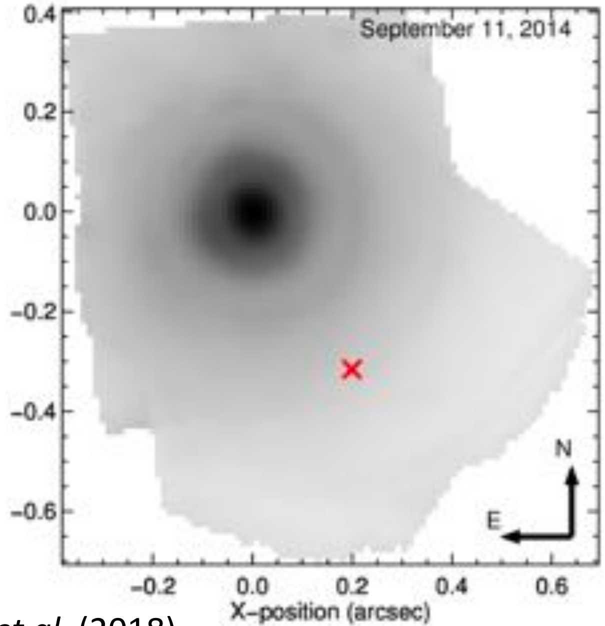

Hoeijmakers et al. (2018)

III) Medium/high spectral resolution

Medium resolution for direct imaging

- Distinguish planetary signal from stellar noise (speckles) thanks to intrinsic molecular lines
- Cross-correlation between the high-passing observed spectrum S_{obs} and a model spectrum S_{th}

$$\boldsymbol{CCF(V_0) = \int S_{obs}(\nu)\times Sth(\nu+\nu\times V_0/c)d\nu}$$

with normalization: $\int \boldsymbol{S^2(\nu)d\nu = 1}$

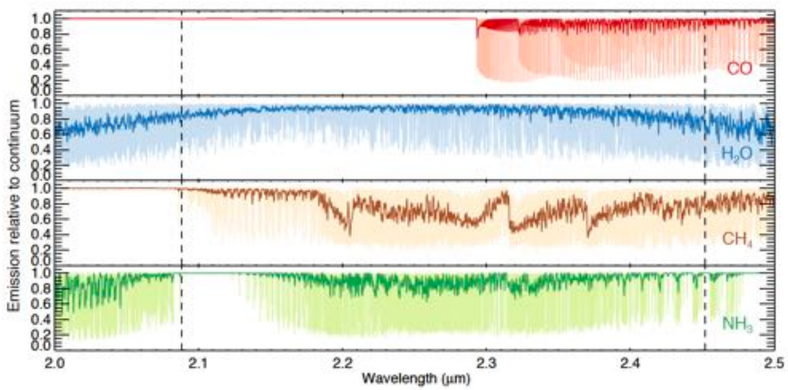

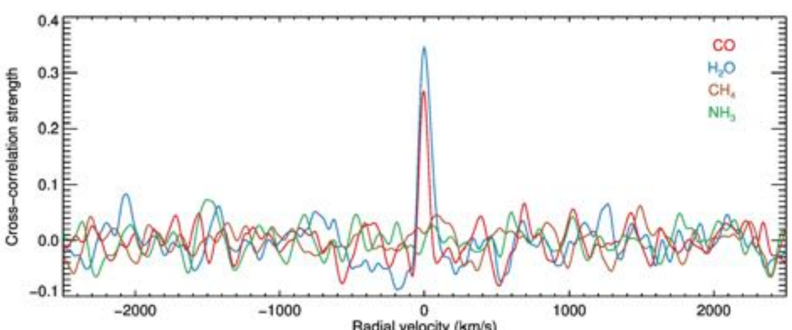

Molecular mapping of beta Pic b

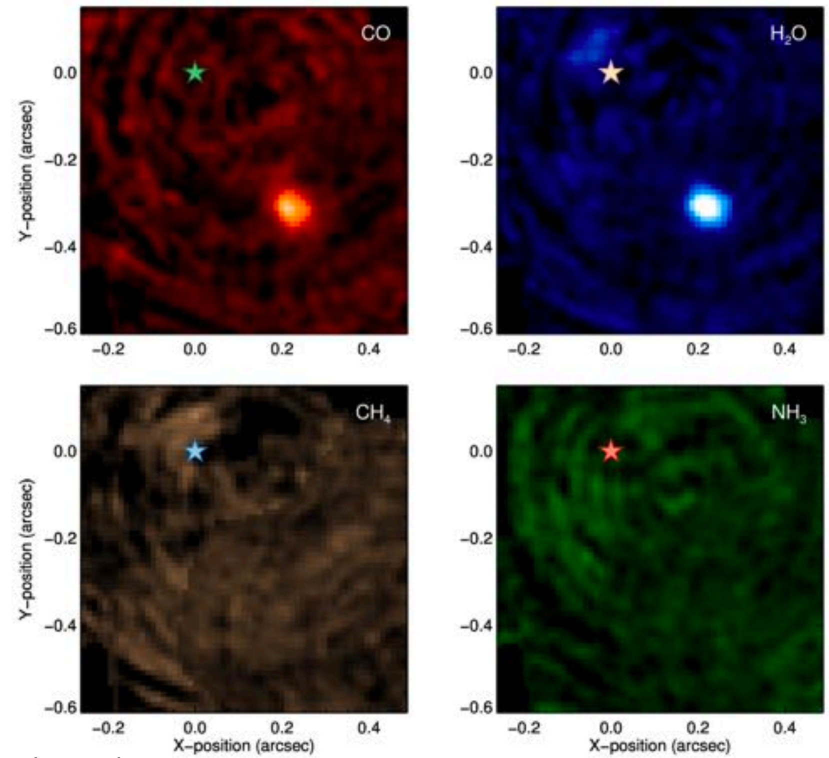

Hoeijmakers et al. (2018)

III) Medium/high spectral resolution

High resolution for transit spectroscopy

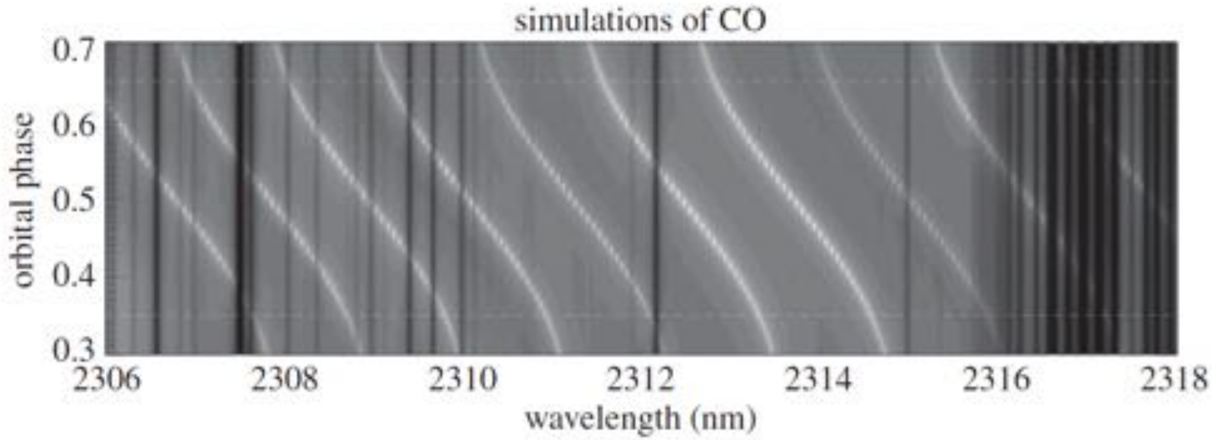

Snellen (2014)

Observation of HD209458 b

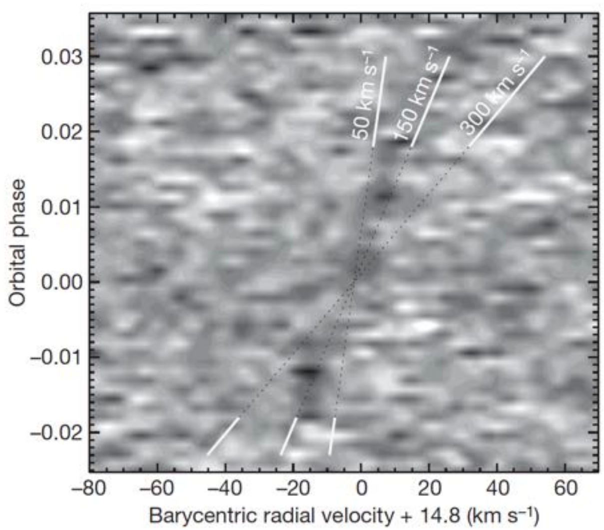

Snellen et al. (2010)

Observation of tau Böotis b

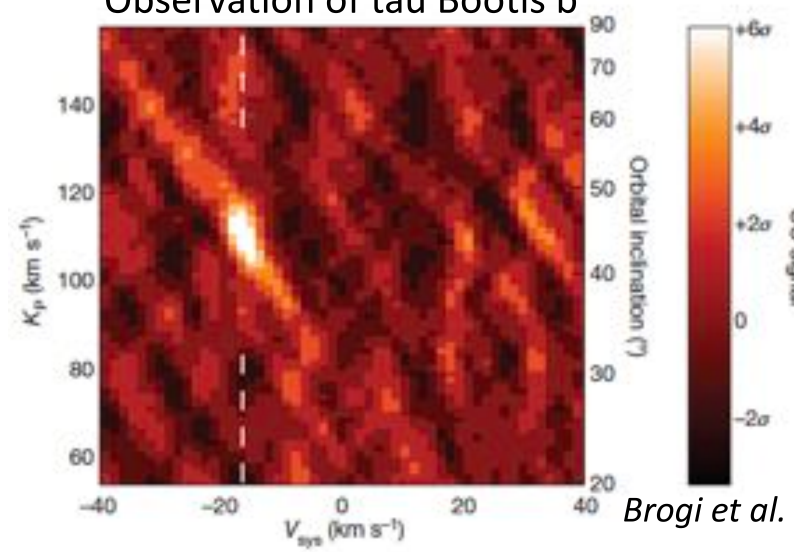

Brogi et al. (2012)

- Detection of CO during transit
- Doppler shift by orbital velocity
- Doppler shift by day-night winds

- Detection of CO in emission
- Stratospheric thermal inversion

Lessons from observations of exoplanet atmospheres

- **Radius & Interior**
  - Hot Jupiters are inflated
  - Gap in the occurrence rate between super-Earths and mini-Neptunes

- **Dynamics & Thermal structure**
  - Superrotation for strongly irradiated planets
  - Stratospheric thermal inversion for the hottest planets

- **Clouds/haze**
  - Most of exoplanets are cloudy/hazy
  - Inhomogeneous clouds distribution

- **Atmospheric composition**
  - Chemical disequilibrium (ex: CO/CH4)
  - Low-mass planets seem to have high-mean molecular weight

- **Atmospheric escape**
  - Atmospheric escape for strongly irradiated planets

IV) Lessons from observations

Inflated hot Jupiters

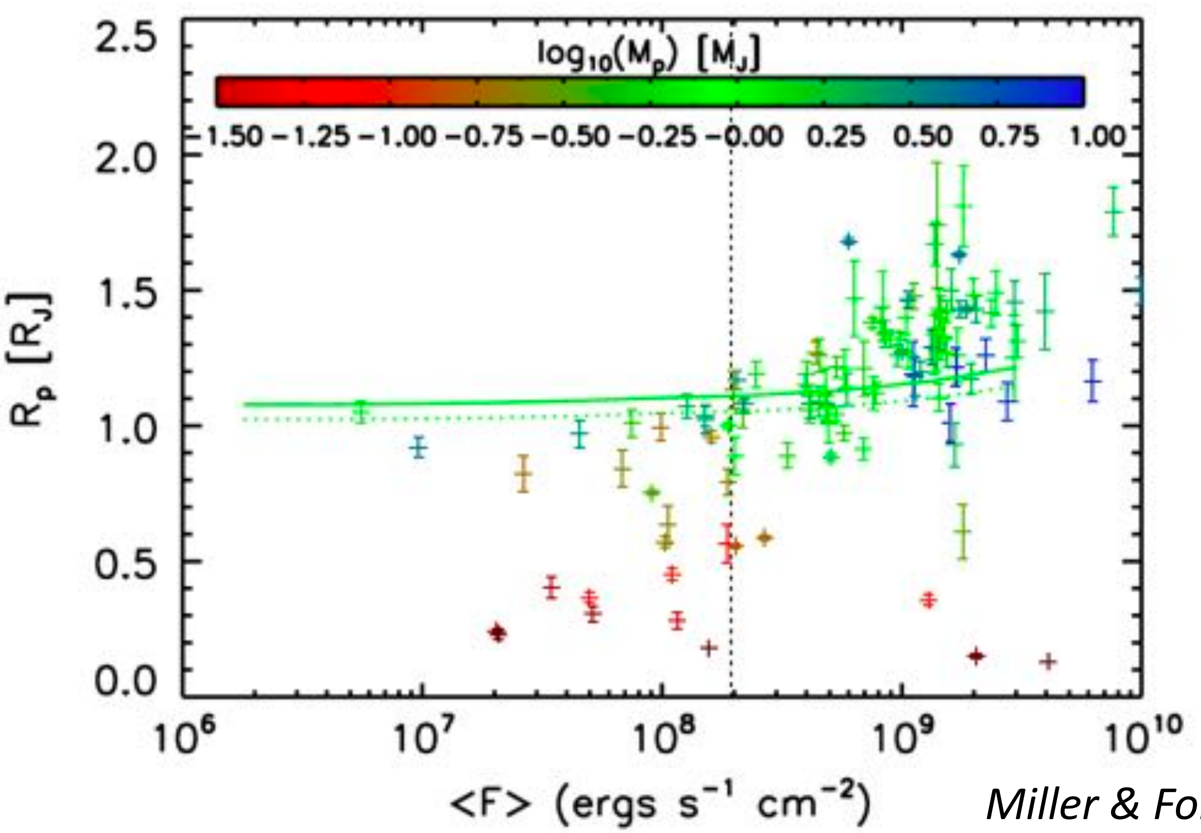

Miller & Fortney (2011)

- **Hot Jupiters are inflated compared to 1D models**
- **Correlation between inflated radii and stellar flux**

IV) Lessons from observations

Inflated hot Jupiters

Explanations for inflated hot Jupiters:

Heat transfer to the adiabatic layer
(10^{-4}% - 1% of the irradiation)

1) Ohmic dissipation

Batygin & Stevenson (2010)

Superrotation + magnetic field + ionization of
H and alkali metals in hot Jupiters → **Induced currents**

Heat production: $P = \frac{J^2}{\sigma}$

Induced currents due to zonal wind flow

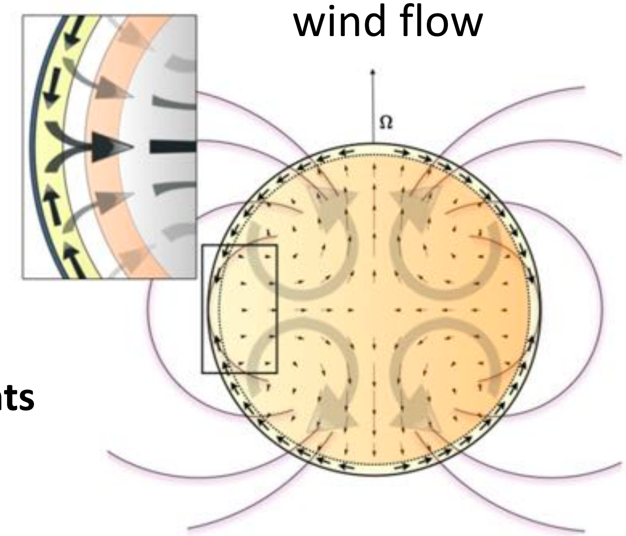

2) Advection of heat from global circulation

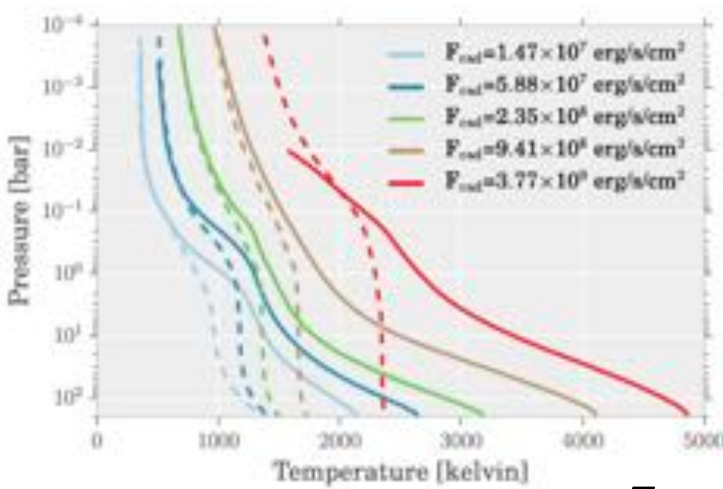

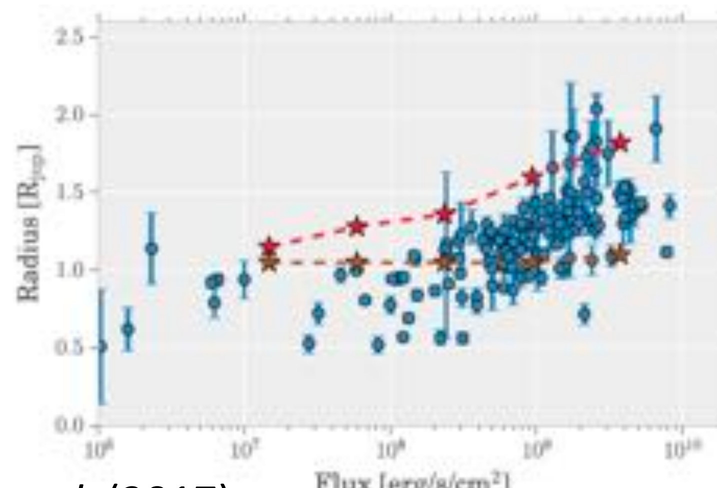

Tremblin et al. (2017)

IV) Lessons from observations

A valley between super-Earths and mini-Neptunes

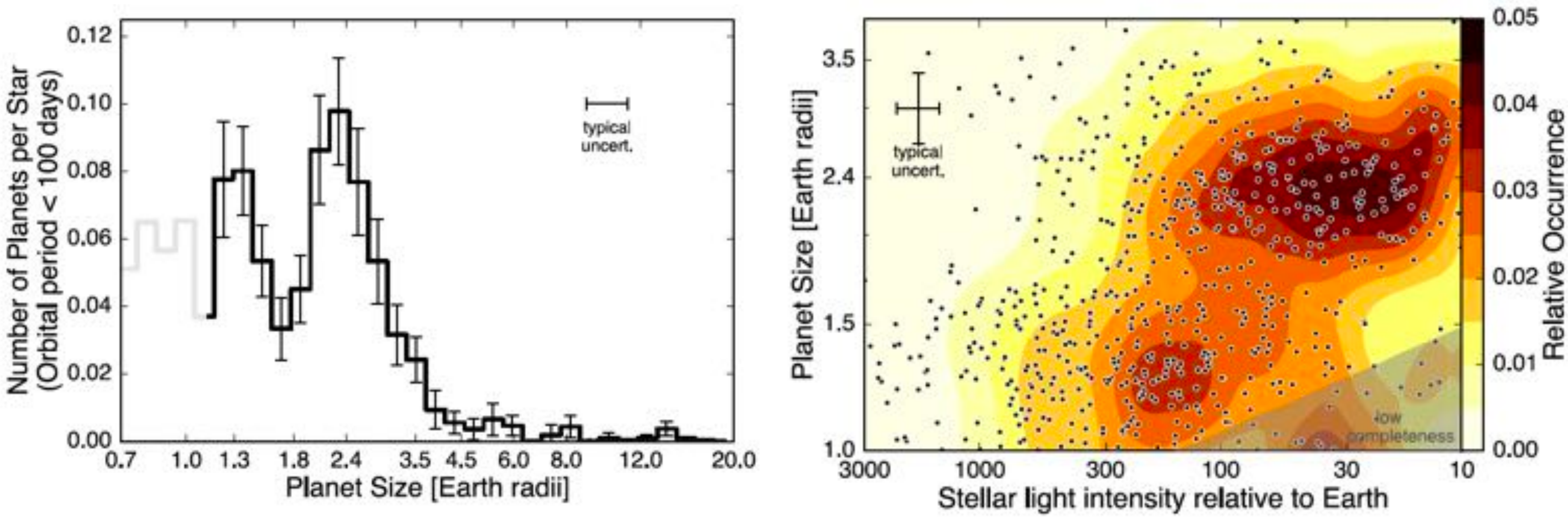

Fulton et al. (2018)

- **Bimodal distribution with a gap at around 1.8 R_E**
- **Transition from mini-Neptunes to super-Earths with increasing instellation**
  - **→ Photoevaporation**

IV) Lessons from observations

A valley between super-Earths and mini-Neptunes

Prediction of a photo-evaporation valley

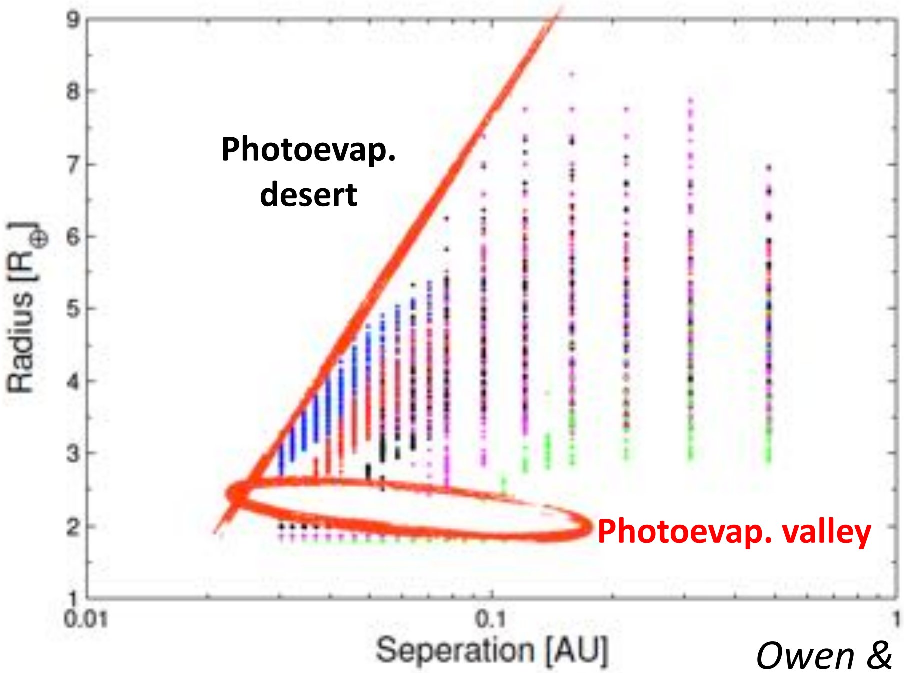

Owen & Wu (2017)

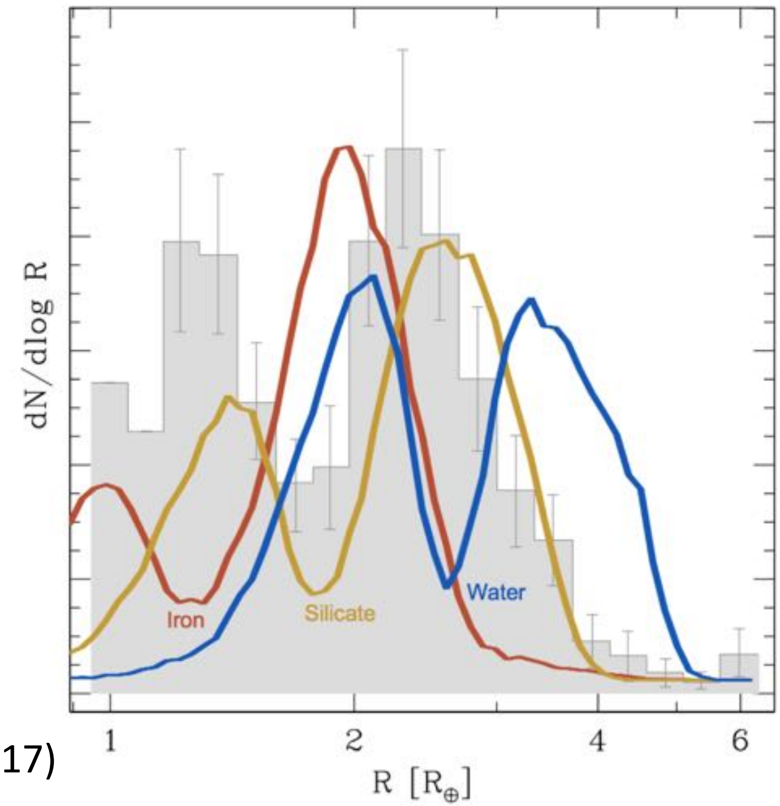

Photoevaporation can predict the 2 peaks. The location of the valley is very sensitive to the core composition —> **cores seem to be Earth-like in composition.**

(Owen & Wu 2017; Jin & Mordasini 2017)

If correct:
No water → formation inside the ice line

Lessons from observations of exoplanet atmospheres

- **Radius & Interior**
  - Hot Jupiters are inflated
  - Gap in the occurrence rate between super-Earths and mini-Neptunes

- **Dynamics & Thermal structure**
  - Superrotation for strongly irradiated planets
  - Stratospheric thermal inversion for the hottest planets

- **Clouds/haze**
  - Most of exoplanets are cloudy/hazy
  - Inhomogeneous clouds distribution

- **Atmospheric composition**
  - Chemical disequilibrium (ex: CO/CH4)
  - Low-mass planets seem to have high-mean molecular weight

- **Atmospheric escape**
  - Atmospheric escape for strongly irradiated planets

IV) Lessons from observations

Superrotation for strongly irradiated planets

Zonal-mean zonal winds for HD189733b

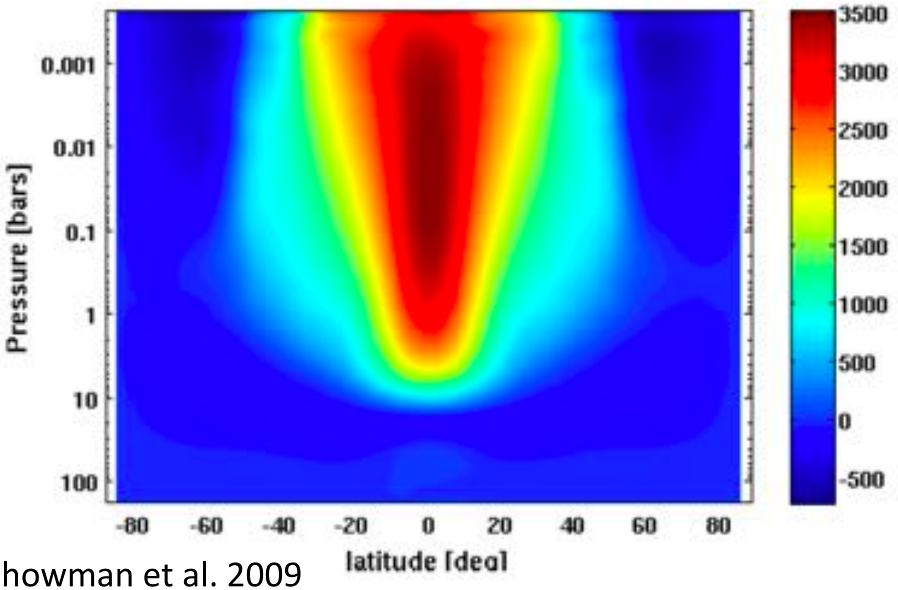

Showman et al. 2009

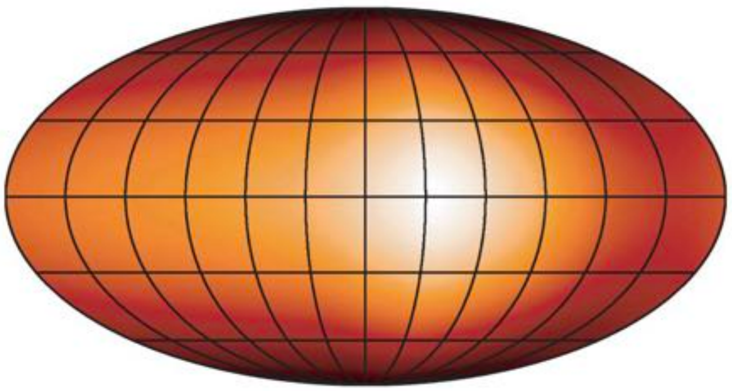

Thermal phase curve and temperature map of HD189733b (Knutson et al. 2007)

- **Presence of an eastward super-rotating equatorial jet**
- **Maximum of temperature shifted east to the substellar point**

Phase offset due to competition between the radiative cooling and the speed of the equatorial jet.

$$\tau_{rad} = \frac{c_p P}{g \sigma T^3}$$

$$\tau_{adv} = \frac{2\pi R}{U}$$

IV) Lessons from observations

Stratospheric thermal inversion for hot planets

Model predictions

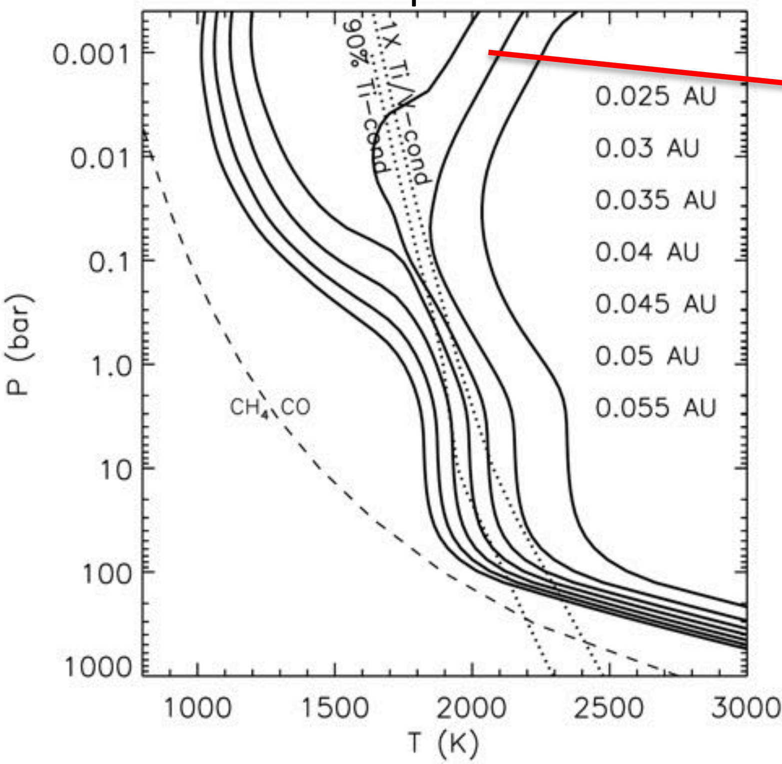

Total molecular opacity (1mbar)

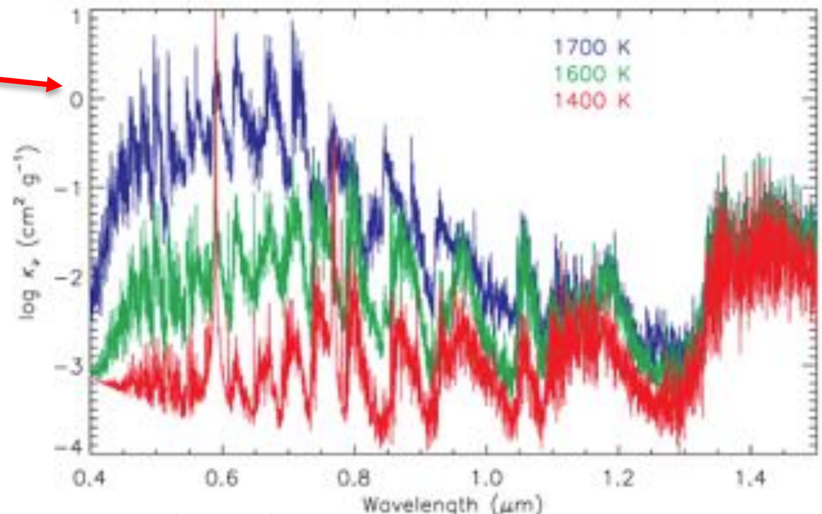

Fortney et al. (2008)

Predictions: Stratospheric thermal inversion due TiO and VO opacity in visible

Observations: fewer planets (ultra-hot) show stratospheric thermal inversion than expected

Possible explanations:

- Cold trapping of TiO/VO on the nightside ?
- High C/O ?
- Photodissociation of TiO/VO by high stellar activity ?

Lessons from observations of exoplanet atmospheres

- **Radius & Interior**
  - Hot Jupiters are inflated
  - Gap in the occurrence rate between super-Earths and mini-Neptunes

- **Dynamics & Thermal structure**
  - Superrotation for strongly irradiated planets
  - Stratospheric thermal inversion for the hottest planets

- **Clouds/haze**
  - Most of exoplanets are cloudy/hazy
  - Inhomogeneous clouds distribution

- **Atmospheric composition**
  - Chemical disequilibrium (ex: CO/CH4)
  - Low-mass planets seem to have high-mean molecular weight

- **Atmospheric escape**
  - Atmospheric escape for strongly irradiated planets

IV) Lessons from observations

Most of exoplanets are cloudy/hazy

A continuum from cloudy to cloud-free planets

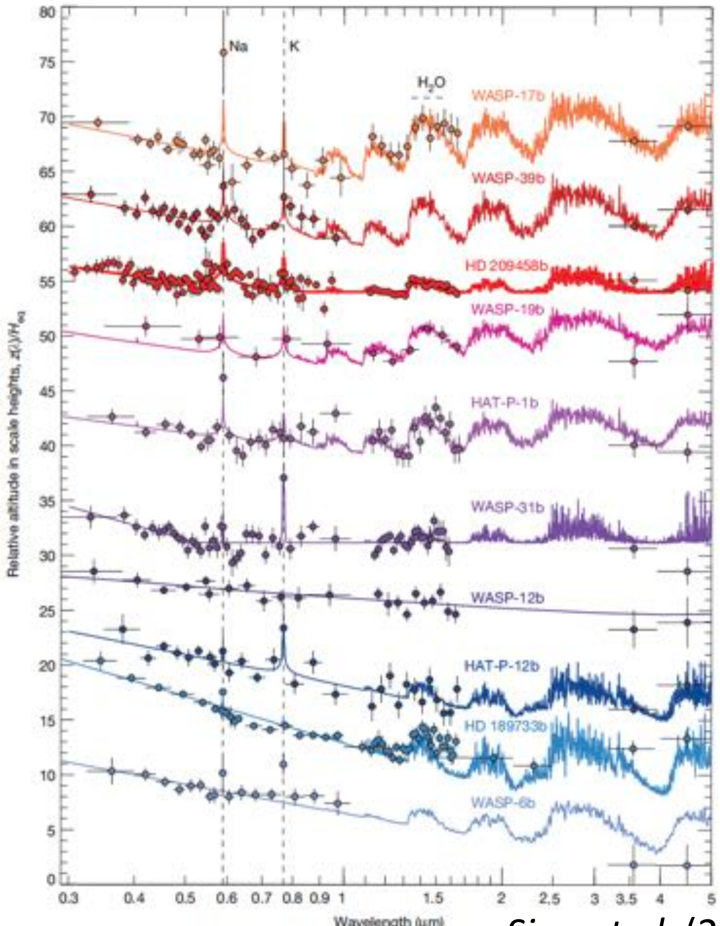

Sing et al. (2015)

→ Flat transit spectrum
→ Mie-scattering slope

Condensate clouds
(thermodynamic phase change)

Haze
(non-equilibrium chemistry)

IV) Lessons from observations

Most of exoplanets are cloudy/hazy

Clouds are everywhere

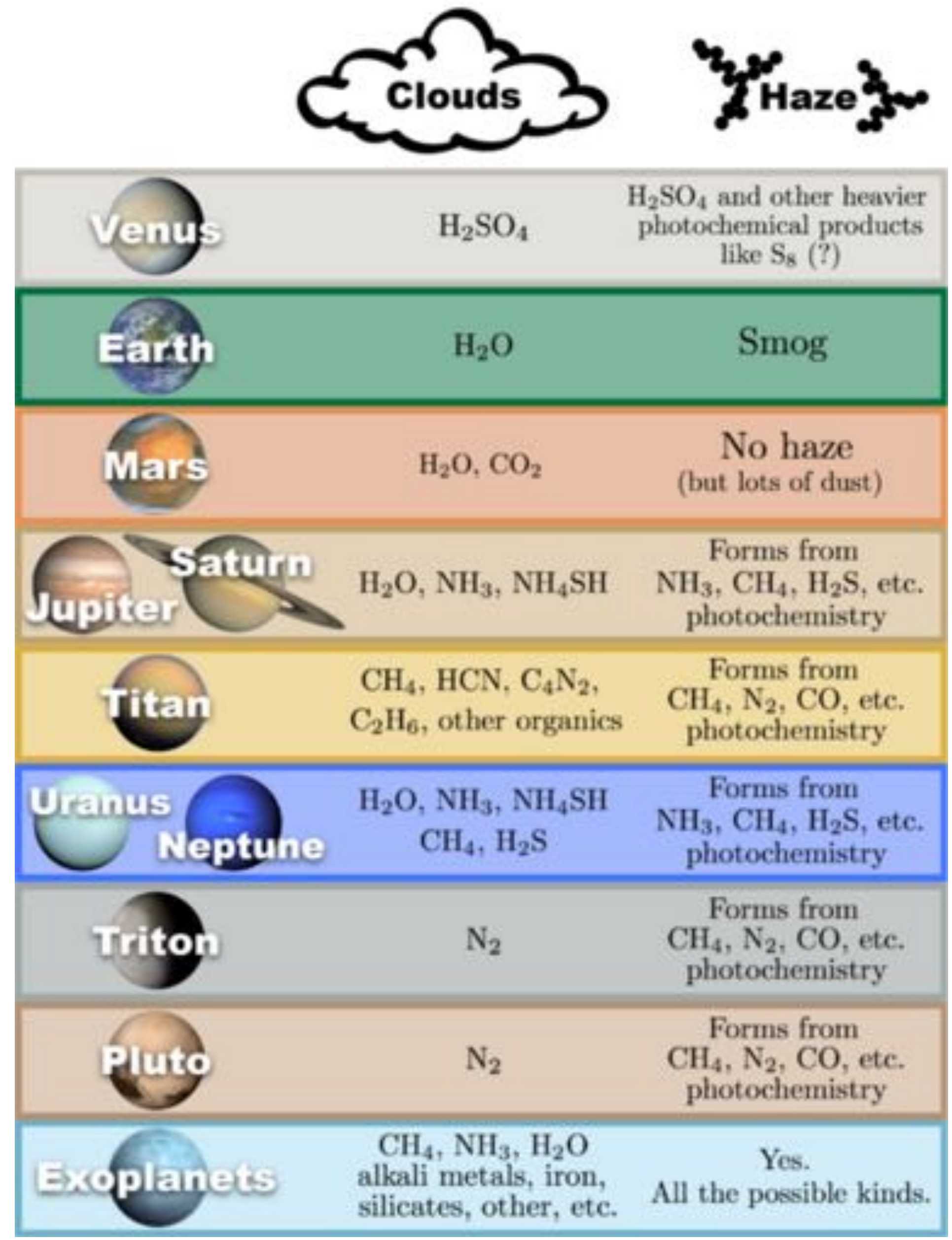

Figure from Sarah Hörst

IV) Lessons from observations

Inhomogeneous cloud distribution

Albedo map

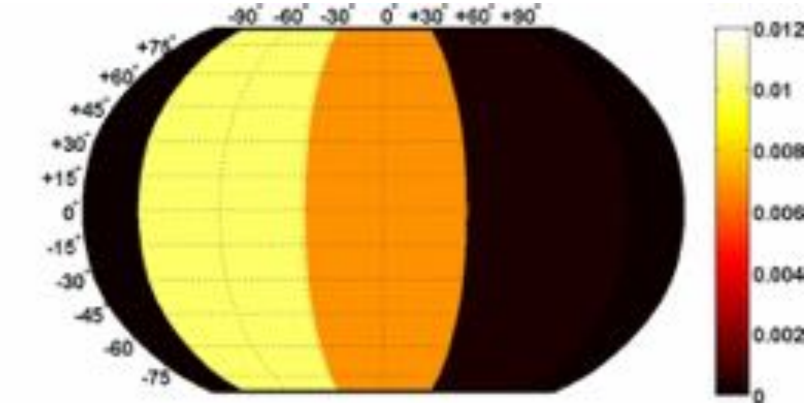

Demory et al. (2013)

→ Evaporation at hot spot
(*Demory et al.* 2013, *Parmentier et al.* 2016)

→ Probably thick clouds on nightside
(*Keating et al.* 2019)

Cloud mapping of brown dwarf

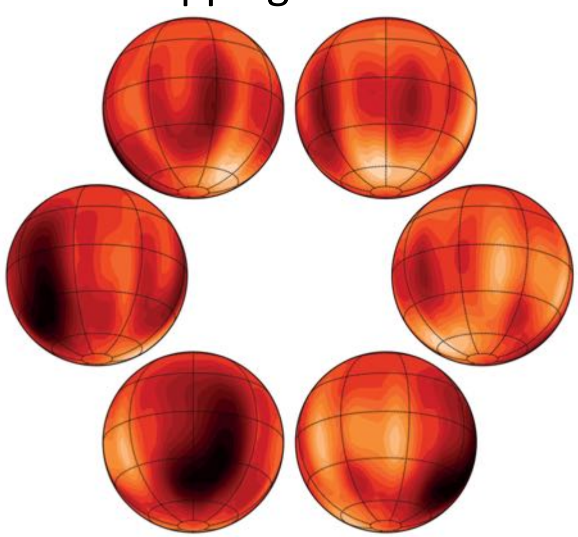

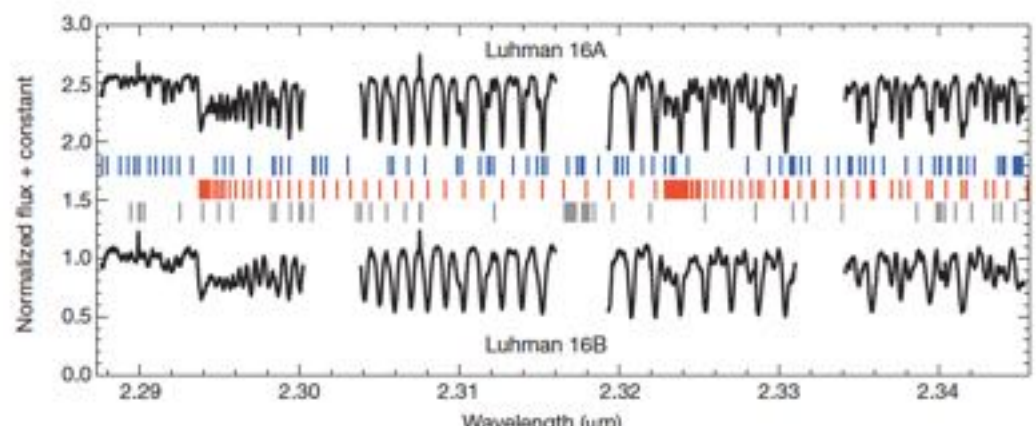

Crossfield et al. (2014)

Lessons from observations of exoplanet atmospheres

- **Radius & Interior**
  - Hot Jupiters are inflated
  - Gap in the occurrence rate between super-Earths and mini-Neptunes

- **Dynamics & Thermal structure**
  - Superrotation for strongly irradiated planets
  - Stratospheric thermal inversion for the hottest planets

- **Clouds/haze**
  - Most of exoplanets are cloudy/hazy
  - Inhomogeneous clouds distribution

- **Atmospheric composition**
  - Chemical disequilibrium (ex: $CO/CH4$)
  - Low-mass planets seem to have high-mean molecular weight

- **Atmospheric escape**
  - Atmospheric escape for strongly irradiated planets

IV) Lessons from observations

Chemical disequilibrium *(See Olivia's course)*

Deviation from chemical equilibrium produced by mixing or photochemistry

Emission spectrum of HR8799e by VLT-GRAVITY

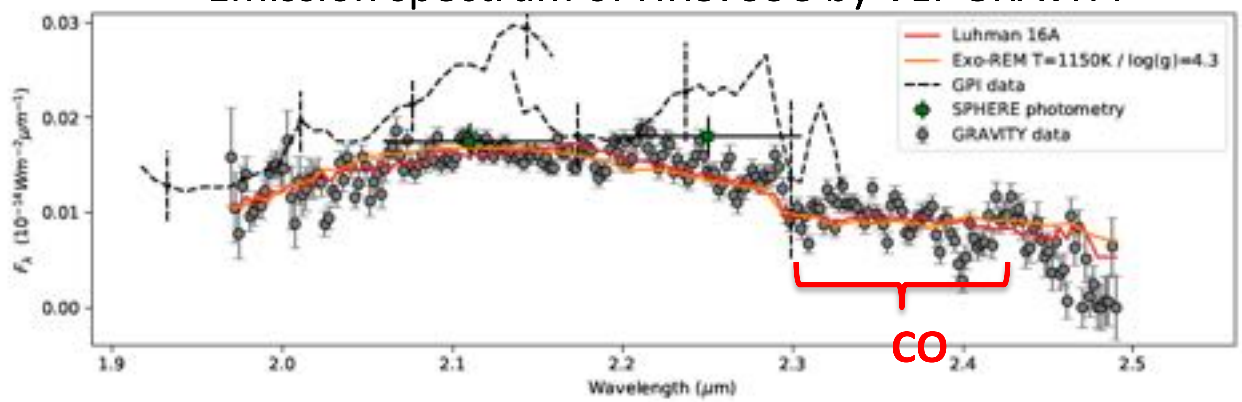

Lacour et al. (2019)

<u>Ex:</u> CO-CH4 conversion in young giant planets
$CO + 3H_3 = CH_4 + H_2O$
CO and CH4 abundances are quenched by vertical mixing

IV) Lessons from observations

Low-mass planets seem to have high-mean molecular weight

GJ1214b

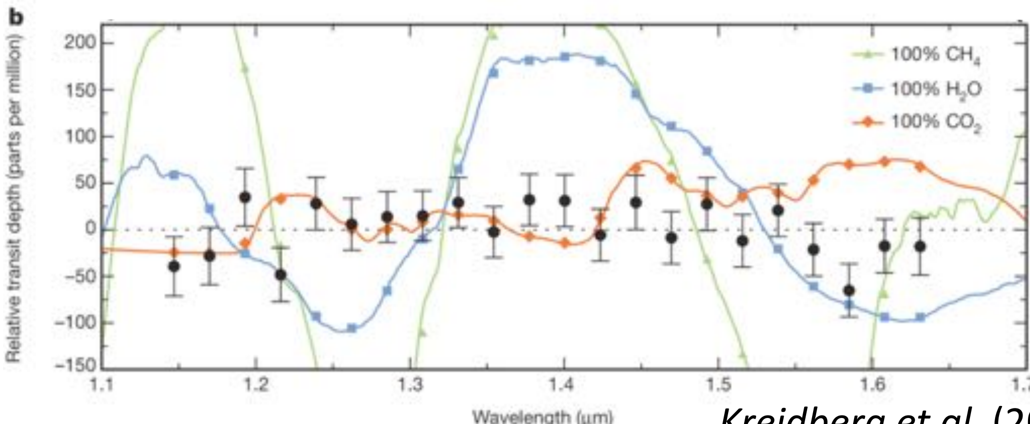

Kreidberg et al. (2014)

K2-18b

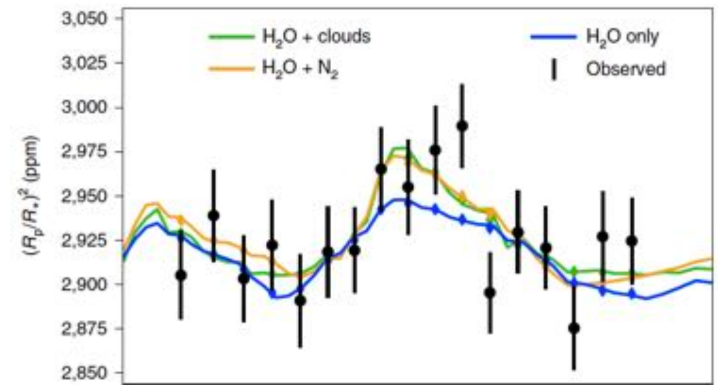

Tsiaras et al. (2019)

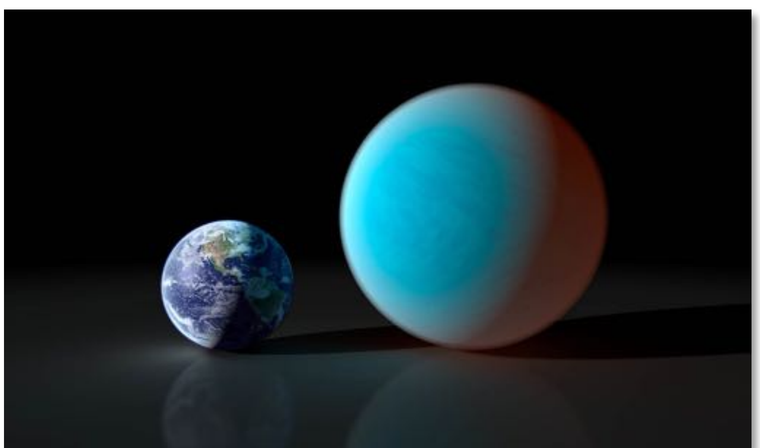

Flat transit spectrum:
→ high mean molecular weight (i.e. high metallicity) + clouds

Lessons from observations of exoplanet atmospheres

- **Radius & Interior**
  - Hot Jupiters are inflated
  - Gap in the occurrence rate between super-Earths and mini-Neptunes

- **Dynamics & Thermal structure**
  - Superrotation for strongly irradiated planets
  - Stratospheric thermal inversion for the hottest planets

- **Clouds/haze**
  - Most of exoplanets are cloudy/hazy
  - Inhomogeneous clouds distribution

- **Atmospheric composition**
  - Chemical disequilibrium (ex: CO/CH4)
  - Low-mass planets seem to have high-mean molecular weight

- **Atmospheric escape**
  - Atmospheric escape for strongly irradiated planets

IV) Lessons from observations

Atmospheric escape for strongly irradiated planets

HD209458 Lyman α profile

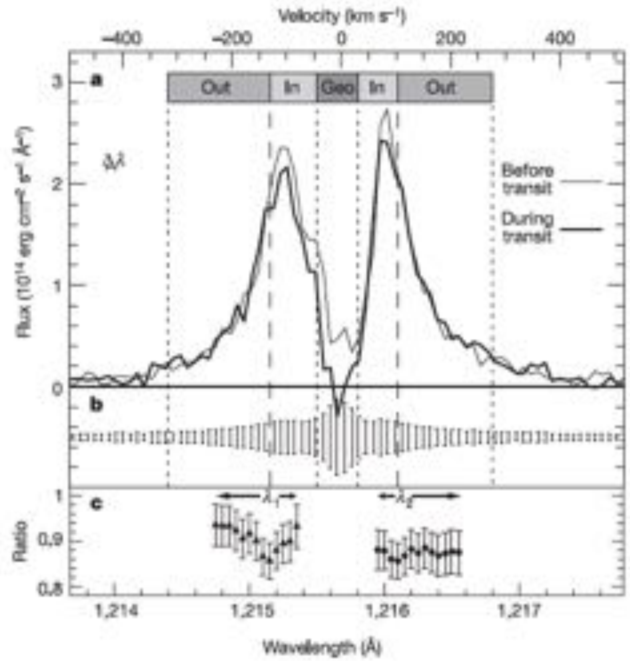

Vidal-Madjar et al. (2003)

GJ436b Lyman α profile

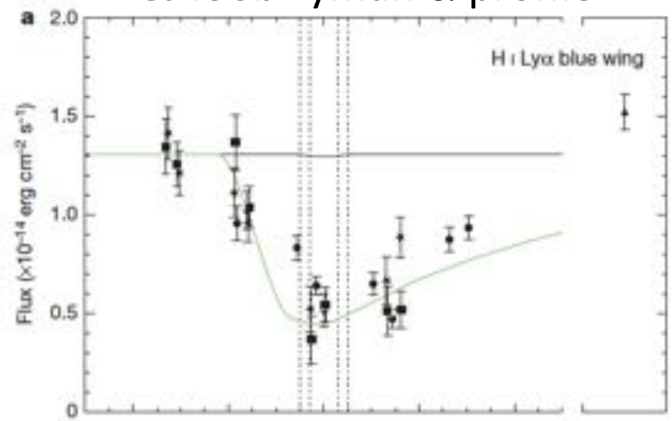

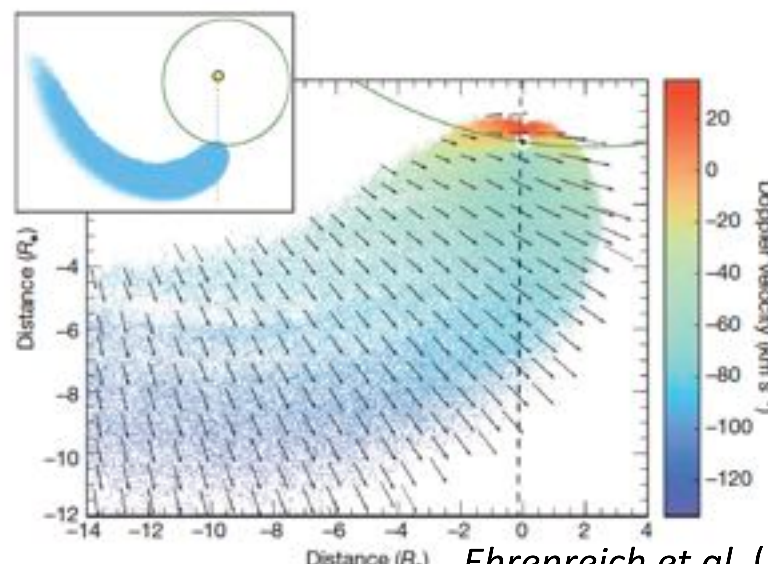

Ehrenreich et al. (2015)

- **Hydrodynamic escape by strong EUV stellar flux**
- **Comet-like H cloud**

Futur telescopes for the characterization of exoplanetary atmospheres

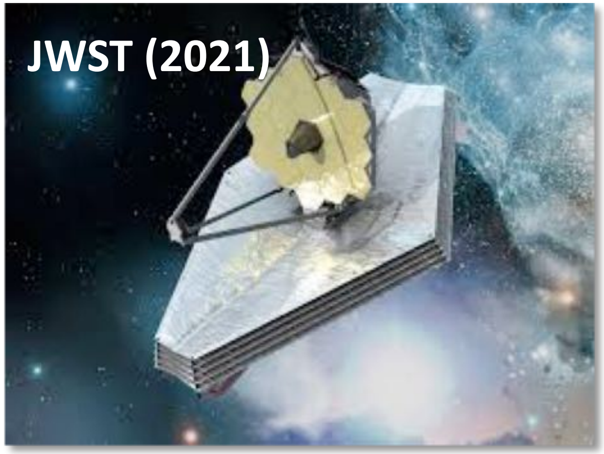

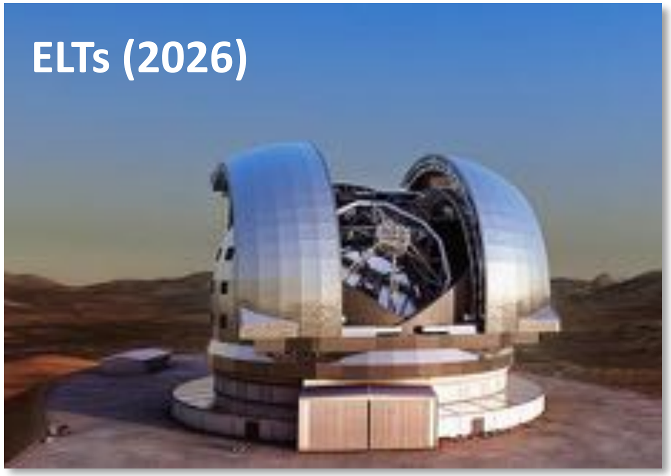

Futur telescopes for the characterization of exoplanetary atmospheres

Futur NASA Great Observatory (2035-2040)

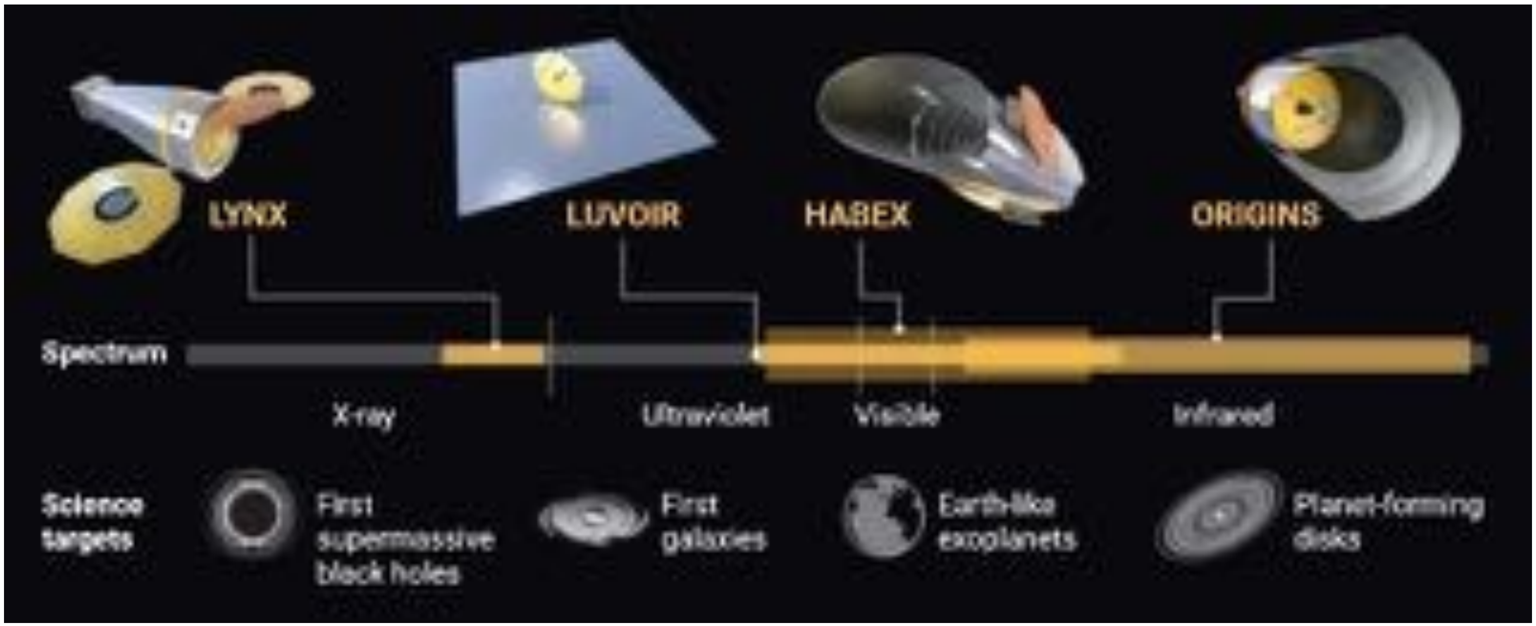

LUVOIR

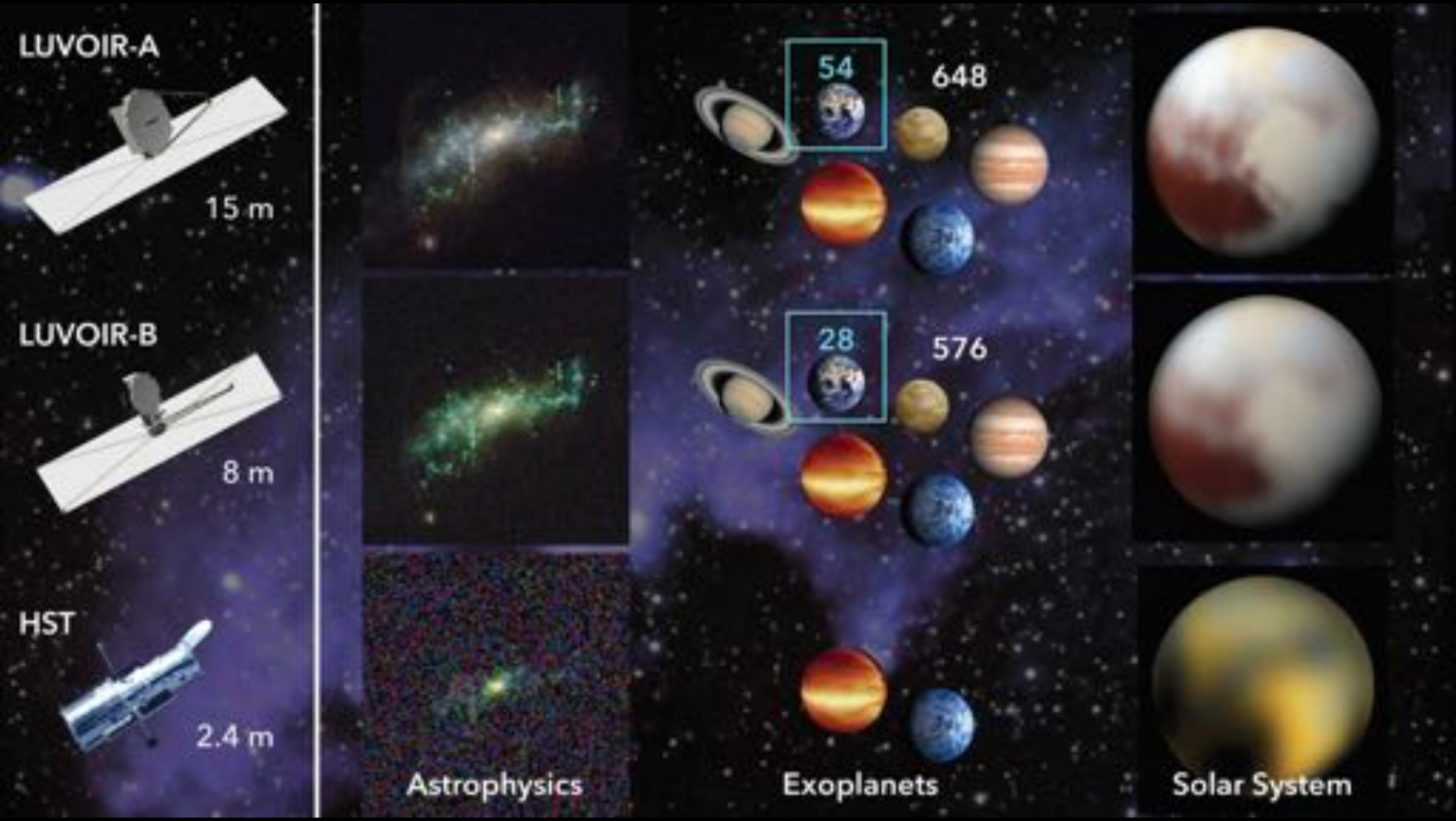

LUVOIR-A
15 m
LUVOIR-B
8 m
HST
2.4 m
54
648
28
576
Astrophysics
Exoplanets
Solar System

HABEX

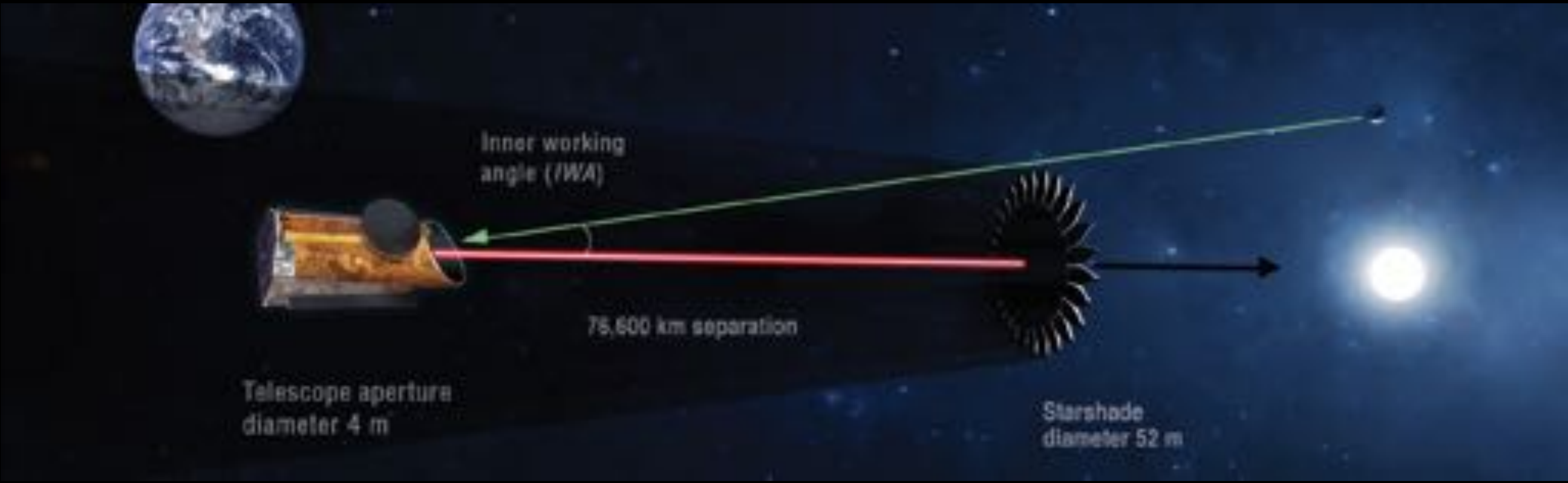
Inner working
angle (IWA)
75,600 km separation
Telescope aperture
diameter 4 m
Starshade
diameter 52 m

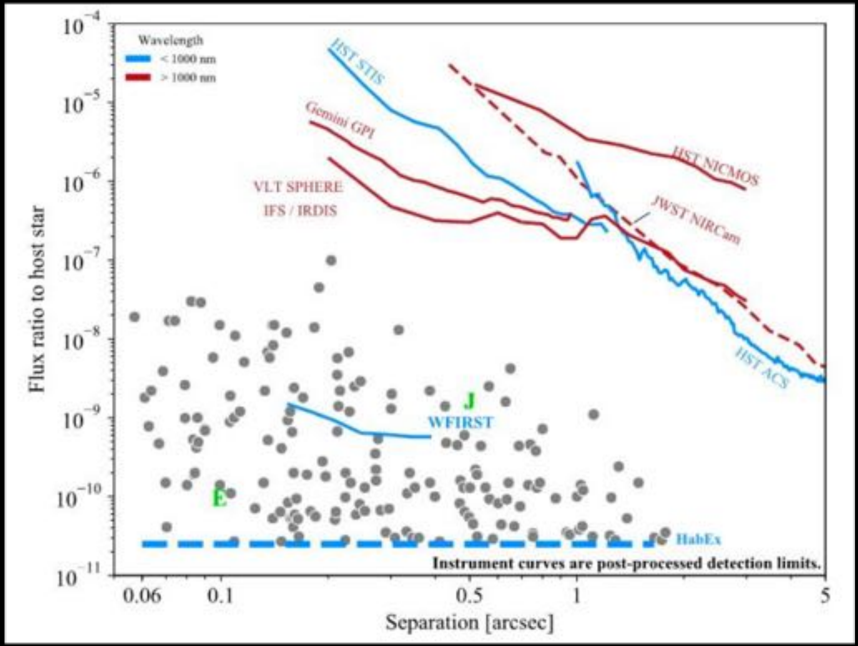
Wavelength
< 1000 nm
> 1000 nm
HST STIS
Gemini GPI
VLT SPHERE
IFS / IRDIS
HST NICMOS
JWST NIRCam
HST ACS
J
WFIRST
E
HabEx
Instrument curves are post-processed detection limits.
Flux ratio to host star
Separation [arcsec]

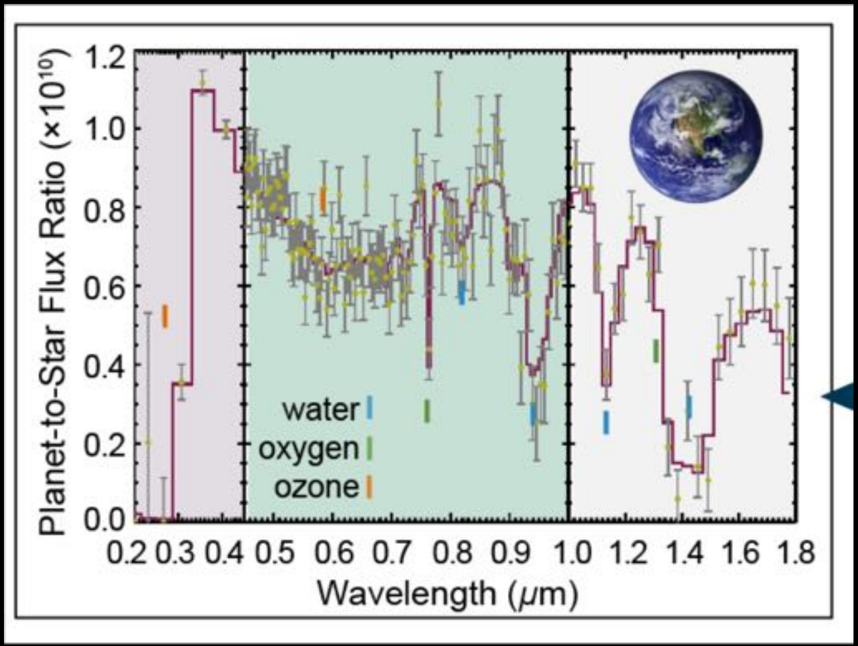
Planet-to-Star Flux Ratio (×10¹⁰)
water
oxygen
ozone
Wavelength (μm)

https://psg.gsfc.nasa.gov/

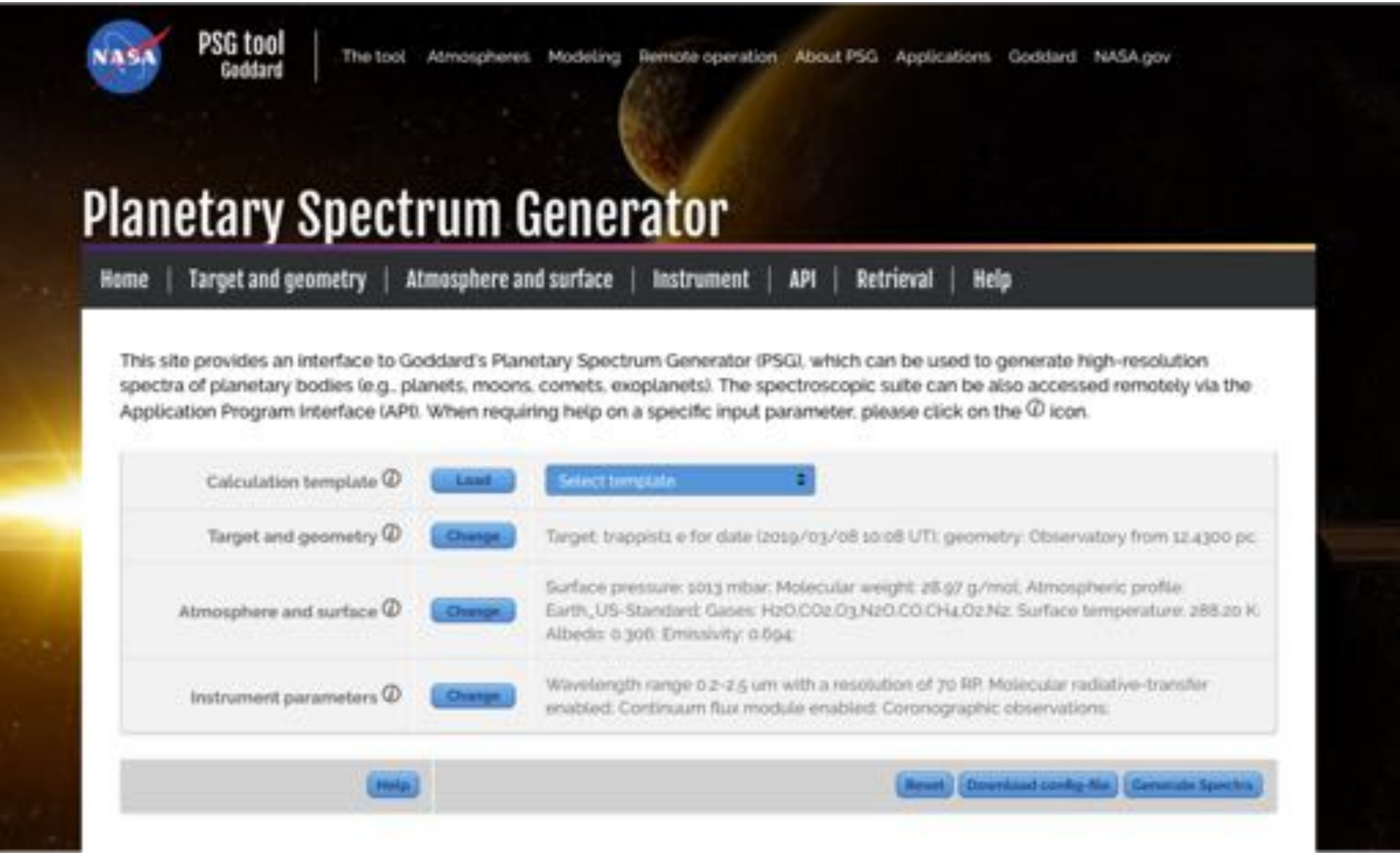

Exemple: GJ1214b with pure H_2O and HST as Kreidberg et al. 2014

Introduction

A diversity of exoplanets

I) Observational techniques

- Transit
- Direct imaging
- Medium/high spectral resolution
- Lessons from observations of exoplanets

II) Modelling exoplanetary atmospheres

- Radiative transfer
- Thermal structure
- Clouds & aerosols

I) Radiative transfer

Definition intensity and flux

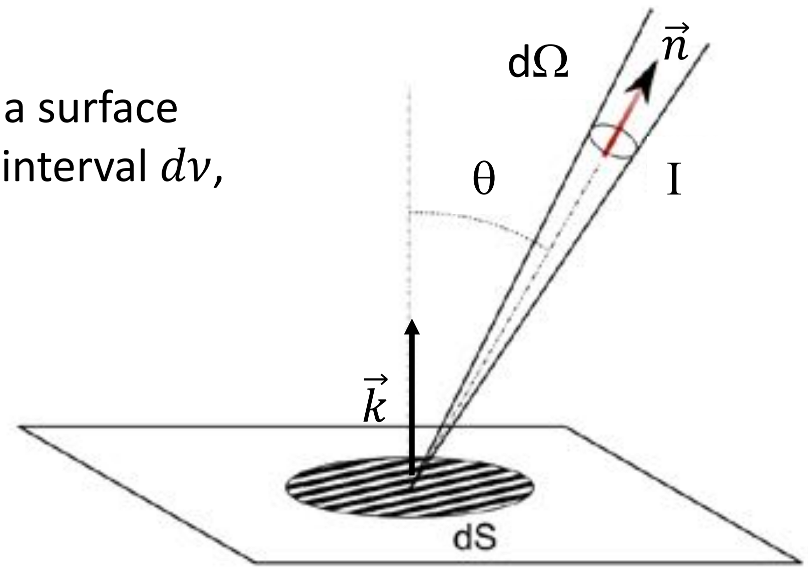

Intensity *I* = amount of energy passing through a surface area dS, within a solid angle $d\Omega$, per frequency interval $d\nu$, per unit time (I in J m^{-2} sr^{-1} Hz^{-1}):

$$dE = I(x, \vec{n}, \nu, t)\, \vec{n} \,.\, \vec{k}\; d\Omega\; dS\; d\nu\; dt$$

Moments:

Mean intensity:

$$J = \int_{\Omega} I(x, \vec{n}, \nu, t) d\Omega$$

Flux:

$$F = \int_{\Omega} I(x, \vec{n}, \nu, t)\vec{n} \,.\, \vec{k} d\Omega = \iint I(x, \theta, \varphi, \nu, t) cos(\theta) \sin(\theta)\, d\theta d\phi$$

I) Radiative transfer

Definition intensity and flux

Blackbody radiation:

$$B(T,\nu) = \frac{2h\nu}{c^2}\frac{1}{e^{h\nu/kT}-1}$$

$$B(T,\lambda) = \frac{2hc^2}{\lambda^5}\frac{1}{e^{hc/\lambda kT}-1}$$

Flux from one hemisphere (isotropic radiation):

$F_s(T,\nu) = \pi B(T,\nu)$

Total flux from one hemisphere (Stefan–Boltzmann law) :

$F_s(T) = \sigma T^4$, $\sigma = 5.67\times10^{-8}$ J K^{-4} m^{-2} s^{-1}

Brightness temperature:

$$T_b = \frac{h\nu}{k}\frac{1}{\ln\left(1+\frac{2\pi h\nu}{c^2 F_s}\right)}$$

with $F_{obs} = F_s\left(\frac{R_p}{Dist}\right)^2$

I) Radiative transfer

Radiative transfer equation for plane-parallel

Optical depth & extinction coefficient:

$$d\tau = -k\,(T, P, \nu)\,\mu\,ds$$

$$k(T, P, \nu) = \sum_i n_i\,(\sigma_i^{abs} + \sigma_i^{scat})$$

Optical mean free path: $l = \frac{1}{k}$

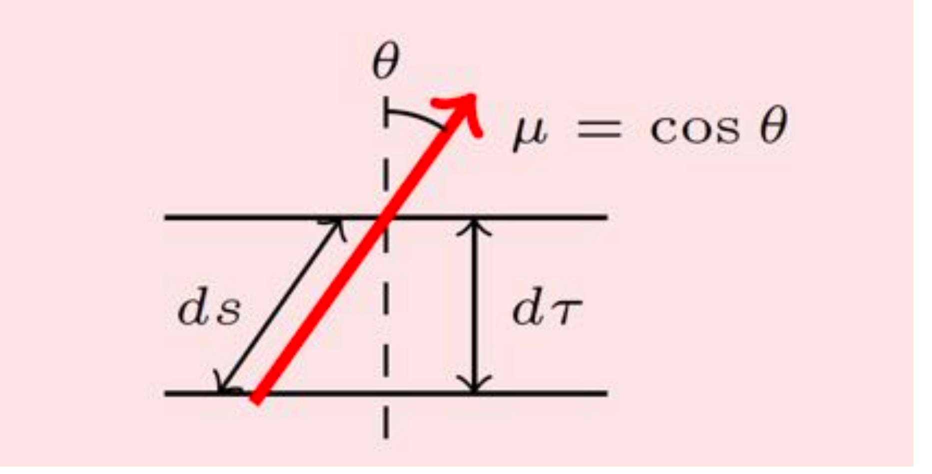

Radiative transfer equation:

$$\mu \frac{dI}{d\tau} = I - S$$

Local thermodynamic Equilibrium (LTE):

$T_{radiation} = T_{kinetics}$

Condition: mean free path of photons ≪ length scale of T variations (for non-LTE see Pierre's talk)

I) Radiative transfer

Source function

$$S_v(\mu,\phi) = (1-\omega_0)B(T,v) + \frac{\omega_0}{4}\iint P(\mu,\mu',\phi,\phi')I\,(v,\mu',\phi')\mathrm{d}\mu' d\phi'$$

Thermal emission — Scattering

$\boldsymbol{\omega_0}$: **single scattering albedo** = $\dfrac{k_{scat}}{k_{scat} + kabs}$

P = scattering phase function

$$\frac{1}{4\pi}\int_{\Omega} P(\Theta)\, d\Omega = 1$$

Rayleigh scattering: $P(\Theta) = \frac{3}{4}(1 + cos^2\Theta)$

$\boldsymbol{g}$: **asymmetry factor** $= \frac{1}{4\pi}\int_{\Omega} cos\Theta\, P(\Theta)\, d\Omega\,, -1 \leq g \leq 1$

$g = 0$ for isotropic or symmetric scattering (e.g. Rayleigh scattering)

I) Radiative transfer

The two-stream approximation

$$\mu \frac{dI}{d\tau} = I - S$$

Goal: to compute the total upward and downward flux

$$J_{\uparrow} \equiv \int_0^{2\pi} \int_0^1 I \, d\mu \, d\phi,$$

$$J_{\downarrow} \equiv \int_0^{2\pi} \int_{-1}^0 I \, d\mu \, d\phi,$$

$$F_{\uparrow} \equiv \int_0^{2\pi} \int_0^1 \mu I \, d\mu \, d\phi,$$

$$F_{\downarrow} \equiv \int_0^{2\pi} \int_{-1}^0 \mu I \, d\mu \, d\phi,$$

Case of stellar radiation with no scattering:

$$F^{\uparrow} = 0$$
$$F^{\downarrow} = F_s e^{-\tau/\mu_*}$$

μ_* is related to the angle of stellar irradiation. For 1D, we use a mean value, generally $\mu_* = 1/\sqrt{3}$ or $\cos(60°)$

I) Radiative transfer

The two-stream approximation

$$\mu \frac{dI}{d\tau} = I - S$$

Goal: to compute the total upward and downward flux

$$J_\uparrow \equiv \int_0^{2\pi} \int_0^1 I \, d\mu \, d\phi,$$

$$J_\downarrow \equiv \int_0^{2\pi} \int_{-1}^0 I \, d\mu \, d\phi,$$

$$F_\uparrow \equiv \int_0^{2\pi} \int_0^1 \mu I \, d\mu \, d\phi,$$

$$F_\downarrow \equiv \int_0^{2\pi} \int_{-1}^0 \mu I \, d\mu \, d\phi,$$

Case of a purely emitting atmosphere:

$$\frac{\partial F^\uparrow}{\partial \tau} = J^\uparrow - 2\pi B$$
$$\frac{\partial F^\downarrow}{\partial \tau} = -J^\downarrow + 2\pi B$$

The two-stream solution consists in approximating I so that it is related to F.

We assume $\frac{F^\uparrow}{J^\uparrow} = \frac{F^\downarrow}{J^\downarrow} = \frac{1}{\gamma}$ (generally $\gamma = \sqrt{3}$)

$$\frac{\partial F^\uparrow}{\partial \tau} = \gamma F^\uparrow - 2\pi B$$
$$\frac{\partial F^\downarrow}{\partial \tau} = -\gamma F^\downarrow + 2\pi B$$

I) Radiative transfer

The two-stream approximation

Case of a purely emitting atmosphere:

$$\frac{\partial F^{\uparrow}}{\partial \tau} = \gamma F^{\uparrow} - 2\pi B$$
$$\frac{\partial F^{\downarrow}}{\partial \tau} = -\gamma F^{\downarrow} + 2\pi B$$

Resolution:

$$F^{\uparrow}(\tau) = F^{\uparrow}_{surf} e^{-\gamma(\tau_0 - \tau)} + \int_{\tau}^{\tau_0} 2\pi B e^{-\gamma(\tau' - \tau)}\, d\tau'$$

$$F^{\downarrow}(\tau) = F^{\downarrow}(\tau = 0) e^{-\gamma\tau} + \int_{0}^{\tau} 2\pi B e^{-\gamma(\tau - \tau')}\, d\tau'$$

Outgoing radiation:

$$OLR = \int_0^{\infty} \left[F^{\uparrow}_{surf} e^{-\gamma\tau_0} + \int_0^{\tau_0} 2\pi B e^{-\gamma\tau}\, d\tau \right] d\nu$$

I) Radiative transfer

The two-stream approximation

Case of a purely emitting atmosphere:

Outgoing radiation:

$$OLR = F^{\uparrow}(\tau_0)e^{-\gamma\tau_0} + \int_0^{\tau_0} 2\pi B e^{-\gamma\tau}\, d\tau$$

Transmittance

Contribution function:

$$cf(P) = B(\nu, T)\frac{de^{-\gamma\tau}}{dlog(P)}$$

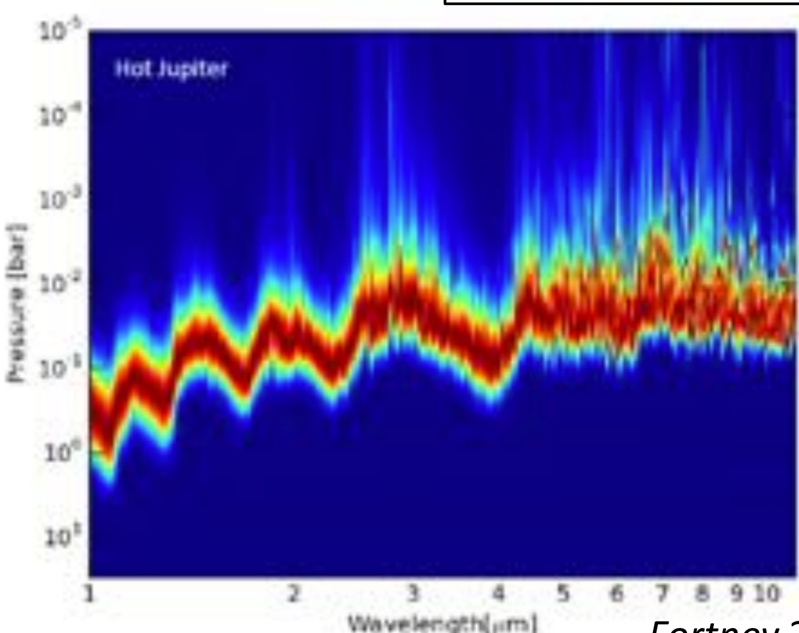

Fortney 2018

Peak of contribution:
at τ ~**2/3** also called the **photosphere**

I) Radiative transfer

The two-stream approximation

Case of a purely emitting atmosphere:

$$\frac{\partial F^{\uparrow}}{\partial \tau} = \gamma F^{\uparrow} - 2\pi B$$
$$\frac{\partial F^{\downarrow}}{\partial \tau} = -\gamma F^{\downarrow} + 2\pi B$$

Radiative equilibrium:

$$\frac{\partial F_\nu}{\partial \tau} = \frac{\partial (F^{\uparrow} - F^{\downarrow})}{\partial \tau} = 0$$

$\Rightarrow$ $\gamma F^{\uparrow} + \gamma F^{\downarrow} = 4\pi B$

$\Rightarrow$ $F_\nu(\tau) = \frac{4\pi}{\gamma^2} \frac{dB}{d\tau}$

With $\gamma = \sqrt{3}$ and $d\tau = k_\nu \, dz$: $\Rightarrow$ $F_\nu(z) = -\frac{4\pi}{3k_\nu} \frac{dB}{dT} \frac{dT}{dz}$

Total flux: $F(z) = \int_0^\infty F_\nu(z) d\nu = -\frac{4\pi}{3} \frac{dT}{dz} \int_0^\infty \frac{1}{k_\nu} \frac{dB}{dT} d\nu$

Diffusive form: $F(z) = -\frac{16}{3} \frac{\sigma T^3}{k_R} \frac{dT}{dz} = -D_R \frac{dT}{dz}$

$$\frac{1}{k_R} = \frac{\int_0^\infty \left(\frac{1}{k_\nu}\right) \left(\frac{dB_\nu}{dT}\right) d\nu}{\int_0^\infty \left(\frac{dB_\nu}{dT}\right) d\nu}$$

k_R is the Rosseland opacity

I) Radiative transfer

The two-stream approximation

$$\mu \frac{dI}{d\tau} = I - S$$

General case for thermal emission with scattering

$$\frac{\partial F^{\uparrow}}{\partial \tau} = \gamma_1 F^{\uparrow} - \gamma_2 F^{\downarrow} - 2\pi(1-\omega_0)B$$
$$\frac{\partial F^{\downarrow}}{\partial \tau} = \gamma_2 F^{\uparrow} - \gamma_1 F^{\downarrow} + 2\pi(1-\omega_0)B$$

Method	γ_1	γ_2	μ_*
Eddington	$[7-\omega_0(4+3g)]/4$	$-[1-\omega_0(4-3g)]/4$	1/2
Quadrature	$\sqrt{3}[1-\omega_0(1+g)/2]$	$\sqrt{3}\omega_0(1+g)/2$	$1/\sqrt{3}$
Hemispheric mean	$2-\omega_0(1+g)$	$\omega_0(1-g)$	1/2

Quadrature for deep atmosphere & Hemisopheric mean for the upper atmosphere

See *Toon et al.* (1989) for the complete solution with multi-layers

I) Radiative transfer

The two-stream approximation

$$\mu \frac{dI}{d\tau} = I - S$$

General case for thermal emission with scattering

$$\frac{\partial F^{\uparrow}}{\partial \tau} = \gamma_1 F^{\uparrow} - \gamma_2 F^{\downarrow} - 2\pi(1-\omega_0)B$$
$$\frac{\partial F^{\downarrow}}{\partial \tau} = \gamma_2 F^{\uparrow} - \gamma_1 F^{\downarrow} + 2\pi(1-\omega_0)B$$

Method	γ_1	γ_2	μ_*
Eddington	$[7-\omega_0(4+3g)]/4$	$-[1-\omega_0(4-3g)]/4$	1/2
Quadrature	$\sqrt{3}[1-\omega_0(1+g)/2]$	$\sqrt{3}\omega_0(1+g)/2$	$1/\sqrt{3}$
Hemispheric mean	$2-\omega_0(1+g)$	$\omega_0(1-g)$	1/2

Quadrature for deep atmosphere & Hemispheric mean for the upper atmosphere

See *Toon et al.* (1989) for the complete solution with multi-layers

I) Radiative transfer

Methods for solving RT

1) <u>Semi-grey analytical model</u>

Optically thin ($\tau < 1$)
Planck mean opacity

$$k_p(T,P,\nu) = \frac{\int_0^\infty k_\nu(T,P,\nu) B_\nu d\nu}{\int_0^\infty B_\nu(T,\nu) d\nu}$$

Optically thick ($\tau > 1$)
Rosseland mean opacity

$$\frac{1}{k_R} = \frac{\int_0^\infty \frac{1}{k_\nu(T,P,\nu)} \frac{dB_\nu}{dT} d\nu}{\int_0^\infty \frac{dB_\nu}{dT} d\nu}$$

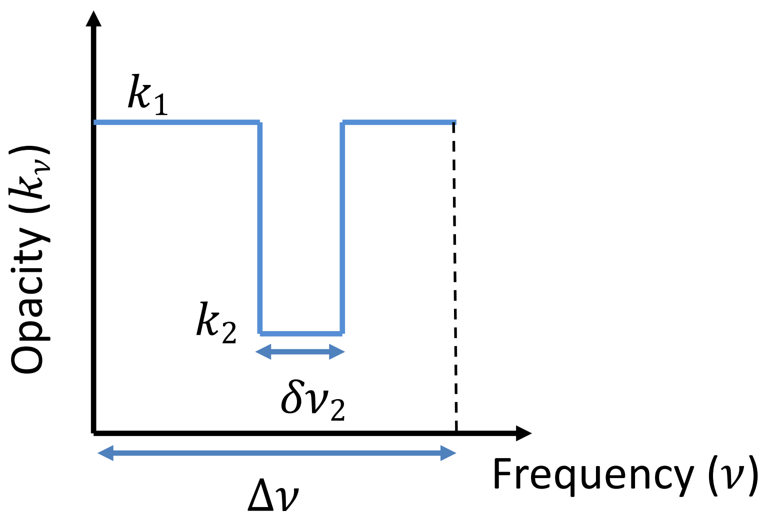

with $k_1 \gg k_2$
$k_p = k_1(\Delta\nu - \delta\nu_2)/\Delta\nu$
$k_R = k_2\delta\nu_2 / \Delta\nu$

Transmittance of a layer Δz:

$$T = \int e^{-k\Delta z} d\nu$$

If $k_1\Delta z \gg 1$ & $k_2\Delta z \ll 1$:
$T \approx k_2\delta\nu_2\Delta z/\Delta\nu = k_R \Delta z$

I) Radiative transfer

Methods for solving RT

1) Semi-grey analytical model

Optically thin ($\tau < 1$)
Planck mean opacity

$$k_p(T,P,\nu) = \frac{\int_0^\infty k_\nu(T,P,\nu) B_\nu d\nu}{\int_0^\infty B_\nu(T,\nu) d\nu}$$

Optically thick ($\tau > 1$)
Rosseland mean opacity

$$\frac{1}{k_R} = \frac{\int_0^\infty \frac{1}{k_\nu(T,P,\nu)} \frac{dB_\nu}{dT} d\nu}{\int_0^\infty \frac{dB_\nu}{dT} d\nu}$$

Mean opacity for H_2-dominated atmosphere:

Table in *Freedman et al.* (2008)

MEAN OPACITIES FOR [M/H] = 0.0

T (K)	P (dyn cm^{-2})	ρ (g cm^{-3})	κ_R (cm^2 g^{-1})	κ_P (cm^2 g^{-1})
75	3E+02	1.1277E−07	2.5619E−06	7.1083E−06
75	3E+03	1.1277E−06	2.5589E−05	6.4309E−05
75	1E+04	3.7591E−06	8.5261E−05	2.1238E−04
75	3E+04	1.1277E−05	2.5571E−04	6.3555E−04
75	1E+05	3.7591E−05	8.5211E−04	2.1167E−03
75	3E+05	1.1277E−04	2.5557E−03	6.3485E−03
75	1E+06	3.7591E−04	8.5180E−03	2.1160E−02
75	3E+06	1.1277E−03	2.5553E−02	6.3478E−02
75	1E+07	3.7591E−03	8.5176E−02	2.1159E−01
100	3E+02	8.4584E−08	4.5393E−06	2.4757E−02
100	3E+03	8.4583E−07	3.9962E−05	2.5407E−03
100	1E+04	2.8193E−06	1.2854E−04	1.0837E−03
100	3E+04	8.4582E−06	3.7709E−04	1.0589E−03
100	1E+05	2.8193E−05	1.2345E−03	2.5780E−03
100	3E+05	8.4582E−05	3.6583E−03	7.3903E−03
100	1E+06	2.8193E−04	1.2104E−02	2.4401E−02
100	3E+06	8.4582E−04	3.6260E−02	7.3044E−02
100	1E+07	2.8193E−03	1.2088E−01	2.4334E−01
100	3E+07	8.4582E−03	3.6261E−01	7.2982E−01

I) Radiative transfer

Methods for solving RT

1) <u>Semi-grey analytical model</u>

Optically thin ($\tau < 1$)
Planck mean opacity

$$k_p(T,P,\nu) = \frac{\int_0^\infty k_\nu(T,P,\nu) B_\nu d\nu}{\int_0^\infty B_\nu(T,\nu) d\nu}$$

Optically thick ($\tau > 1$)
Rosseland mean opacity

$$\frac{1}{k_R} = \frac{\int_0^\infty \frac{1}{k_\nu(T,P,\nu)} \frac{dB_\nu}{dT} d\nu}{\int_0^\infty \frac{dB_\nu}{dT} d\nu}$$

Mean opacity for H_2-dominated atmosphere:

Parameterization in *Freedman et al.* (2018)

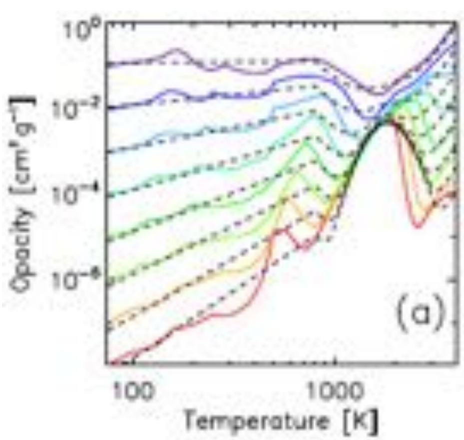

$$\kappa_{\mathrm{gas}} = \kappa_{\mathrm{lowP}} + \kappa_{\mathrm{highP}}$$

$$\log_{10}\kappa_{\mathrm{lowP}} = c_1 \tan^{-1}(\log_{10}T - c_2) - \frac{c_3}{\log_{10}P + c_4} e^{(\log_{10}T - c_5)^2} + c_6 \mathrm{met} + c_7$$

$$\log_{10}\kappa_{\mathrm{highP}} = c_8 + c_9 \log_{10}T + c_{10}(\log_{10}T)^2 + \log_{10}P(c_{11} + c_{12}\log_{10}T) + c_{13}\mathrm{met}\left[\frac{1}{2} + \frac{1}{\pi}\tan^{-1}\left(\frac{\log_{10}T - 2.5}{0.2}\right)\right]$$

Table 2
Coefficients used for opacity fit

	For all T		$T < 800$ K	$T > 800$ K
c_1	10.602	c_8	-14.051	82.241
c_2	2.882	c_9	3.055	-55.456
c_3	6.09×10^{-15}	c_{10}	0.024	8.754
c_4	2.954	c_{11}	1.877	0.7048
c_5	-2.526	c_{12}	-0.445	-0.0414
c_6	0.843	c_{13}	0.8321	0.8321
c_7	-5.490	...	...	...

I) Radiative transfer

Methods for solving RT

1) Semi-grey analytical model

Only for computing the thermal structure (e.g. for retrieval or thermal evolution)

- Model of *Guillot et al.* (2010):

Two parameters (k_{vis} and k_{ir}) for visible (stellar) and infrared (planetary) radiation

- Models with sub-bands:

e.g. *Parmentier et al.* (2014) and *Robinson & Catling* (2012):

One parameter for visible (k_{vis}) and three parameters for infrared (k_{ir1}, k_{ir2}, $\beta = \frac{\delta\nu_2}{\Delta\nu}$)

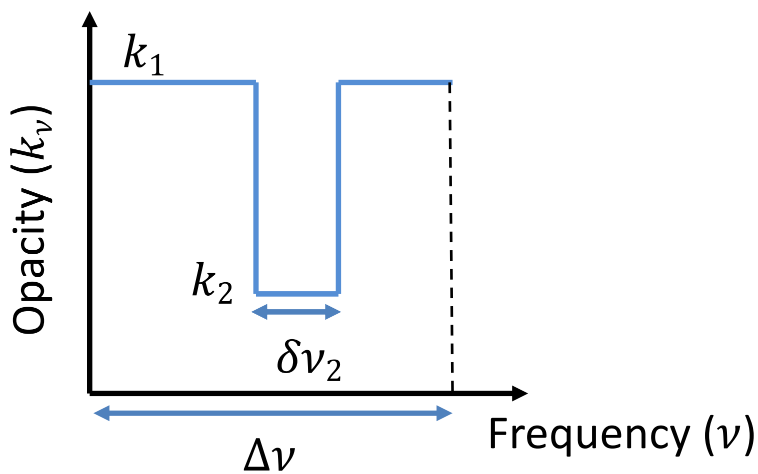

I) Radiative transfer

Methods for solving RT

2) <u>Correlated-k method</u>

$$T = \int_{\nu}^{\nu+\Delta\nu} \exp[-k(\nu)\Delta z] \frac{d\nu}{\Delta\nu}$$

Going from frequency space to g-space, where *g* is the cumulative opacity distribution function: $dg = f(k)dk$

$$T \approx \sum_{i}^{N_g} exp[-ki\Delta z]\, \Delta g_i$$

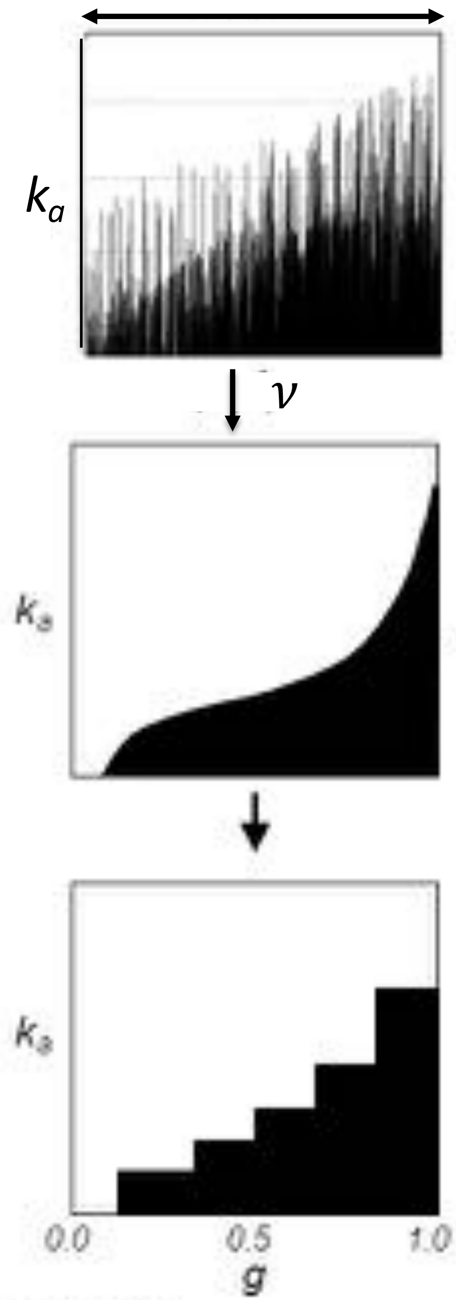

Fast method, excellent for low and medium resolution
Widely used for atmospheric models and 3D GCM

I) Radiative transfer

Methods for solving RT

2) <u>Correlated-k method</u>

Possibility to combine mutliple species

$$\boldsymbol{T = \int_{\nu}^{\nu+\Delta\nu} \mathbf{exp}[-X_1 k_1(\nu) + X_2 k_2(\nu)\Delta z]\,\frac{d\nu}{\Delta\nu}}$$

We assume that k_1 and k_2 are uncorrelated

$$\boldsymbol{T = \left[\int_{\nu}^{\nu+\Delta\nu} e^{-X_1 k_1(\nu)\Delta z}\,\frac{d\nu}{\Delta\nu}\right]\left[\int_{\nu}^{\nu+\Delta\nu} e^{-X_2 k_2(\nu)\Delta z}\,\frac{d\nu}{\Delta\nu}\right]}$$

Going from frequency space to g-space:

$$\boldsymbol{T \approx \sum_{i}^{N_g}\sum_{j}^{N_g} exp[-X_1 k_{1i} + X_2 k_{2j}\Delta z]\,\Delta g_i \Delta g_j}$$

Equivalent to a single gas with: $\boldsymbol{k_{ij} = X_1 k_{1i} + X_2 k_{2j}}$ and $\boldsymbol{\Delta g_{ij} = \Delta g_i \Delta g_j}$

→ ordering of increasing $\boldsymbol{k_{ij}}$ → interpolate on g-space → iterate with another specie

I) Radiative transfer

Methods for solving RT

3) Line-by-line models

For computing accurate transmittance & spectra at medium/high resolution

- Ex: LBLRTM

http://rtweb.aer.com/lblrtm_frame.html

Earth atmospheric transmittance at Mauna Kea & Dome C (computed with LBLRTM)

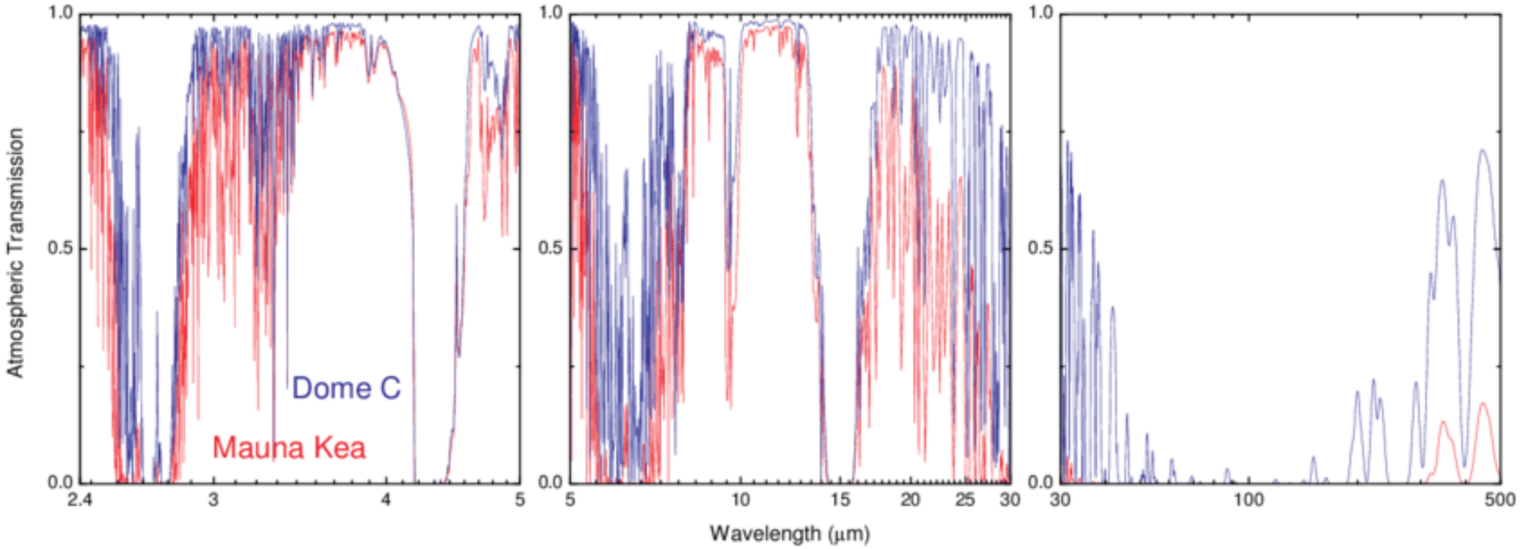

Burton et al. (2004)

I) Radiative transfer

A first look at the greenhouse effect

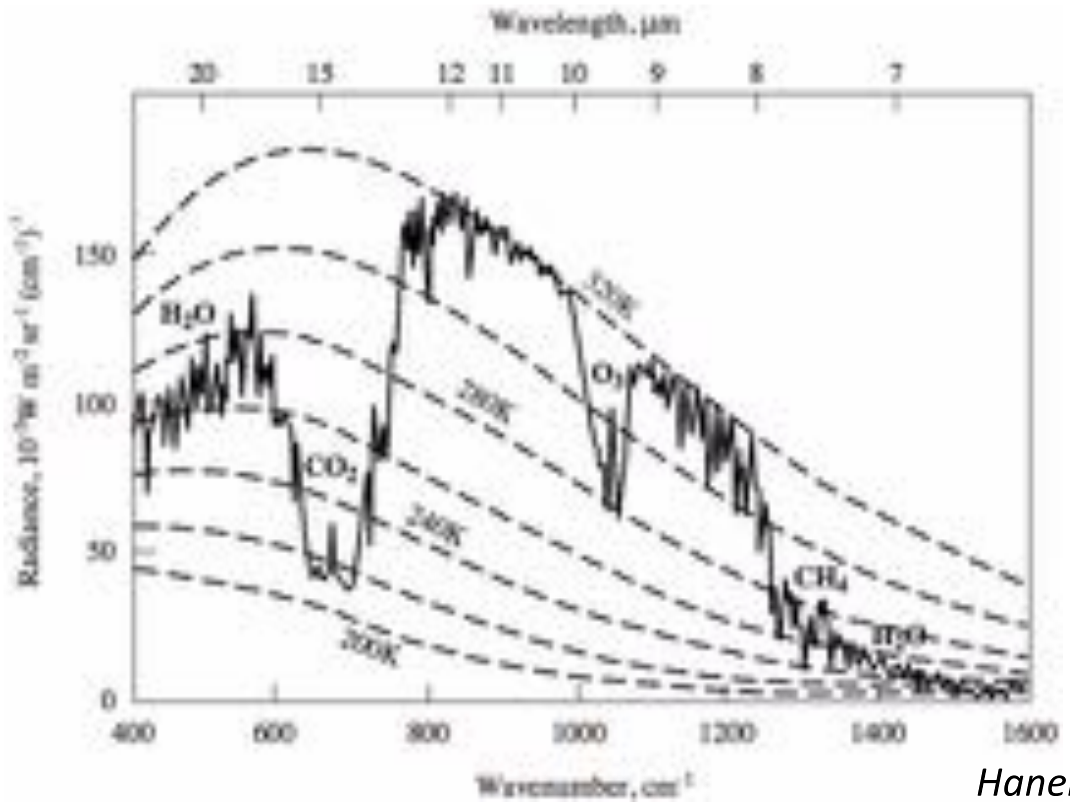

Hanel et al. (1972)

<u>Outgoing radiation:</u>

$$OLR = \int_0^{\infty} \left[F^{\uparrow}{}_{surf} e^{-\gamma\tau_0} + \int_0^{\tau_0} 2\pi B e^{-\gamma\tau}\, d\tau \right] d\nu$$

Transmittance

I) Radiative transfer

A first look at the greenhouse effect

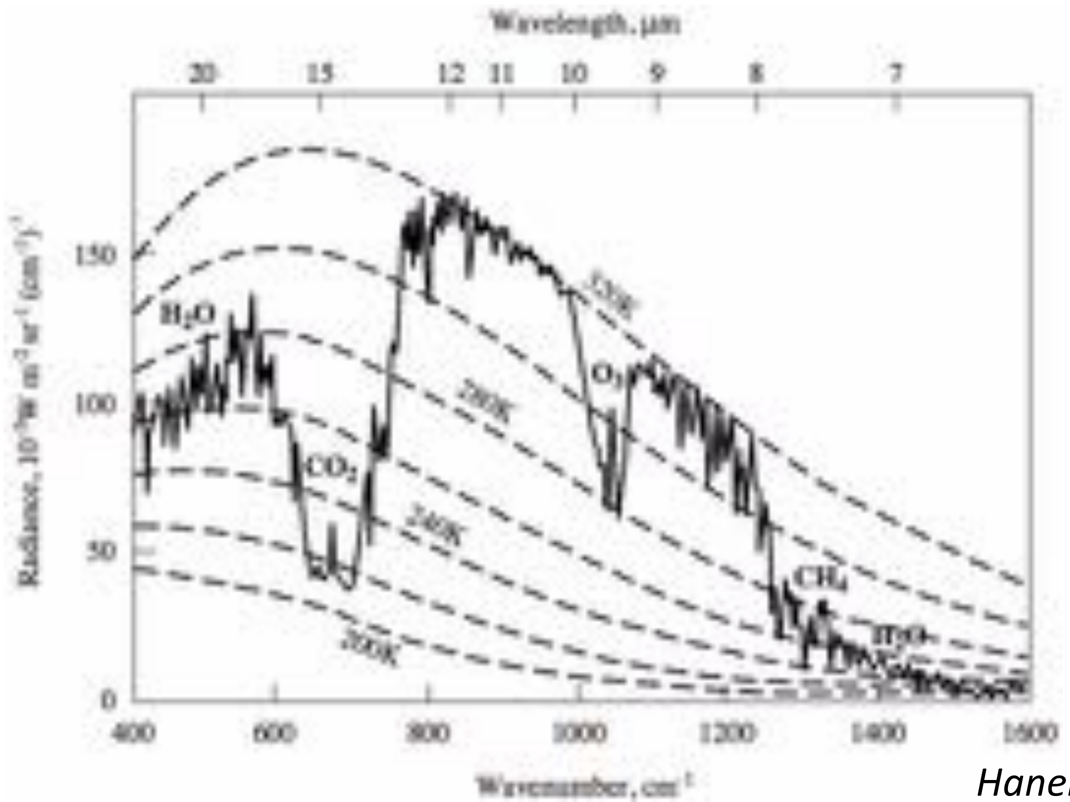

Hanel et al. (1972)

The efficiency of a greenhouse gas is related to how much it reduces spectral windows

<u>Question:</u> What is the strongest greenhouse gase between CO_2 and CH_4 ?

1) For current Earth's atmosphere
2) For a pure N_2 atmosphere

I) Radiative transfer

A first look at the greenhouse effect

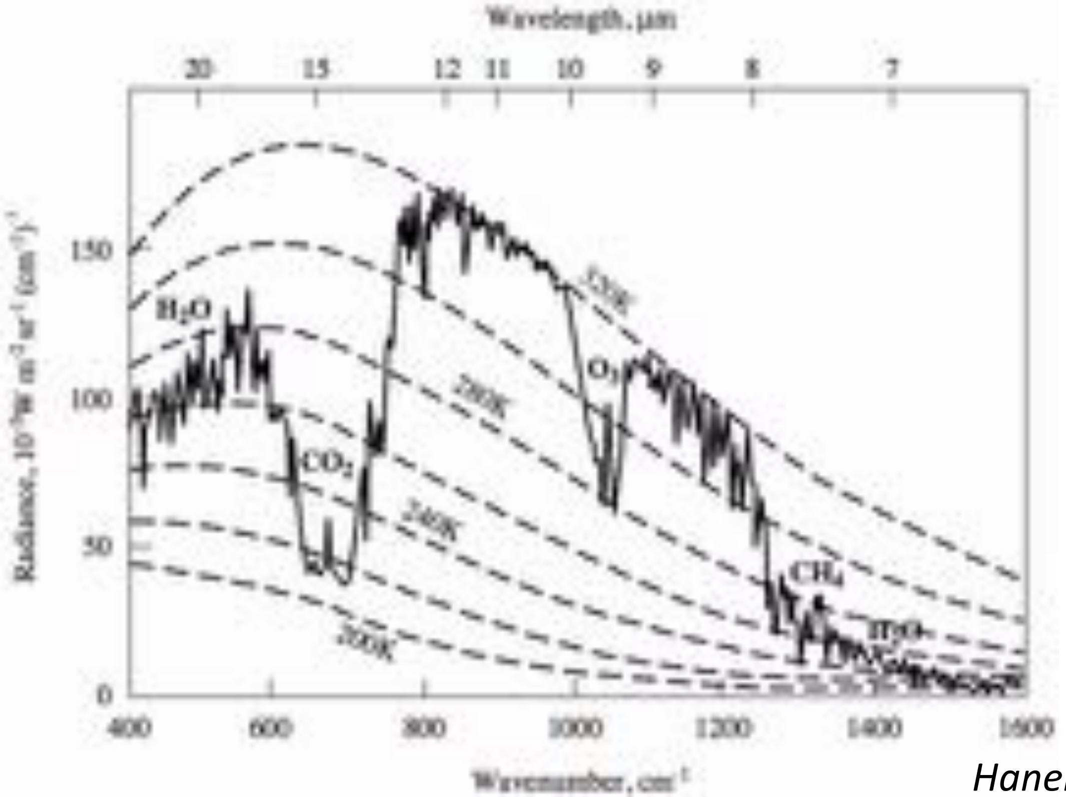

Hanel et al. (1972)

The efficiency of a greenhouse gas is related to how much it reduces spectral windows

<u>Question:</u> What is the strongest greenhouse gase between CO_2 and CH_4 ?

1) For current Earth's atmosphere → $CH_4 \approx 20 \times CO_2$
2) For a pure N_2 atmosphere → $CO_2 \approx 6 \times CH_4$

I) Radiative transfer

A first look at the greenhouse effect

Radiative forcing of a greenhouse gas:

$$\mathbf{\Delta F = ASR - OLR(C) = OLR(C_0) - OLR(C)}$$

$\Delta FCO_2 = 5.35 \times \ln\left(\frac{C}{C_0}\right)$ (CO_2 concentration C in ppm)

$\Delta FCH_4 = 0.036 \times \left(\sqrt{C} - \sqrt{C_0}\right)$ (CH_4 concentration C in ppb)

Mhyre et al. (1998)

Climate sensitivity: **$S = \Delta T$ for $2 \times CO_2$**

IPPC report: S=1.5-4.5 K → $\frac{S}{\Delta F_{2\times CO_2}} \approx 0.8\ \mathrm{K\ W^{-1}\ m^2}$

I) Radiative transfer

A first look at the greenhouse effect

<u>Radiative forcing of a greenhouse gas:</u>

$$\mathbf{\Delta F = ASR - OLR(C) = OLR(C_0) - OLR(C)}$$

$\Delta FCO_2 = 5.35 \times \ln\left(\frac{C}{C_0}\right)$ (CO_2 concentration C in ppm) *Mhyre et al.* (1998)

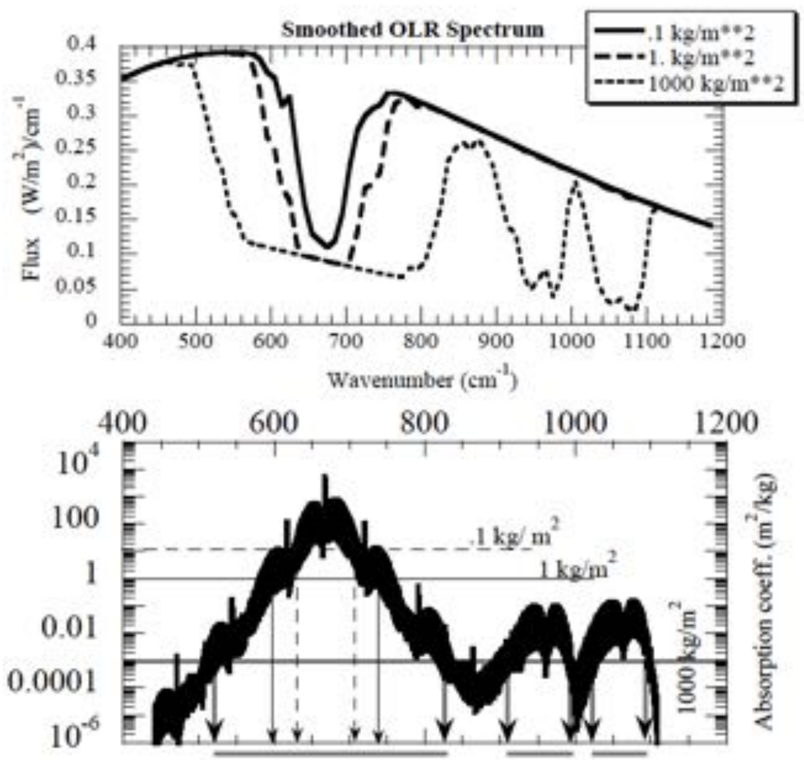

Width of the optically thick band $\propto \ln(C)$

from Pierrehumbert

II) Thermal structure

Skin temperature (radiative)

Stratosphere (radiative)

Troposphere (convective)

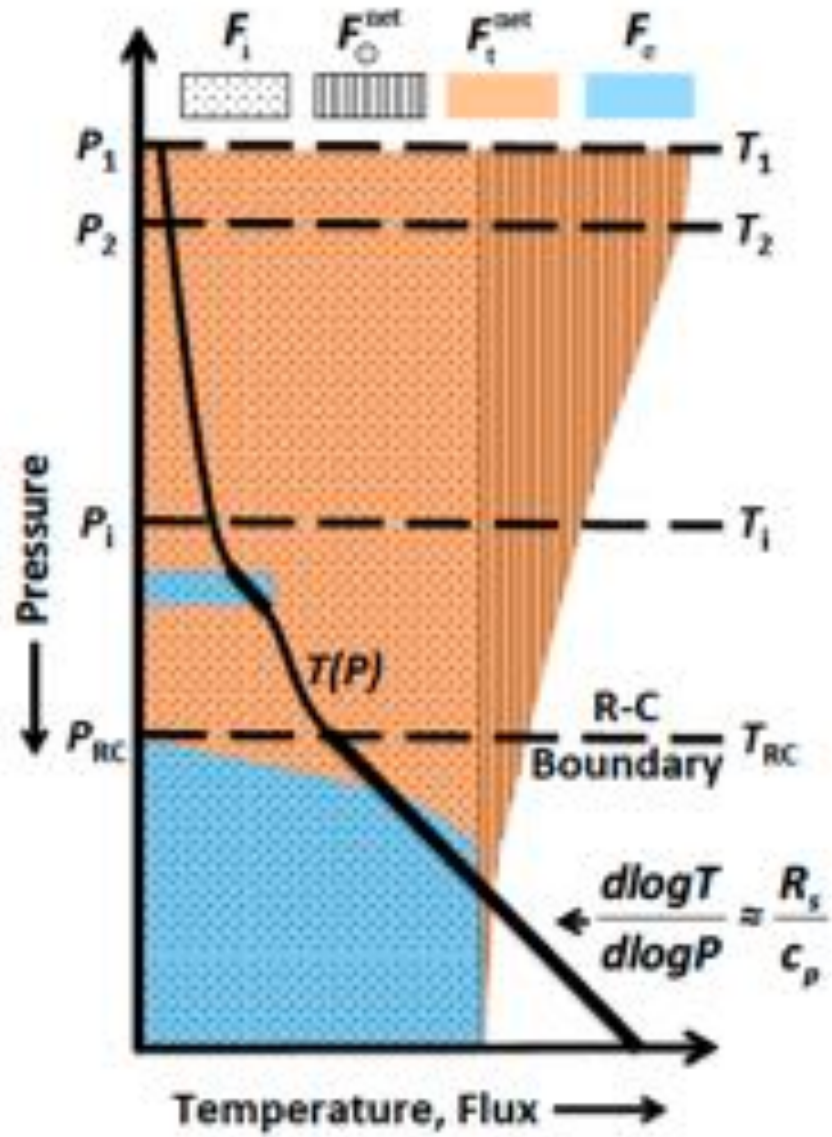

Marley & Robinson (2014)

II) Thermal structure

Resolution of the two-stream for semi-grey case with no scattering

1) Grey atmosphere heated from below

Thermal emission

$$\frac{\partial F^{\uparrow}}{\partial \tau} = \gamma F^{\uparrow} - 2\pi B$$
$$\frac{\partial F^{\downarrow}}{\partial \tau} = -\gamma F^{\downarrow} + 2\pi B$$

- Internal flux: $F_{int} = \sigma T_{int}^4 = \sigma T_{eff}^4$
- We choose $\gamma = \sqrt{3}$ in the deep atmosphere
- $$T(\tau = 0) = T_{skin} = 2^{-1/4} T_{int}$$

Heating:
$$\rho c_v \frac{\partial T}{\partial t} = -\frac{dF}{dz} = 0 \text{ at equilibrium}$$

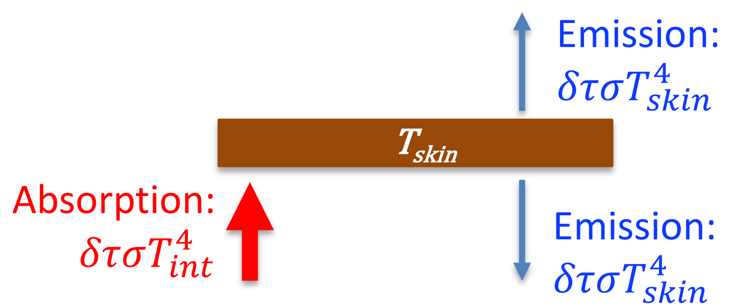

Beautiful exercice: show that
$$T^4 = \frac{3}{4} T_{int}^4 \left(\tau + \frac{2}{3}\right)$$

II) Thermal structure

Resolution of the two-stream for semi-grey case with no scattering

1) Grey atmosphere heated from below

Thermal emission

(1) $$\frac{\partial F^{\uparrow}}{\partial \tau} = \gamma F^{\uparrow} - 2\pi B$$

(2) $$\frac{\partial F^{\downarrow}}{\partial \tau} = -\gamma F^{\downarrow} + 2\pi B$$

- Internal flux: $F_{int} = \sigma T_{int}^4 = \sigma T_{eff}^4$
- We choose $\gamma = \sqrt{3}$ in the deep atmosphere
- $T(\tau = 0) = T_{skin} = 2^{-1/4} T_{int}$

(1)-(2) → $$\frac{\partial F}{\partial \tau} = \gamma(F^{\uparrow} + F^{\downarrow}) - 4\pi B$$

$\int d\nu$ → $$\frac{\partial F_{tot}}{\partial \tau} = \gamma({F_{tot}}^{\uparrow} + {F_{tot}}^{\downarrow}) - 4\sigma T^4 = 0$$

Derivative → $$3(Ftot^{\uparrow} - {F_{tot}}^{\downarrow}) - 4\sigma \frac{\partial T^4}{\partial \tau} = 0$$ → $$3T_{int}^4 - 4\frac{\partial T^4}{\partial \tau} = 0$$

Integration → $$T^4 = \frac{3}{4} T_{int}^4 \left(\tau + \frac{2}{3}\right)$$

At the ground: $$T_g^4 - T^4(\tau_g) = T_{int}^4$$
$$T_g^4 = \frac{3}{4} T_{int}^4 (\tau + 2)$$

II) Thermal structure

Resolution of the two-stream for semi-grey case with no scattering

2) Grey atmosphere heated from above and below

➡ Model of *Guillot et al.* (2010)

- Internal flux: $F_{int} = \sigma T_{int}^4$
- Stellar flux: $F_{ext} = \sigma T_{irr}^4$
- Effective temperature: $T_{eff}^4 = f T_{irr}^4 + T_{int}^4$
- $\tau = \tau_{ir}$; $\gamma = k_{vis}/k_{ir}$

$$T^4 = \frac{3}{4} T_{int}^4 \left(\tau + \frac{2}{3}\right) + \frac{3}{4} T_{irr}^4 f \left[\frac{2}{3} + \frac{1}{\gamma\sqrt{3}} + \left(\frac{\gamma}{\sqrt{3}} - \frac{1}{\gamma\sqrt{3}}\right) e^{-\gamma\tau\sqrt{3}}\right]$$

f = 1 at substellar point,
f = 1/2 for a day-side average
f = 1/4 for an average over the whole planet

$$T_{skin}^4 = \frac{1}{2} T_{int}^4 + \frac{3}{4} T_{irr}^4 f \left[\frac{2}{3} + \frac{\gamma}{\sqrt{3}}\right]$$

II) Thermal structure

Resolution of the two-stream for semi-grey case with no scattering

2) Grey atmosphere heated from above and below

➡ Model of *Guillot et al.* (2010)

- Internal flux: $F_{int} = \sigma T_{int}^4$
- Stellar flux: $F_{ext} = \sigma T_{irr}^4$
- Effective temperature: $T_{eff}^4 = f T_{irr}^4 + T_{int}^4$
- $\tau = \tau_{ir}$; $\gamma = k_{vis}/k_{ir}$

$$T^4 = \frac{3}{4} T_{int}^4 \left(\tau + \frac{2}{3}\right) + \frac{3}{4} T_{irr}^4 f \left[\frac{2}{3} + \frac{1}{\gamma\sqrt{3}} + \left(\frac{\gamma}{\sqrt{3}} - \frac{1}{\gamma\sqrt{3}}\right) e^{-\gamma\tau\sqrt{3}}\right]$$

For τ>>1: $$T_{deep}^4 = \frac{3}{4}\tau T_{int}^4 + \frac{3}{4} T_{irr}^4 f \left[\frac{2}{3} + \frac{1}{\gamma\sqrt{3}}\right]$$

<u>For inflated hot Jupiters:</u>

Heat transfer to the deep atmosphere (10^{-4}% - 1% F_{ext} into F_{int})

➡ Huge change for the temperature in the deep atmosphere

II) Thermal structure

Resolution of the two-stream for semi-grey case with no scattering

2) Grey atmosphere heated from above and below

➡ Model of *Guillot et al.* (2010)

- Internal flux: $F_{int} = \sigma T_{int}^4$
- Stellar flux: $F_{ext} = \sigma T_{irr}^4$
- Effective temperature: $T_{eff}^4 = f T_{irr}^4 + T_{int}^4$
- $\tau = \tau_{ir}$; $\gamma = k_{vis}/k_{ir}$

T profiles for γ =0.01-100

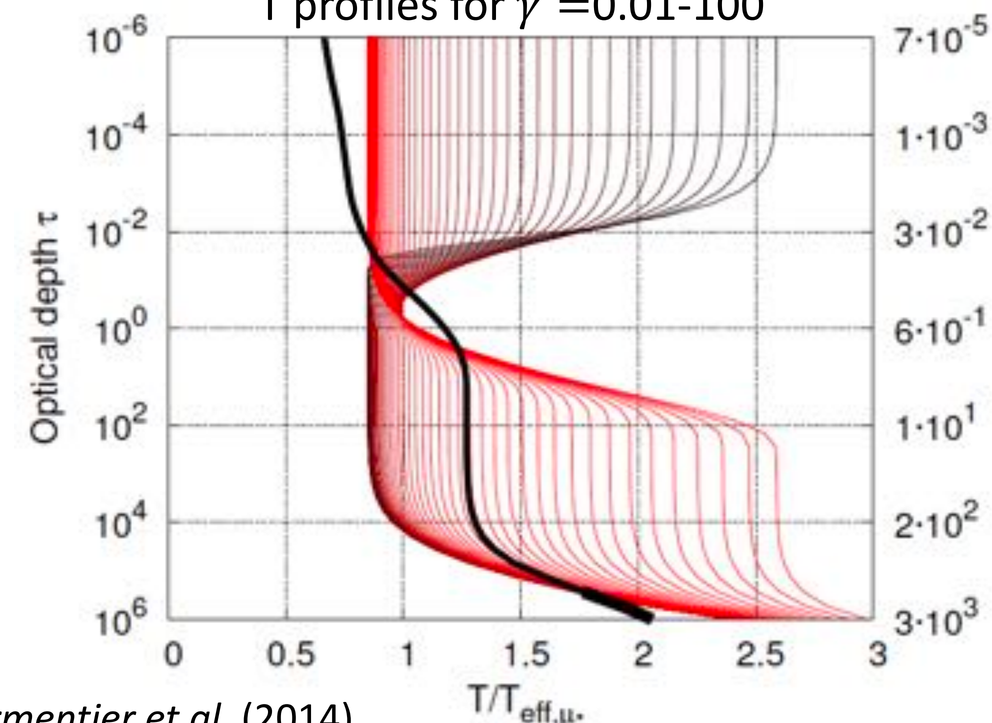

Parmentier et al. (2014)

Stratospheric thermal inversion for $\gamma > 1$

$$T_{deep}^4 = \frac{3}{4} T_{irr}^4 f \left[\frac{2}{3} + \frac{1}{\gamma\sqrt{3}}\right]$$

II) Thermal structure

Troposphere and convective instability

Adiabatic lapse rate

For an air parcel with no heat transfer:

$$\Gamma_d = -\frac{dT}{dz} = \frac{g}{C_p} \iff \frac{dlnT}{dlnP} = \frac{R}{C_p} \leftrightarrow T = T_0 \left(\frac{P_0}{P}\right)^{R/Cp}$$

Stability of an air parcel

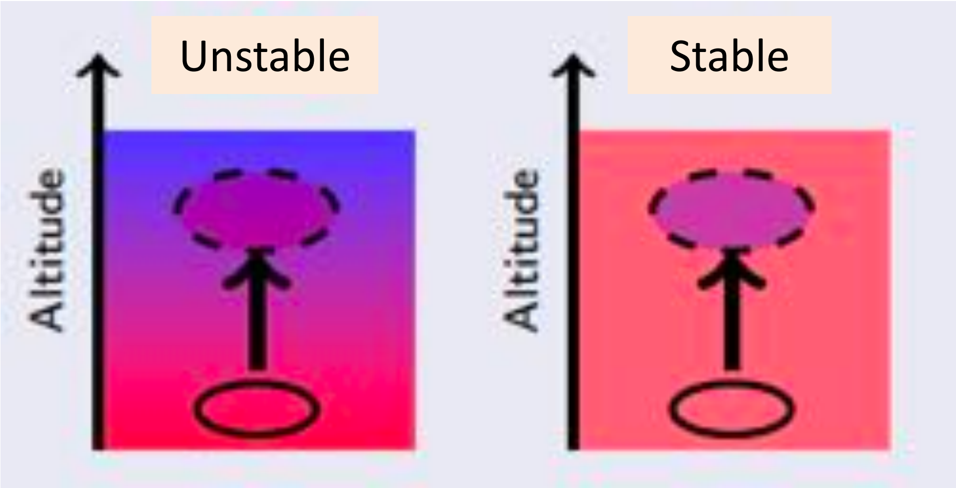

$\boldsymbol{\Gamma > \Gamma_d}$ $\boldsymbol{\Gamma < \Gamma_d}$

II) Thermal structure

Troposphere and convective instability

Question: For a grey atmosphere heated from below, where is the air unstable ?

1) For $\tau \propto P$ (constant absorption)
2) For $\tau \propto P^2$ (opacity controlled by pressure-broadening or CIA)

$$T^4 = \frac{3}{4} T_{int}^4 \left(\tau + \frac{2}{3}\right)$$

We assume $\frac{R}{C_p} = \frac{2}{7}$ (e.g. N_2) or $\frac{R}{C_p} = \frac{2}{9}$ (e.g. CO_2)

II) Thermal structure

Troposphere and convective instability

Question: For a grey atmosphere heated from below, where is the air unstable ?
1) For $\tau \propto P$ (constant absorption)
2) For $\tau \propto P^2$ (opacity controlled by pressure-broadening or CIA)

$$T^4 = \frac{3}{4} T_{int}^4 \left(\tau + \frac{2}{3}\right)$$

We assume $\frac{R}{C_p} = \frac{2}{7}$ (e.g. N_2) or $\frac{R}{C_p} = \frac{2}{9}$ (e.g. CO_2)

$$\frac{dlnT}{dlnP} = \frac{P}{4(\tau + \frac{2}{3})} \frac{d\tau}{dP}$$

1) $\frac{dlnT}{dlnP} = \frac{\tau}{4(\tau + \frac{2}{3})}$ ➡ $\frac{dlnT}{dlnP}(max) = 1/4$

$\frac{dlnT}{dlnP}(max) < \frac{R}{C_p}$ for N_2

Always stable

$\frac{dlnT}{dlnP}(max) > \frac{R}{C_p}$ for CO_2

Potentially unstable

2) $\frac{dlnT}{dlnP} = \frac{\tau}{2(\tau + \frac{2}{3})}$ ➡ $\frac{dlnT}{dlnP}(max) = 1/2$

$\frac{dlnT}{dlnP}(max) < \frac{R}{C_p}$ for N_2 & CO_2 ⇨ Convection for $\tau = 8/9$ (N_2) & $8/15$ (CO_2)

$\boldsymbol{\tau \approx 1}$

II) Thermal structure

Tropopause & stratospheric thermal inversion

No analytical general solution to the radiative-convective TP profile

→ determination doing iterations

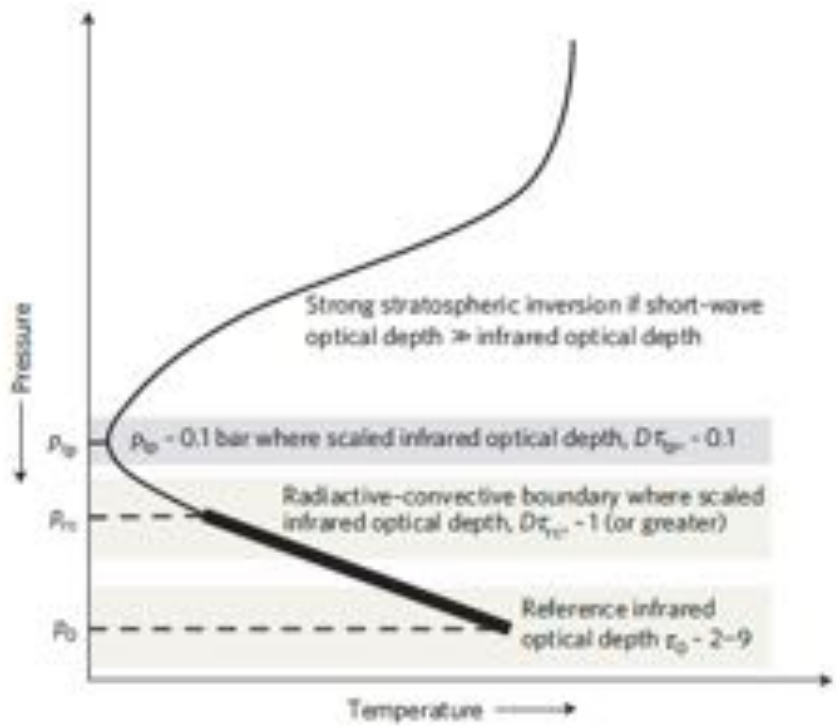

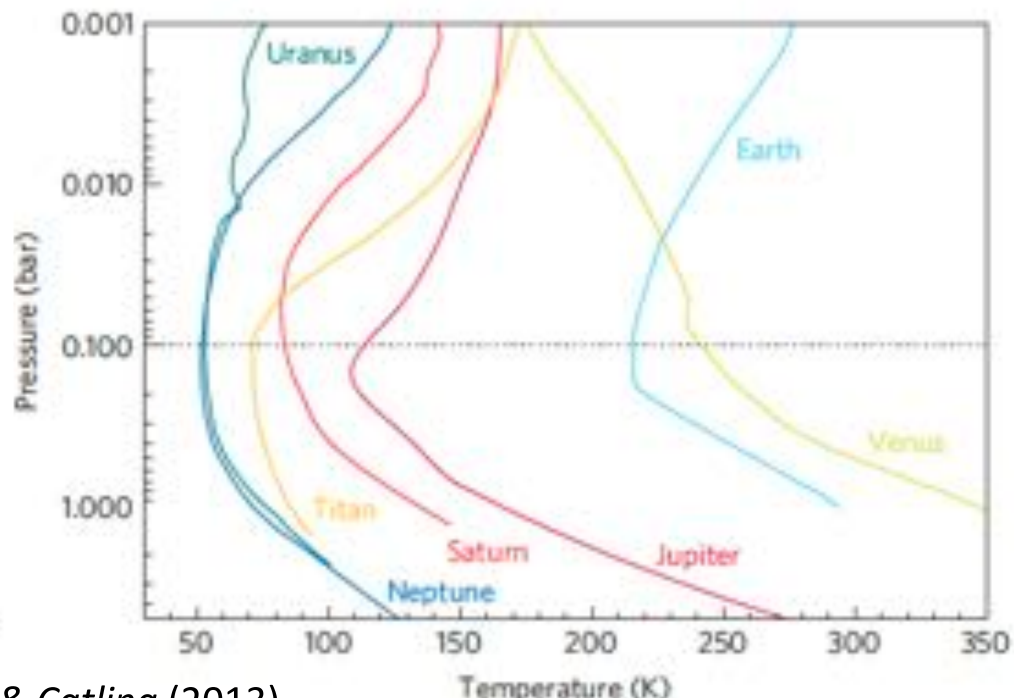

Robinson & Catling (2013)

Tropopause generally at 0.1 bar

III) Clouds & Aerosols

Cloud impact on planetary atmospheres

- Atmospheric composition/chemistry
- Radiative transfert (scattering & absorption)
- Atmospheric dynamics
- Temperature and climate

→ **Atmospheric retrieval**

III) Clouds & Aerosols

Cloud impact on planetary atmospheres

- Atmospheric composition/chemistry
- Radiative transfert (scattering & absorption)
- Atmospheric dynamics
- Temperature and climate

→ **Atmospheric retrieval**

Clouds seen by astronomers

Clouds seen by atmospheric scientists

III) Clouds & Aerosols

Cloud impact on planetary atmospheres

- Atmospheric composition/chemistry
- Radiative transfert (scattering & absorption)
- Atmospheric dynamics
- Temperature and climate

Need for atmospheric models with clouds simulated properly and self-consistently

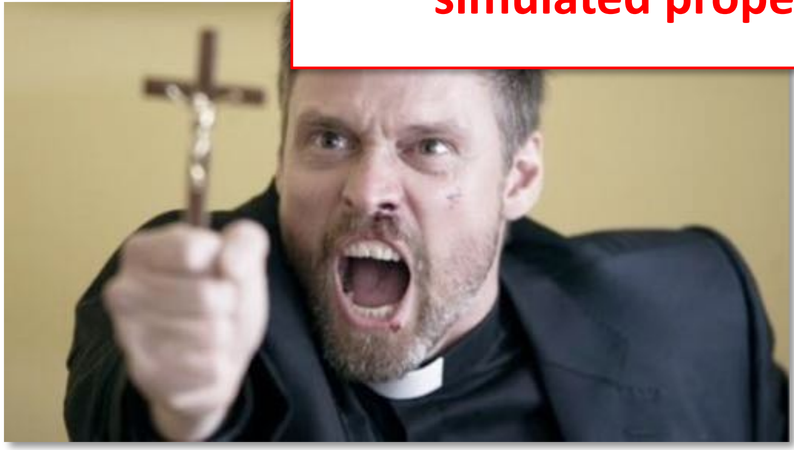

Clouds seen by astronomers

Clouds seen by atmospheric scientists

III) Clouds & Aerosols

Phase diagram

Likely liqu

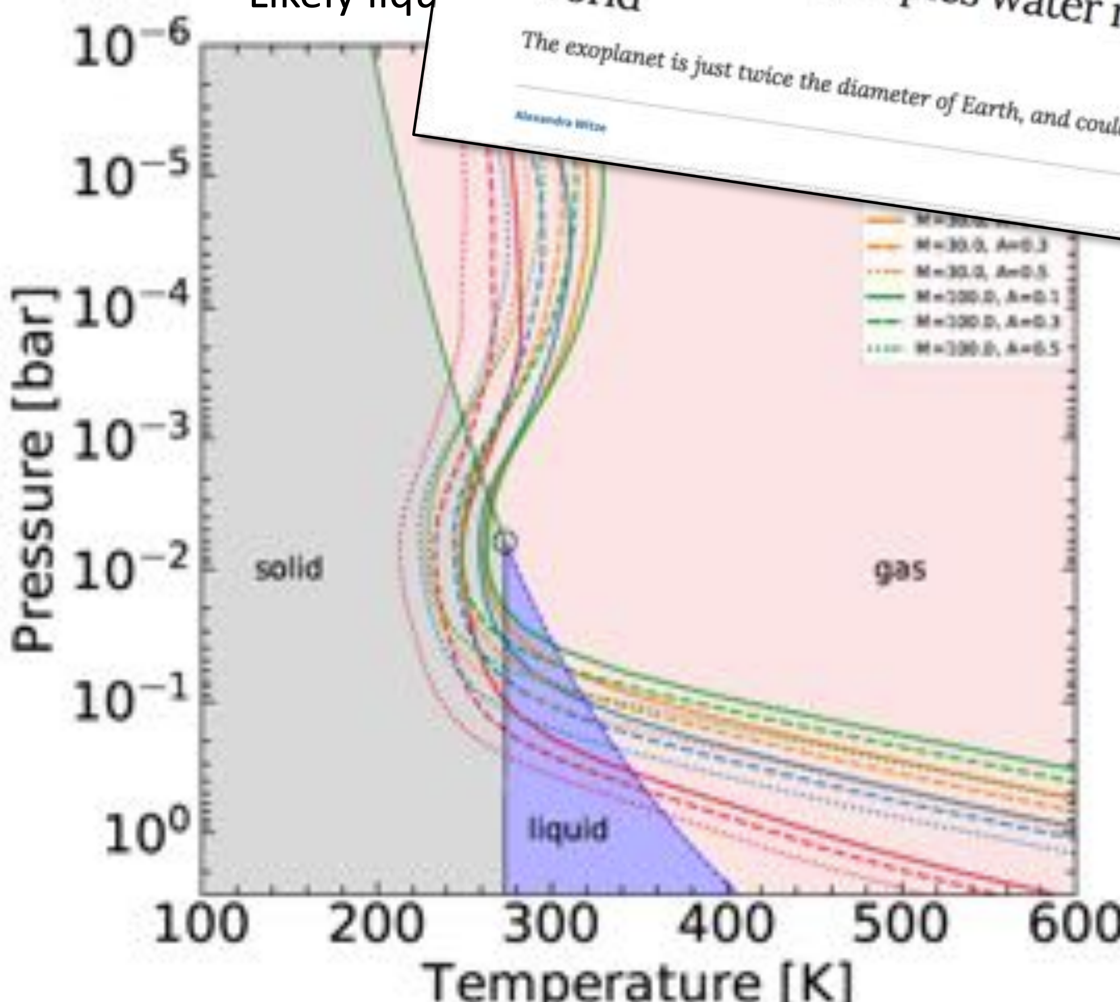

nature

NEWS · 11 SEPTEMBER 2019

Hubble telescope spies water raining on distant world

The exoplanet is just twice the diameter of Earth, and could potentially host life.

Alexandra Witze

Benneke et al. 2019

III) Clouds & Ae

Phase diagram

Transition gas → condensed phase
what matters is the partial pressure
not the total pressure

Likely liquid water clouds on K2-18b !!!

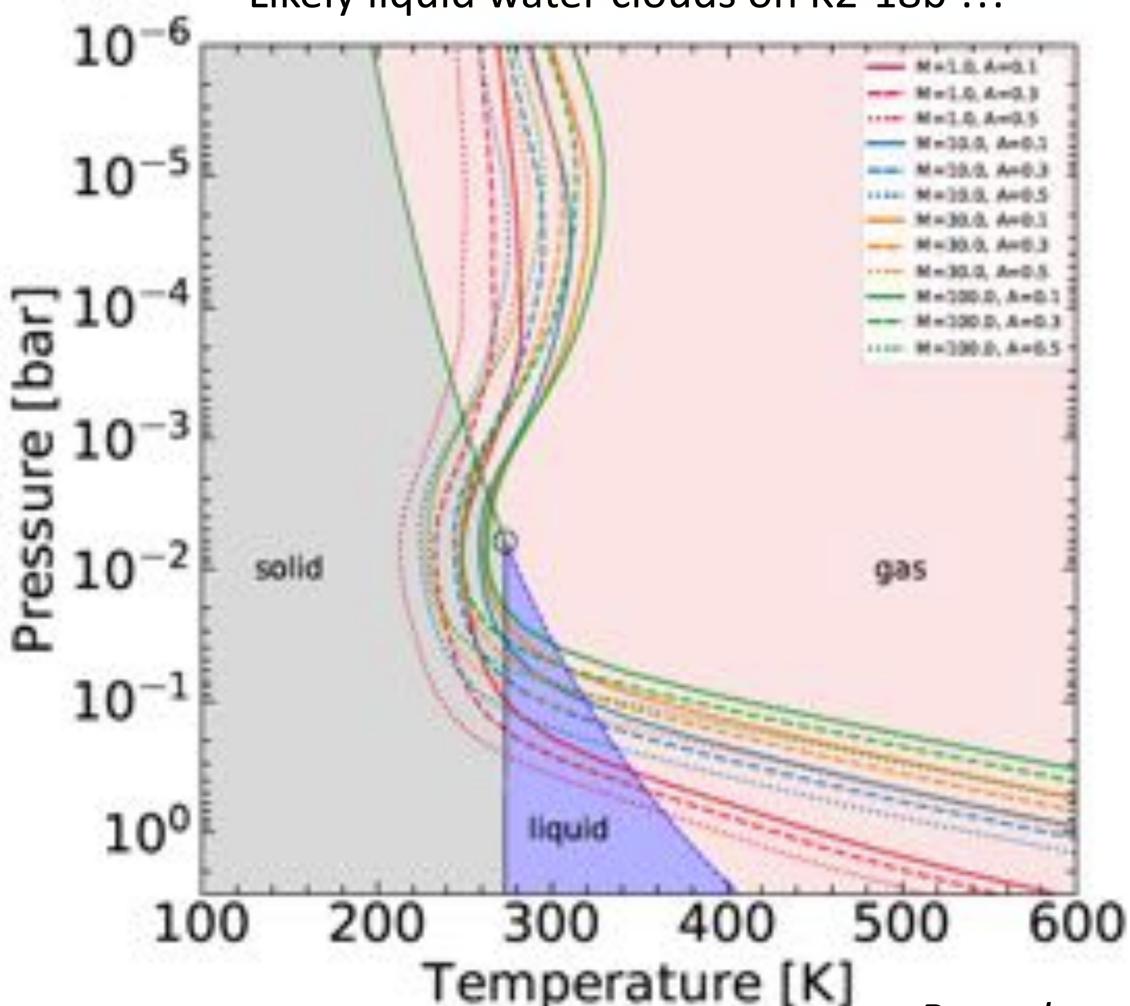

1xsolar: $P_{H2O} \approx 10^{-3} P_{tot}$

100xsolar: $P_{H2O} \approx 0.1 P_{tot}$

No condensation or just water ice for these TP profiles !

Benneke et al. 2019

III) Clouds & Aerosols

Condensation curves

Temperature condensation curves for solar metallicity

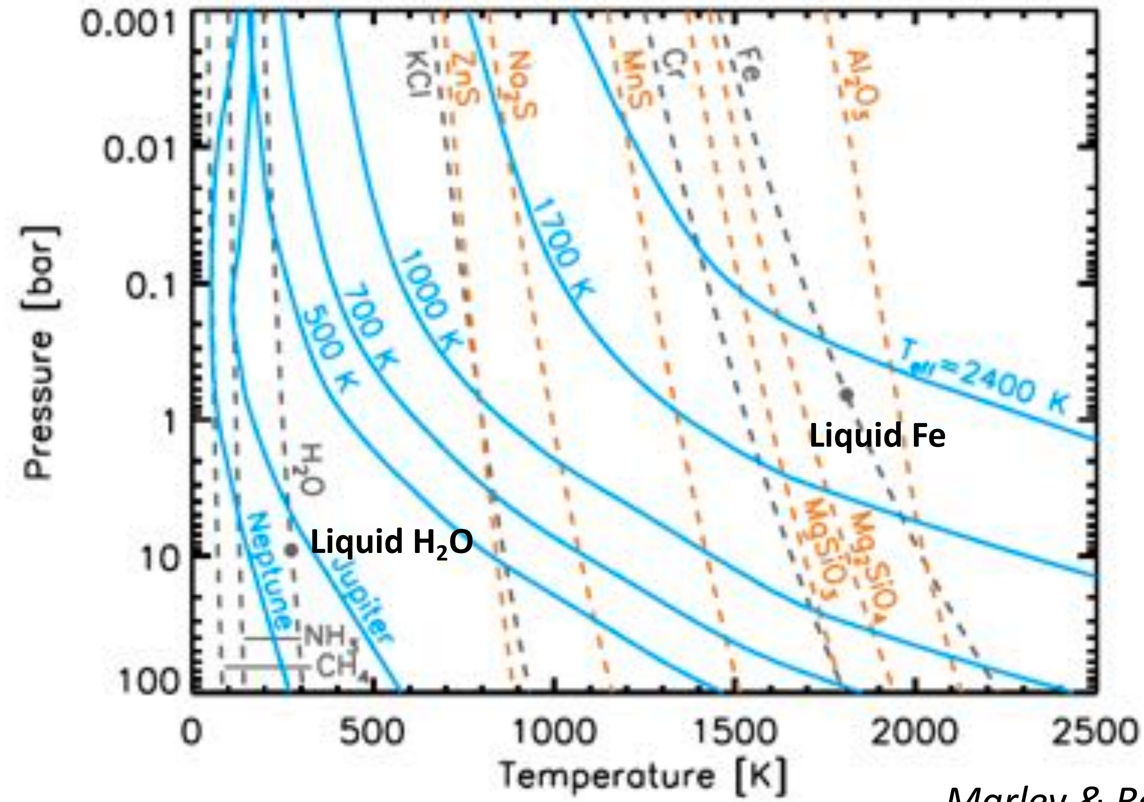

Marley & Robinson (2014)

Elemental abundances from *Lodders et al.* (2003)

Temperature condensation curves from *Visscher et al.* (2006, 2010)

Clausius-Clapeyron relation: $P_{sat} = P_{sat}(T_0)e^{-\frac{L}{R}\left(\frac{1}{T}-\frac{1}{T_0}\right)}$

III) Clouds & Aerosols

1D Cloud models

1) Model with f_{sed} from Ackerman & Marley 2001

At equilibrium :

$$\frac{\partial q_c}{\partial z} = -\frac{\partial q_s}{\partial z} - \frac{V_{sed}}{K_{zz}} q_c$$

- q_c = mass mixing ratio of condensate
- q_s = mass mixing ratio of vapor at saturation
- V_{sed}= sedimentation speed
- K_{zz} = eddy diffusion coefficient

Mixing length theory:

$$K_{zz} = \frac{H}{3}\left(\frac{L}{H}\right)^{4/3}\left(\frac{rF_{conv}}{c_p\rho_a}\right)^{1/3}$$

Ackerman & Marley 2001

- Mixing length: *L=H*
- $F_{conv}=\sigma T_{eff}^4$

Assumption: $\boldsymbol{f_{sed} = \frac{HV_{sed}}{K_{zz}}}$ = **constant** (generally f_{sed}= 1-5)

Above condensation: $q_c = q_{c0}\left(\frac{P}{P_0}\right)^{f_{sed}}$

III) Clouds & Aerosols

1D Cloud models

2) Model with simple microphysics using timescales from Rossow 1978

e.g. BT-Settl (*Allard et al.* 2001) and Exo-REM (*Charnay et al.* 2018)

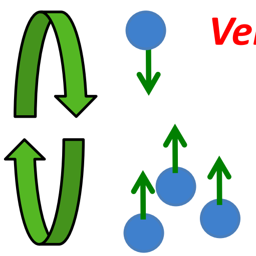

Vertical mixing

$$\tau_{mixing} = \frac{H^2}{K_{zz}}$$

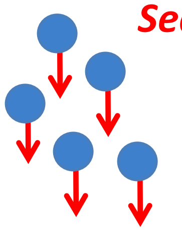

Sedimentation

$$\tau_{sed} = \frac{H}{v_{sed}}$$

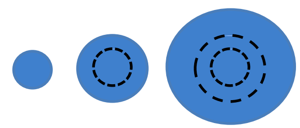

Condensation growth

$$\tau_{cond} = \frac{r^2}{(2 f \eta q_s S)} \rho_c$$

$$S = 10^{-3} - 10^{-1}$$

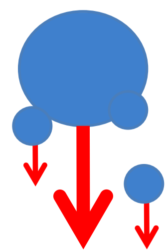

Coalescence

$$\tau_{coal} = \frac{4 r \rho_c}{3 \alpha v_{sed} \rho_{air} q_c}$$

III) Clouds & Aerosols

1D Cloud models

3) Models with full microphysics

e.g. Drift-Phoenix (*Woitke & Helling* 2003)

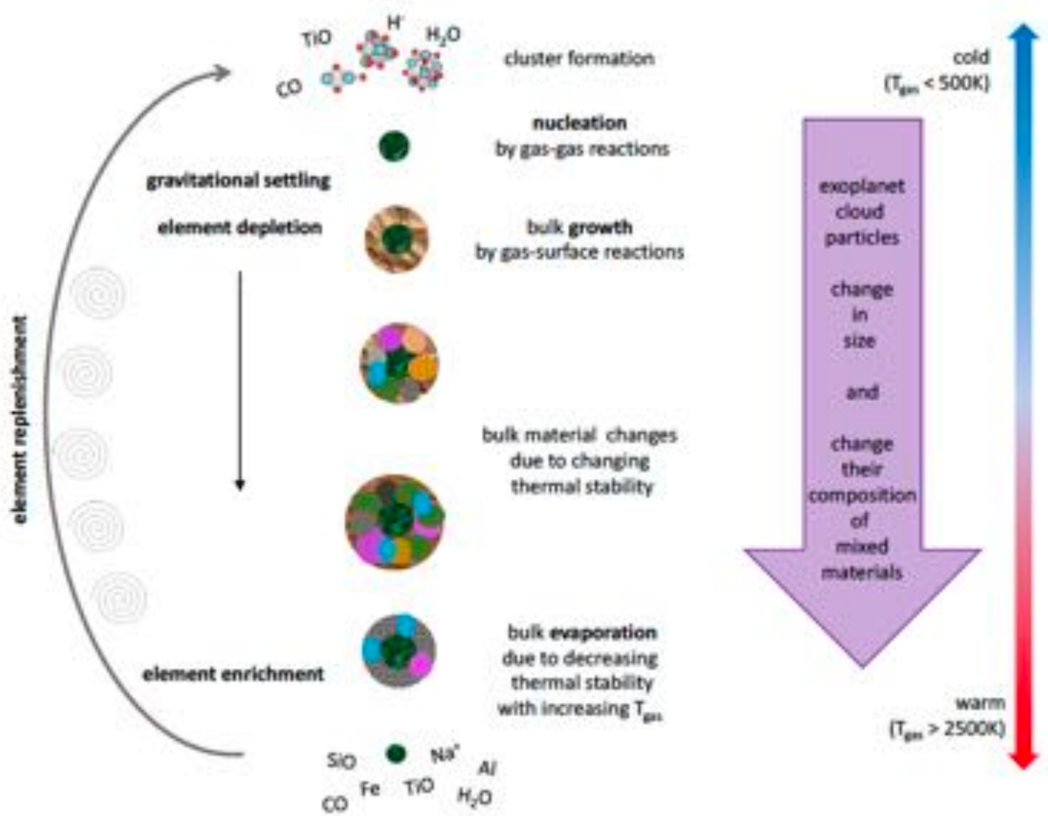

III) Clouds & Aerosols

Opacity

We usually compute aerosol optical properties ($Q_{ext}=\sigma_{ext}/\pi r^2$, ω_0, g) from Mie Theory with optical indexes and assuming spherical particules

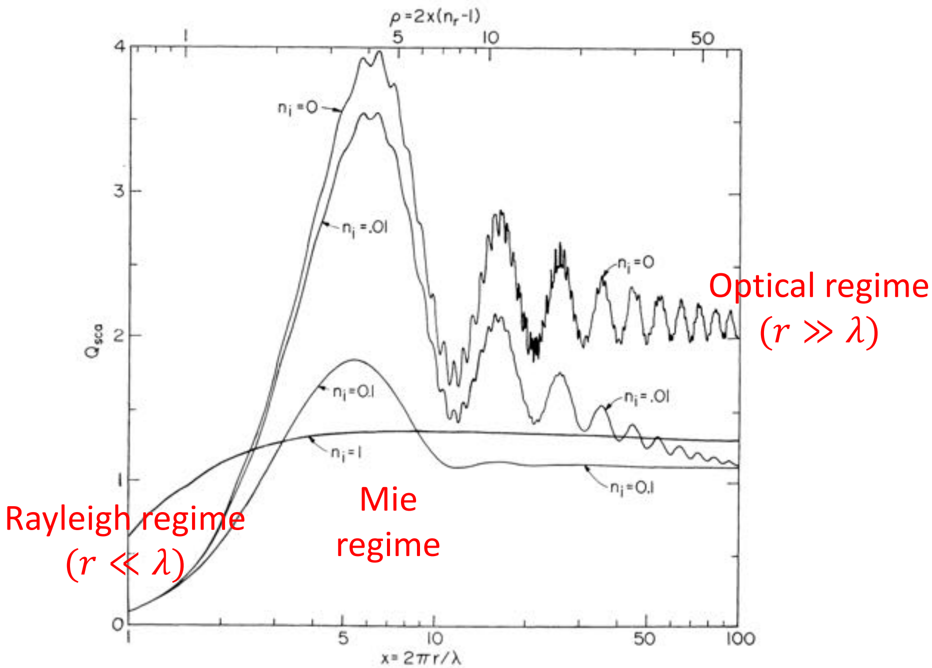

Hansen & Travis (1974)

Optical indexes
(*Kitzmann et al.* 2017)

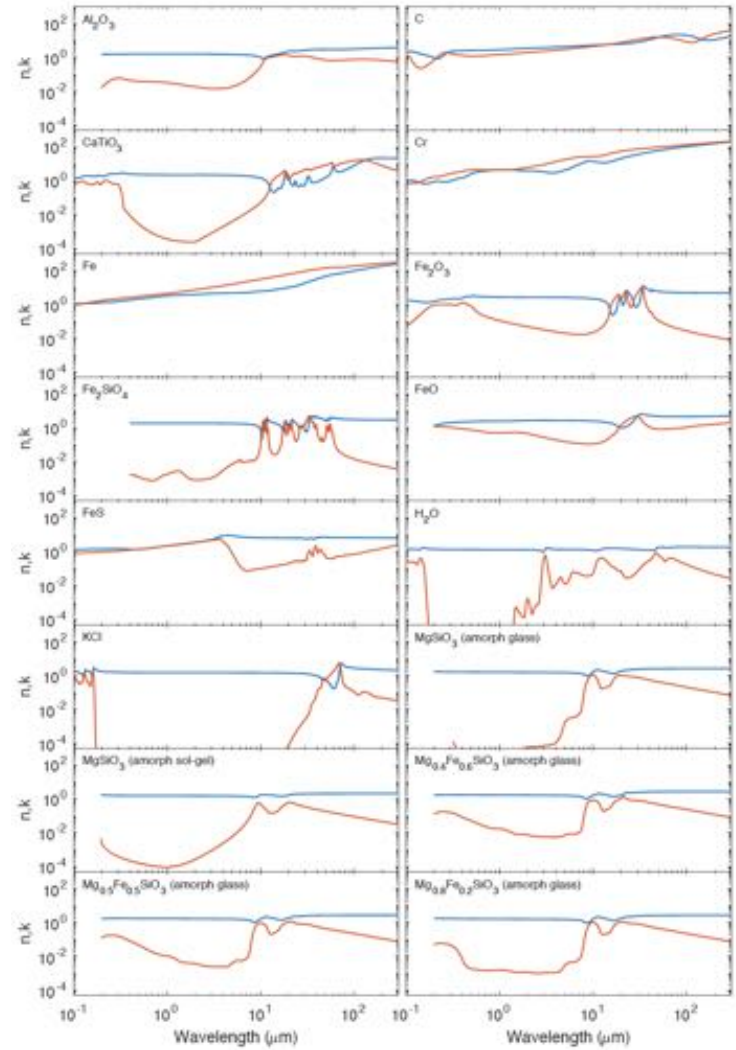

Cloud optical depth: $\tau_c = \frac{3}{4}\frac{Q_{ext}w}{\rho r e}$

w: mass column
ρ: volumic mass
r_e: effective radius

III) Clouds & Aerosols

Radiative effects

1) **Scattering of stellar radiation**

→ surface cooling by albedo effect

Cloud albedo for pure scattering cloud ($\omega_0 \rightarrow 1$) using the two-stream approximation:

$$A_c = \frac{\sqrt{3}(1-gc)\tau_c}{2+\sqrt{3}(1-gc)\tau_c}$$

Hansen & Lacis (1974)

2) **Absorption of stellar flux**

→ local warming & surface cooling (anti-greenhouse effect, e.g. Titan's haze)

3) **Absorption/emission of thermal radiation**

→ surface warming by greenhouse effect

- Stronger effect for upper clouds (e.g. cirrus)
- Same effect for back-scattering of thermal flux

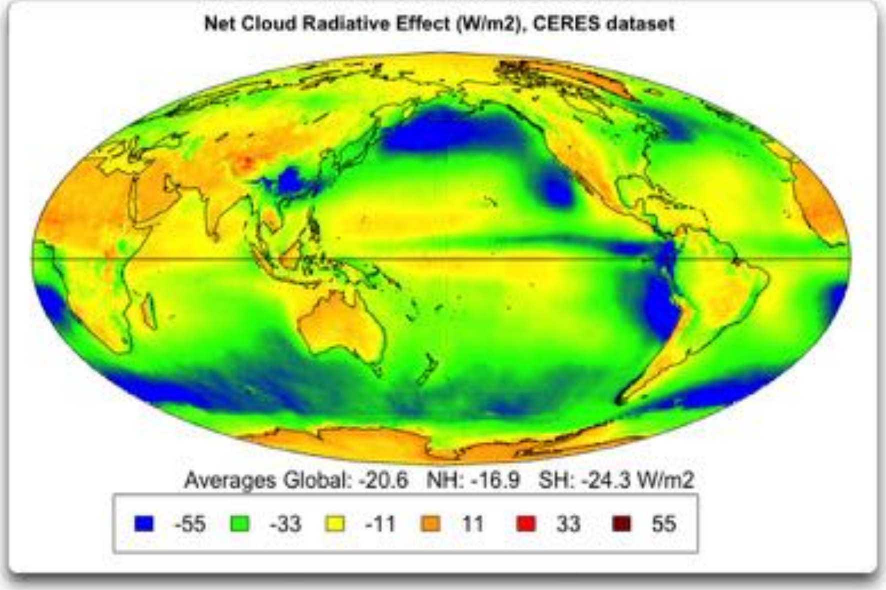

On Earth, clouds globally have a net cooling effect

III) Clouds & Aerosols

Radiative effects: absorption/emission of thermal radiation

Emission spectra and brightness temperature (Teff=1300K, log(g)=5)

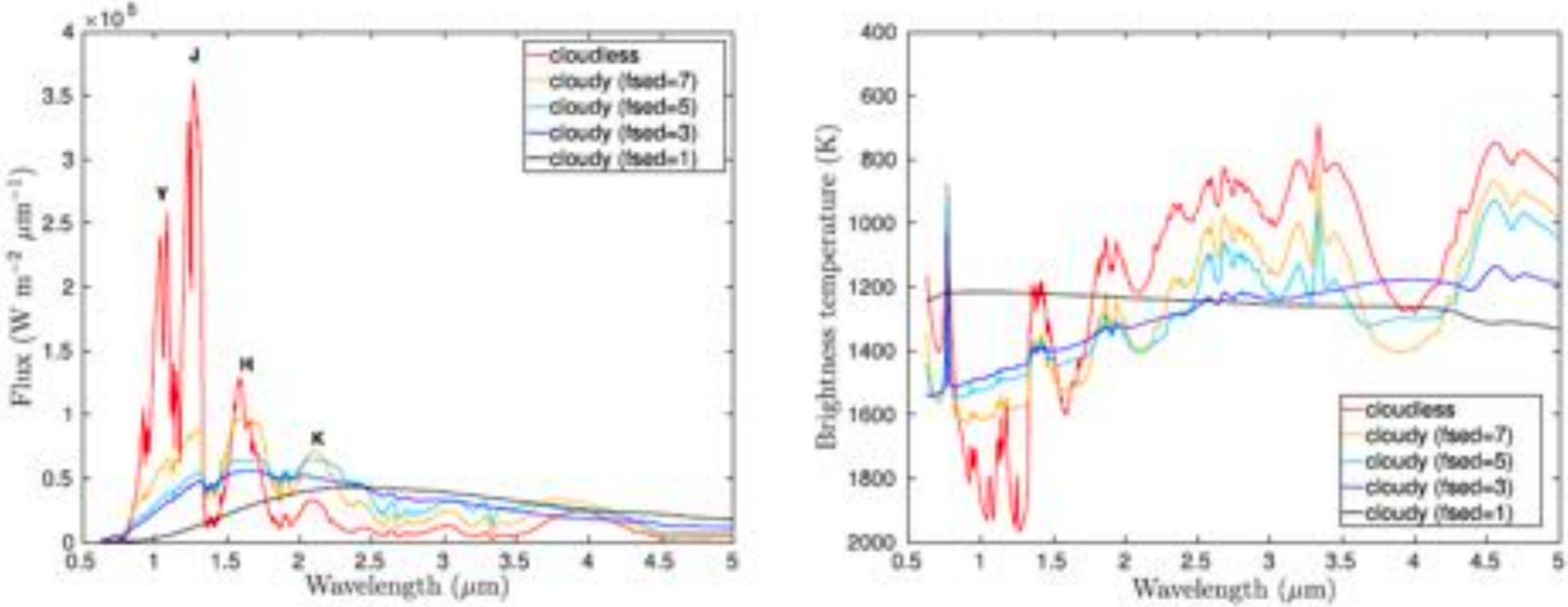

Charnay et al. (2018)

- Clouds produce a decrease of flux in spectral windows and an increase in spectral bands (greenhouse warming).
- With thick clouds, spectrum close to a blackbody

III) Clouds & Aerosols

LT transition for brown dwarfs

Color-magnitude diagram of brown dwarfs

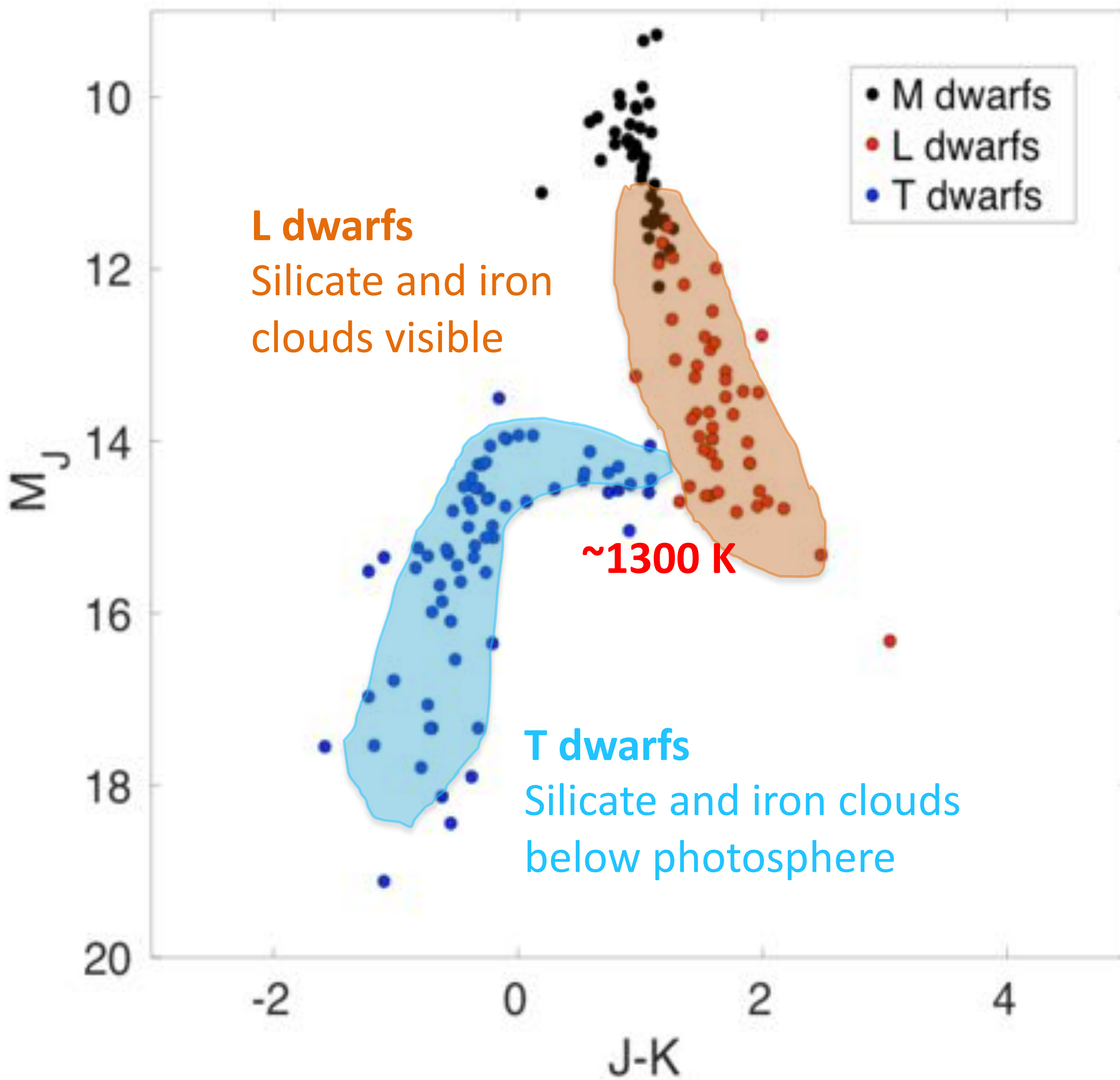

III) Clouds & Aerosols

LT transition for brown dwarfs

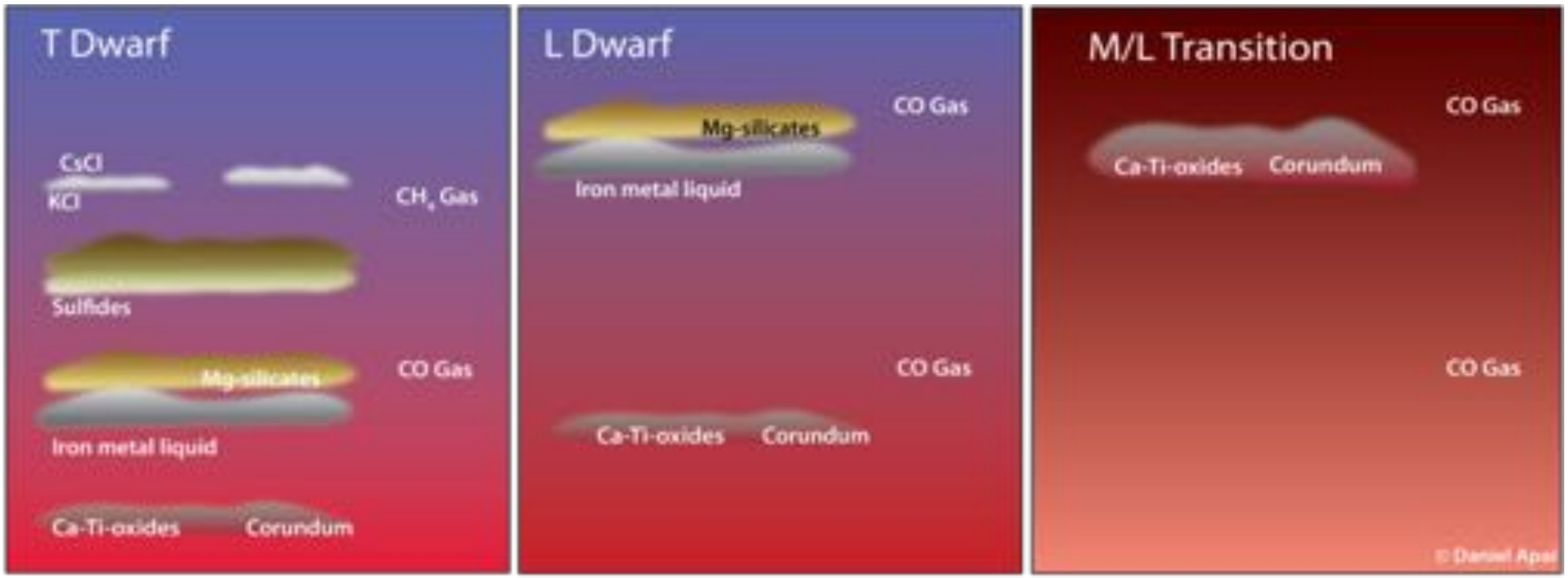

III) Clouds & Aerosols

LT transition for brown dwarfs

Teff= 700/900/1300/1600 K, log(g)=5 (g in cm/s²)

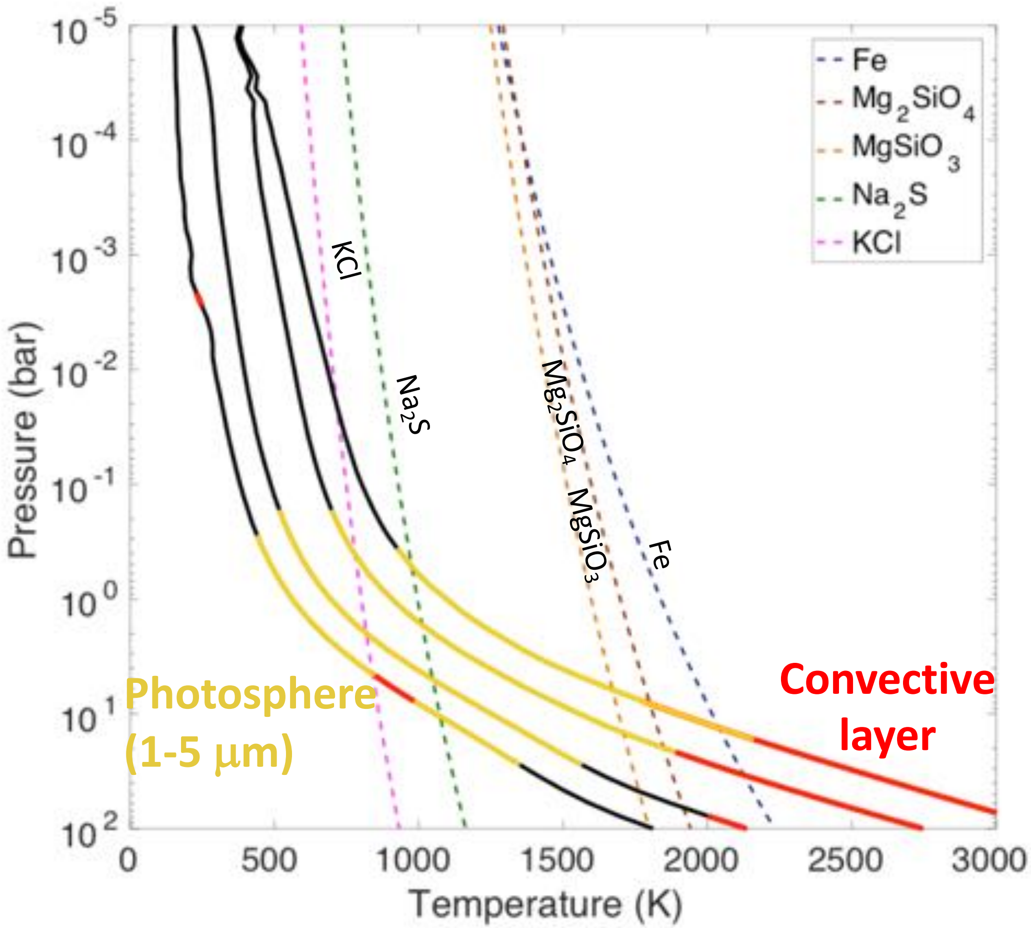

Charnay et al. (2018)

Cloud below photosphere for T_{eff}<1300 K

⇒ LT transition

What’s next

For strongly irradiated exoplanets, we need 3D GCM !

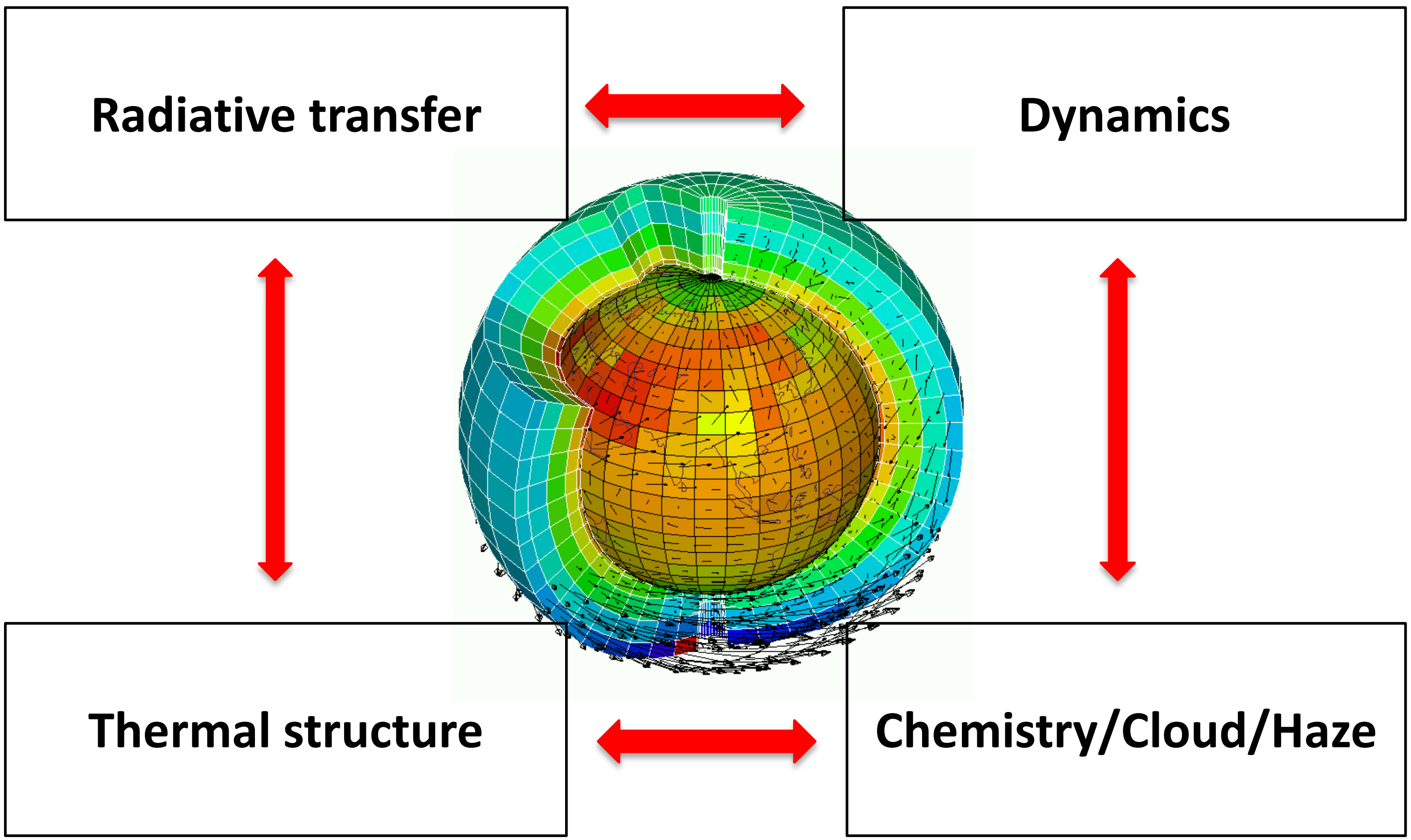

Current and future space telescopes for exoplanets

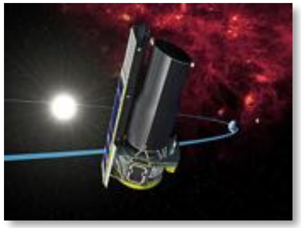

- **Spitzer**

Photometry (3.6, 4.5 μm)

- **HST**

Spectroscopy (1.1 - 1.7 μm)

- **Kepler**

Photometry (0.4 - 0.9 μm)

- **TESS**

Photometry (0.6 - 1 μm)

- **CHEOPS** (2019)

Photometry (0.4 - 1 μm)

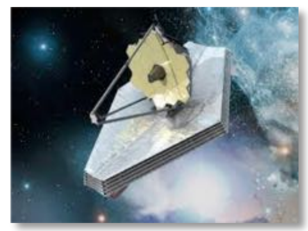

- **JWST** (2021)

Spectroscopy
(NIRISS, NIRSpec & MIRI)

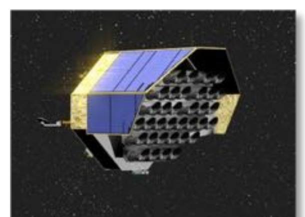

- **PLATO** (2026)

Photometry (0.5 - 1 μm)

- **ARIEL** (2028)

Photometry (0.5 - 0.95 μm)
Spectroscopy (0.95 - 7.95 μm)

~